

27 the deep geodynamic processes, the inherited heterogeneity of the pre-Neoproterozoic
28 basement, the tectonic evolution of Rodinia, Gondwana and Pangea amalgamation and
29 breakup, and environmental conditions influenced by the drifting through the South Pole
30 towards its present-day equatorial position and global climatic fluctuations between icehouse
31 and greenhouse conditions.

32

33 **Key Words:** Congo Basin, Intracratonic basins, Basin Tectonic Evolution, Sediments.

34

35 **1. Introduction**

36

37 The Congo Basin (CB), also known as “Cuvette Centrale”, is a roughly circular basin
38 located in the center of the African plate (Fig. 1). It extends for about 1.2 million km² from
39 the Central African Republic (CAR) in the North to Angola in the South, occupying most of
40 the Democratic Republic of Congo (DRC) and the Republic of Congo (RC). It is considered
41 as a typical intracratonic basin, due to its slow and long-lived subsidence history and the
42 largely unknown formation mechanisms (Veach, 1935; Crosby et al., 2010; Kadima et al.,
43 2011a; Buitter et al., 2012). Hydrocarbon exploration in the CB, using geological and
44 geophysical methods, started in the 1950’s and continued during the following decades
45 (Evrard, 1957; Jones et al., 1960; Lawrence and Makazu, 1988, Daly et al., 1992), along with
46 field campaigns in its peripheral parts (Raucq, 1957, 1970; Verbeek, 1970; Lepersonne, 1977;
47 JNOC, 1984). Despite the possible geo-resources potential of this basin (Delvaux and
48 Fernandez, 2015), the existing geophysical and geological data have not been fully exploited
49 and important scientific questions concerning its structure and tectonic evolution remain. The
50 CB has been repeatedly reactivated by global and local compressional and extensional
51 tectonic events (Hartley and Allen, 1994; Kadima et al., 2015; Linol et al., 2015a). During the

52 first part of its development, it also shared its intraplate history with other intracratonic basin
53 in the Gondwana supercontinent. The CB is thus a natural laboratory to investigate the
54 processes that govern the long-term evolution of continental interiors.

55 The history of the geological and geophysical investigations in the CB has been
56 reviewed in Kadima et al. (2011a, 2015). In the 1950's, field works, gravity surveys, and
57 several seismic refractions profiles were carried out. The first exploration campaigns were
58 undertaken between 1952 and 1956 by REMINA (Société de Recherche Minière en Afrique),
59 a.o. with the drilling of two fully cored stratigraphic wells (Fig. 2), in the localities of Samba
60 (2.039 m deep; Cahen et al., 1959) and Dekese (1.856 m deep; Cahen et al., 1960) (Fig. 2).
61 The resulting data and documentation of these campaigns (original data and notes,
62 publications, geological samples, and the entire cores) were donated to the Royal Museum for
63 Central Africa (RMCA) for further use in scientific studies.

64 A second exploration campaign was organised by a consortium of oil companies in
65 the 1970's, acquiring ~2600 km of seismic reflection profiles, airborne aeromagnetic surveys
66 covering most part of the basin in the DRC, and additional field sampling. Two deep (~4.3-
67 4.6 km) exploration wells, taking mostly drilling cuttings (Mbandaka-1 and Gilson-1) were
68 drilled in 1981 by Esso Zaire (Fig. 2).

69 In recent years, renewed interest was driven by the availability of a high resolution
70 global gravity field dataset derived from the GOCE satellite that allowed for the first time to
71 recover geological features across the entire African continent, also in areas with scarce field
72 observations (Braitenberg, 2014). The satellite gravity data led to several new geodynamic
73 models to explain the huge geoid anomaly centred on the CB and the long-term evolution of
74 the basin (Downey and Gurnis, 2009; Crosby et al., 2010; Kadima et al., 2011b, Buitter et al.,
75 2012). The available geological and geophysical data were used to revise and/or update the
76 stratigraphy and tectonic evolution of the basin (Kadima et al., 2011a, 2015; Sachse et al.,

77 2012; Linol et al., 2015a; 2015b; 2015c; Lucazeau et al., 2015; Caillaud et al., 2017; François
78 et al., 2017). A new field campaign in the CB was initiated to evaluate its hydrocarbon
79 potential (Delvaux and Fernandez, 2015).

80

81 *1.1. Existing views on the CB evolution and formation*

82

83 The CB has a long and complex history of sediment accumulation, tectonic
84 reactivations and erosion, initiated in the Precambrian with different extensional phases
85 interrupted by short-lived compressional phases (Lucazeau et al. 2015), similarly to other
86 intracratonic basins (Lindsay et al., 2002; Burke and Gunnell, 2008). The CB overlies a thick
87 rigid lithosphere (~200 km; Crosby et al., 2010) and requires a deep compensation level to
88 explain the underlying long-wave negative gravity anomaly, one of the largest on Earth
89 (Hartley and Allen, 1994; Downey et al., 2011; Buiter et al., 2012). This anomaly is
90 considered as the result of the combined effects of the low density of its thick sedimentary
91 units (~9 km) and the presence of a high-density body below the crust, which isostatically
92 compensates the sediments (Hartley and Allen, 1994).

93 According to Kadima et al. (2011a) and Buiter et al. (2012), a large part of the older
94 subsidence history of the CB is controlled by post-rift thermal subsidence. Further studies
95 link the CB formation to tectonic uplift of swells surrounding the basin (Burke and Gunnell,
96 2008) or to lithospheric delamination (Downey et al., 2011). These studies have based their
97 hypotheses on the stratigraphy reconstructed from the interpretation of the seismic reflection
98 profiles, calibrated by the four deep wells (Samba, Dekese, Mbandaka, and Gilson; Fig. 2).

99

100 *1.2. Study approach*

101

102 Despite the already abundant literature on the subject, the spatio-temporal evolution
103 of the CB within the global plate tectonic and climatic context is still poorly known. In a
104 considerable effort, the available litho- and biostratigraphic data have been recently
105 highlighted in several recent papers, but they have not yet been fully used at the scale of the
106 basin. We construct here a three-dimensional geological and stratigraphic model of the CB
107 for the main time periods, in order to investigate the architecture and evolution of the CB.

108 To achieve this, we reconstructed the structure of the basin using all the available
109 seismic and geological data (seismic reflection, seismic refraction, borehole, and field data),
110 taking advantage of the apparent lateral continuity of the stratigraphic units. We re-examined
111 the calibrated seismic reflection profiles and interpreted the total of about 2600 km of seismic
112 profiles, acquired along 35 lines in the CB, between 1974 and 1976, by an Esso-Texaco
113 consortium. The obtained model will be validated by aeromagnetic, satellite gravity data, and
114 density measurements from rock samples in a next paper (Maddaloni et al., 2020).

115 The interpreted two-way travel time (TWT) profiles were converted into depth
116 profiles and used to compute a series of major sedimentary layers by kriging interpolation.
117 The obtained results enable to identify the main sedimentary depocenters of the CB and
118 reconstruct its tectonic and geological history in greater details than in previous studies. In
119 particular, from the work of Daly et al. (1992) and Kadima et al. (2011a), we provide a new
120 lithostratigraphic subdivision with newly defined Supergroup and Group. Furthermore, the
121 analysis of the seismic reflection profiles led us to identify several small tectonic features
122 reflecting the influence of far-field compressional tectonic events within the basin. The ~
123 1.000 Ma evolution of the CB is then placed into a broad tectonic context of Rodinia,
124 Gondwana and Pangea amalgamation and breakup, and glacial climatic fluctuation with
125 several glacial events.

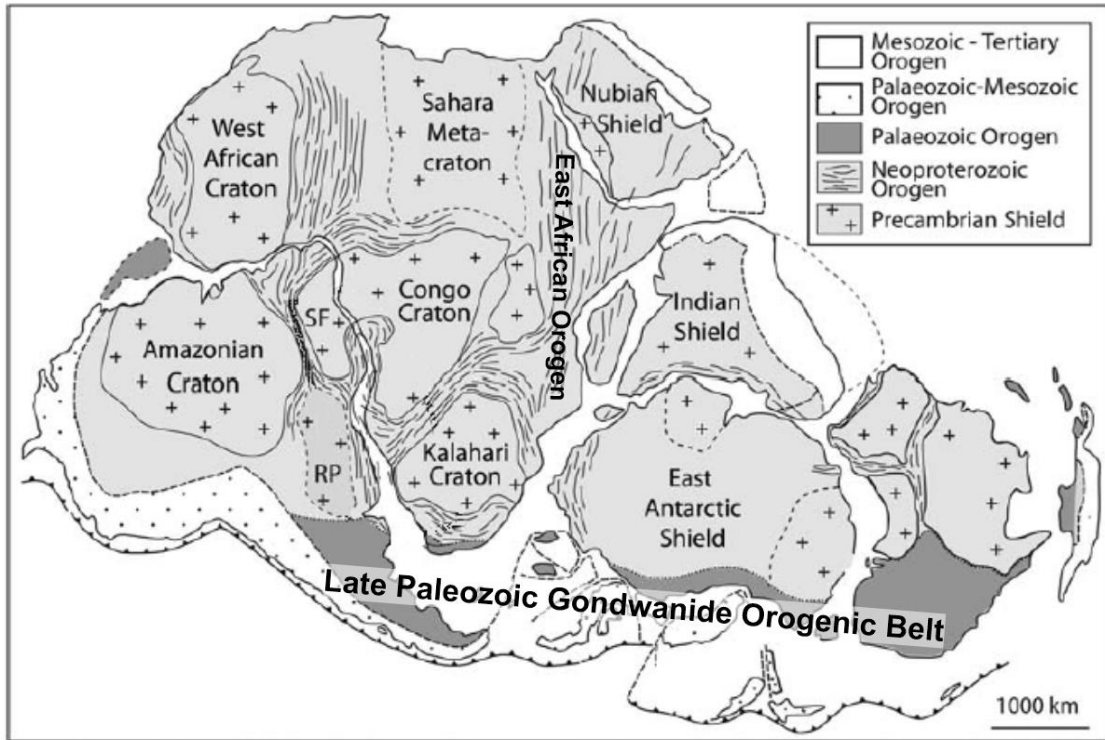
126

127 **2. Tectonic setting and factors controlling the evolution of the Congo Basin**

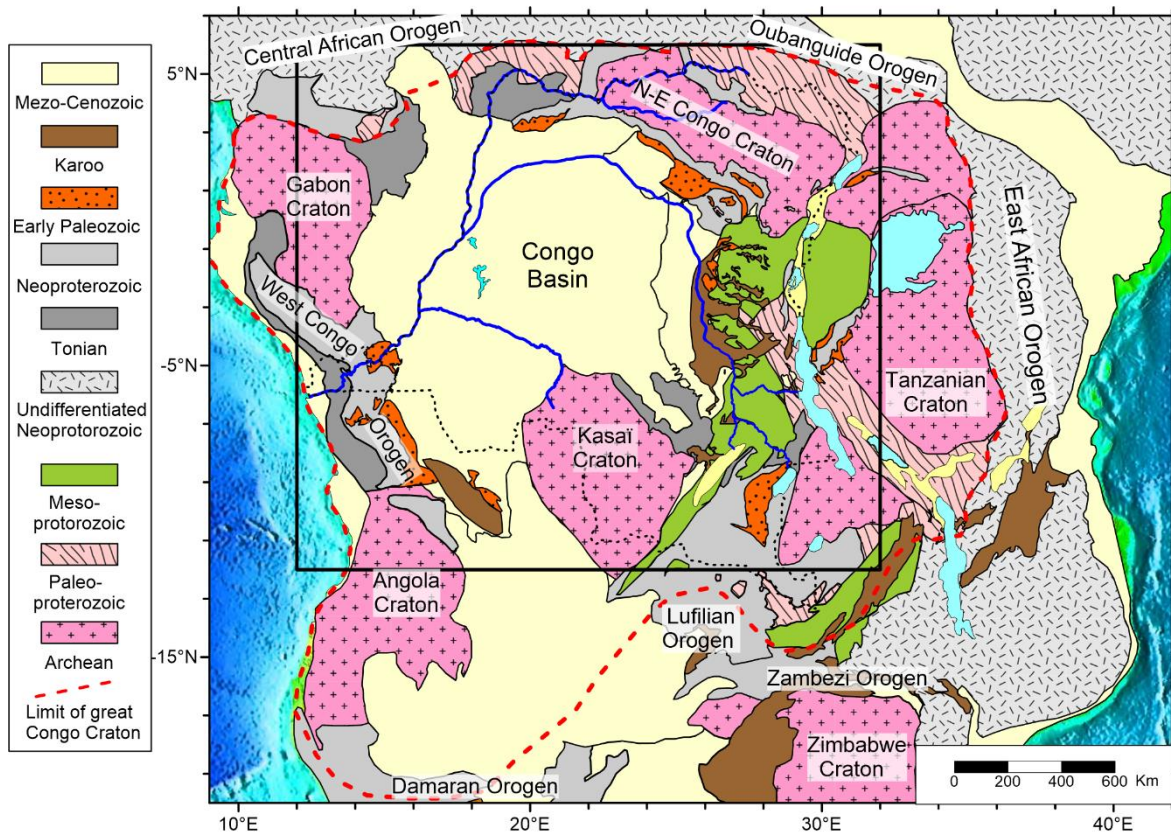
128

129 The CB started to form in early Neoproterozoic (Kadima et al., 2011b, 2015), or, as
130 we will show in this study, possibly even earlier, in late Mesoproterozoic. It developed within
131 the Precambrian basement of Central Africa (Fig. 1), originally defined as the Congo Craton
132 by Cahen (1954). De Waele et al. (2008) and Fernandez-Alonso et al. (2015) expanded the
133 definition of the Congo Craton to the assemblage of several central-African Archean nuclei
134 plus the Sao-Francisco and Tanzania cratons; all welded together at the end of the
135 Mesoproterozoic by Meso- and Paleoproterozoic belts. Others named this assemblage the
136 Central African Shield (de Wit and Linol, 2015) or the great Congo Craton (Kadima et al.,
137 2015). We prefer here to keep the Congo Craton term as understood by De Waele et al.
138 (2008) and Fernandez-Alonso et al. (2015). The Congo Craton is surrounded from all sides
139 by Neoproterozoic belts (Abdelsalaam et al., 2002; Frimmel et al., 2006; Gray et al., 2008;
140 Collins and Pisarevsky, 2005; Fritz et al., 2013; Foster et al., 2015).

141



142



143

144 **Fig. 1.** Geological setting of the Congo Basin. **a:** Map of Gondwana (adapted from Gray et
 145 al., 2008), with position of the Gondwanide orogenic belt from Trauw & de Wit (1999). **b.**
 146 Congo Craton and surrounding Pan-African orogenic belts (adapted from Kadima et al.,
 147 2015). Black rectangle delimits the Congo Basin as detailed in Figure 2.

148

149 Since the late Mesoproterozoic, as the result of Rodinia amalgamation, the Congo
150 Craton comprised the NE-Congo, Gabon, Angola, Kasai, Tanzania, and São Francisco
151 cratons, together with the Bangweulu block (Collins and Pisarevsky, 2005; Fernandez et al.,
152 2015). During Gondwana amalgamation, it interacted between 650 and 540 Ma with the West
153 African craton along the Central African Orogenic Belt (Toteu et al., 2004; Saha-Fouotsa,
154 2019). At about 630 Ma, it entered in continental collision with the Sahara Metacraton,
155 generating the Oubanguide Orogen (Poidevin, 1985) and with Neoproterozoic India in the
156 East, generating the East African Orogen (Fritz et al., 2013). At about 570 Ma, closure of the
157 ocean embayment between the São Francisco Craton (eastern Brazil) and the Gabon-Angola
158 cratonic nuclei generated the Araçuaí-West Congo Orogen (Pedrosa-Soares et al., 2008;
159 Santiago et al., 2020). Convergence and collision between the southern margin of the Congo
160 Craton and the Zimbabwe Craton (small northern part of the Kalahari Craton) generated the
161 Damara Orogen in the west, peaking at about 565 Ma (Frimmel et al., 2011) and, in the east,
162 the twin Lufilian Orogen, peaking at about 595 Ma (Cailteux and De Putter, 2019) and
163 Zambezi Orogen, peaking at 560-550Ma (Kuribara et al., 2018). Late tectonic convergence
164 between the Dharwar Craton (India) relative to the Congo Craton at ~530 Ma generated
165 intraplate reactivations between the Congo-Bangweulu and the Tanzania cratons (Delvaux et
166 al. 2012) and also within the Lufilian Orogen (Kipata et al, 2013; Cailteux and De Putter,
167 2019). All these tectonic events are likely to have caused late Neoproterozoic (Pan-African)
168 intraplate deformations in the heterogeneous Congo Craton, which could have been recorded
169 in the CB.

170 The CB developed over three NW elongated Archean nuclei (Gabon, Kasai and NE-
171 Congo) that form the central core of the Congo Craton, and surrounding the concealed central
172 part of the Congo Craton (de Wit and Linol, 2015). The presence of cratonic lithosphere

173 beneath the CB has recently been confirmed by seismic tomography by Celli et al. (2020),
174 who identified at least three distinct high-velocity blocks. These blocks represent remnants of
175 likely larger Archean nuclei, which were partly eroded by their interactions with thermo-
176 chemical mantle plumes (e.g., Hu et al., 2018) or by other processes (e.g., Liao et al., 2017).
177 Therefore, the original heterogeneous structures of the Archean cratons and their possible
178 successive modifications during geological time are responsible for the primary basement
179 anisotropy and the following development of the CB.

180 After the final junction between East and West Gondwana, at about 530 Ma, the CB
181 became located in the center of the Gondwana supercontinent. A new paleo-pacific active
182 margin formed along the southern edge of the continent during the Phanerozoic (Milani and
183 de Wit, 2008). Once amalgamated, the entire Gondwana supercontinent drifted first
184 southwards, then northwards, bringing the CB into a polar-centered, and back into an
185 equatorial position. According to the apparent polar wander curve for Gondwana (Scotese et
186 al., 1999; Torsvik and Cocks, 2011; 2013), the South pole was located in W Africa
187 (Mali/Algeria) in early Cambrian, NW Africa (Morocco) in early Ordovician, SW Africa
188 (Ivory Coast) in late Ordovician, western coast of Central Africa (Namibia) in early
189 Devonian, Namibia in late Devonian (Frasnian), Central Africa in late Devonian
190 (Famennian), north of the CB in early Carboniferous (Tournaisian-Visean), and central
191 Antarctica (then adjacent to South Africa) in late Carboniferous. From that period, the
192 general tendency for the Gondwana continent was to drift northwards, bringing the CB
193 progressively into a more equatorial position. In parallel, the global climate fluctuated with
194 several ice ages (Ice House), during which one or two poles were covered by permanent ice,
195 followed by global warming and warm ages (Hot House), without permanent ice cover at the
196 poles. Major Ice House periods occurred during the Cryogenian (coinciding with the
197 assembly of Gondwana), late Ordovician - earliest Silurian (brief but extensive), and in late

198 Devonian–Carboniferous to early Permian (Frakes et al., 1992). The regional paleoclimatic
199 conditions of the plate interior were controlled by the latitudinal movement of Gondwana,
200 global climate evolution, and morphology of the plate interior.

201 During the lifespan of the Gondwana supercontinent, interactions with the adjacent
202 plates generated plate-boundary forces that propagated into the continental interior as far-
203 field stresses (Daly et al., 1991; de Wit and Ransome, 1992). Collision with Laurentia on its
204 NW edge in the late Carboniferous – early Permian resulted in the Appalachian-Mauritanian-
205 Variscan orogeny (Kröner and Römer, 2013). Subduction along the southern margin of
206 Gondwana resulted in the Gondwanides orogeny (Fig. 1a) with the Sierra de la Ventana-Cape
207 Fold Belt in the late Permian – early Triassic (Trouw and de Wit, 1999; Milani and de Wit,
208 2008) and earlier collisions (Ordovician-Devonian) in the NW, along the South American
209 domain (Milani and de Wit, 2008). Gondwana breakup which started around 200 Ma ago
210 (early Jurassic), also influenced the tectonic evolution of the CB, with the giant Okavango
211 mafic dyke swarm across NE Botswana emplaced at 178-179 Ma (Le Gall et al., 2005), the
212 late Jurassic opening of the Indian Ocean (Sinha et al., 2019), the early Cretaceous opening of
213 the South Atlantic Ocean (Heine et al., 2013), and the Neogene East African rifting
214 (Macgregor, 2015).

215 According to Kadima et al. (2011a, 2011b), the CB started as a failed rift system. The
216 fossil rift would be represented by the WNW-trending Kiri basement high that separates the
217 basin in two parts and coincides with pronounced axial magnetic and gravity anomalies.
218 Following Daly et al. (1992), the Kiri High formed by crustal contraction and uplift in the late
219 Paleozoic times, reactivating (inverting) the former rift structure. Kadima et al. (2011a),
220 instead, using combined gravity and magnetic modeling, proposed that the poorly defined
221 seismic zone with transparent seismic facies which mark the ‘basement’ of the Kiri High (see
222 Figure 7 below) can be adequately modelled by intermediate salt (evaporate) and sediment

223 density, instead of an uplifted crystalline basement. They therefore propose a gradual lateral
224 change in density from the adjacent basins towards the Kiri High. They also suggested that
225 observed tectonic structures of the CB are the typical product of the inversion processes
226 during the two major tectonic events (Pan-African and Permo-Triassic) and induced by
227 movement of salt present in the Neoproterozoic sediments.

228

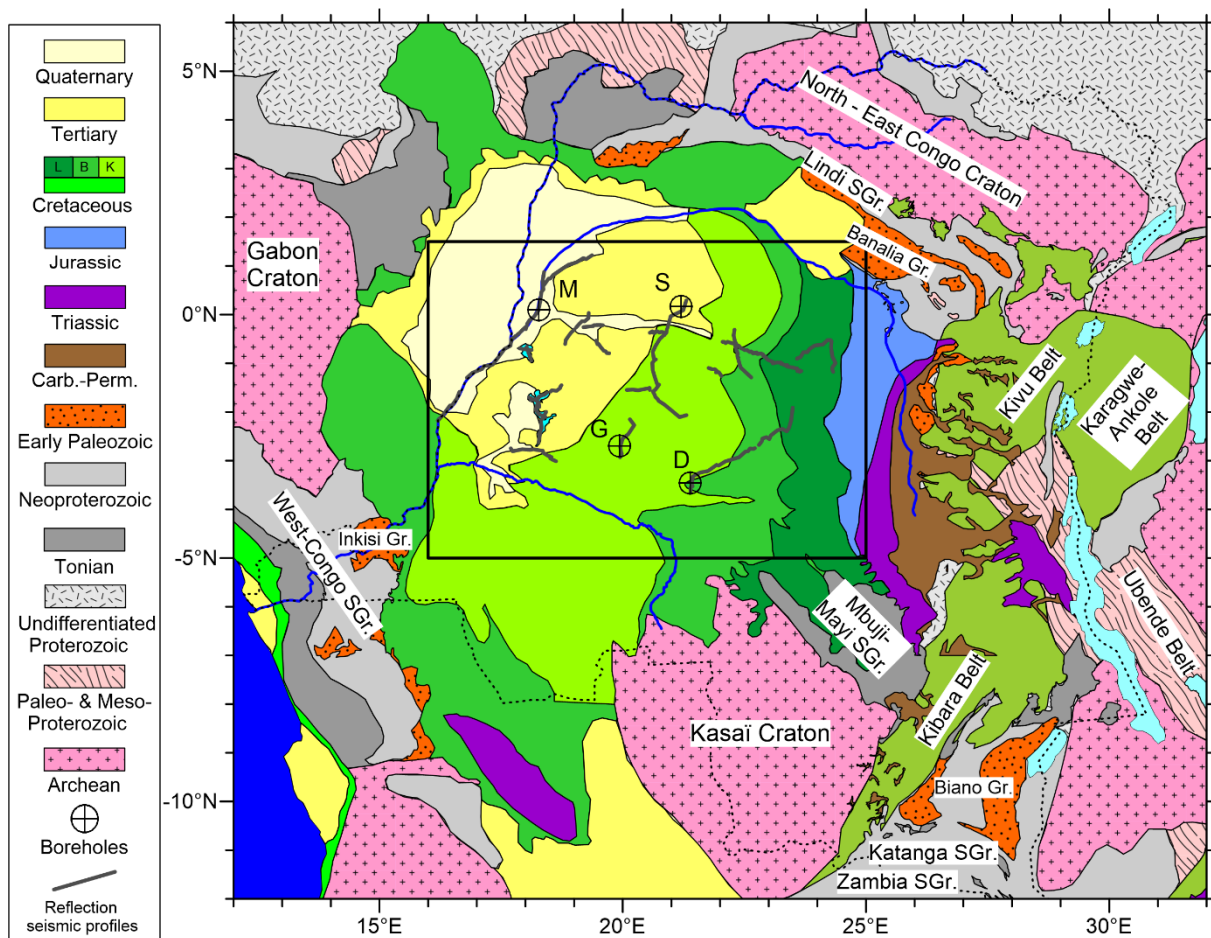
229 **3. Data obtained from exploration campaigns**

230

231 A first exploration campaign in the Congo Basin was conducted in 1952-1956 by the
232 ‘Syndicat pour l’étude géologique et minière de la Cuvette congolaise’, with field work,
233 refraction seismics and two c. 2000m deep stratigraphic wells, fully cored (Samba and
234 Dekese) drilled by the REMINA. The resulting data (outcrop samples, drill cores), reports
235 and publications are stored in RMCA collections and available for research. Furthermore,
236 between 1970 and 1984, Shell, Texaco, and JNOC oil companies acquired new data with
237 aeromagnetic surveys. They also acquired more additional gravity data, geochemical
238 sampling, and about 2600 km of seismic reflection profiles, in the CB over an area of
239 500.000 km² between the Congo and Kasai rivers. The seismic profiles were recorded both
240 along watercourses (lines R) and roads (lines L) (Fig. 2). In 1981, the exploration wells
241 Mbandaka-1 (4350 m; Esso Zaire S.A.R.L., 1981a) and Gilson-1 (4563 m; Esso Zaire
242 S.A.R.L., 1981b) were drilled by the Esso Oil Company (Fig. 2). The cuttings of the cores
243 were sampled every 10 m, but they are no longer accessible. The Mbandaka-1 well
244 terminated in massive salt deposits of Proterozoic age with anhydrite inter-beds, after
245 encountering stromatolitic carbonates, while the Gilson-1 well terminated in massive
246 dolomite. None of the four wells reached the crystalline basement. Only the Jurassic to
247 Recent sediments encountered in the Dekese and Samba wells were accurately dated

248 paleontologically but the stratigraphic position of the deeper deposits is more problematic.
 249 Analysis of the data lead to a preliminary subdivision of the basin stratigraphy in three major
 250 sedimentary sequences (Proterozoic, Paleozoic-Triassic and Jurassic-Cretaceous) separated
 251 by major tectonic unconformities (Pan-African and Basal Jurassic) and allowed to define its
 252 global architecture and tectonic evolution (ECL, 1988; Lawrence and Makazu, 1988; Daly et
 253 al, 1992; Kadima et al., 2011a).

254



255

256 **Fig. 2.** Surface geology of the Congo Basin (adapted from Kadima et al., 2015). Black
 257 circles: deep wells: D (Dekese), G (Gilson-1), M (Mbandaka-1), S (Samba). Broken black
 258 lines identify reflection seismic lines. Black rectangle delimits location of the study area.

259

260 **4. Revised seismic stratigraphy of the Congo basin**

261

262 The bowl-shaped CB (hence its name “Cuvette Centrale”) shows progressively older
263 outcropping geological series towards its periphery (Fig. 2). Integrating this with the well
264 data and thanks to the remarkable lateral continuity of the stratigraphic units, Daly et al
265 (1992) proposed a first general stratigraphic column of the CB. It was revised by Kadima et
266 al. (2011a, 2015) and Linol et al. (2015b, 2015c) based on the re-analysis of some key
267 seismic profiles and well data. The lithostratigraphic units are named according to the last
268 version of the Geological map of the RDC at 1/2.500.000 (Fernandez-Alonso et al., 2017) as
269 detailed in his Explanatory Notice (Fernandez-Alonso et al., 2017), published by the Ministry
270 of Mines of the DRC. A series of stratigraphic names have been changed according to the
271 Stratigraphic Guide of the International Commission on Stratigraphy (ICS). In particular, the
272 formations described in the literature as Haute-Lueki and Stanleyville Groups are now
273 respectively named as Lueki and Kisangani Groups.

274

275 *4.1 Lithostratigraphy and age control from well and outcrop data*

276

277 The lithostratigraphy of the CB is known from a few deep and shallow wells and from
278 surface outcrops. The good lateral continuity of the sedimentary layers and seismic reflection
279 profiles allows extending the stratigraphic framework over the entire basin. Almost all
280 stratigraphic sequences, from the late Mesoproterozoic to the Cenozoic, are illustrated by
281 well and/or outcrop data (Fig. 3). The Proterozoic to Cambrian sequences are exposed along
282 the margins of the CB (Delpomdor and Pr eat, 2015). The pre-Jurassic sequences of the deep
283 Gilson and Mbandaka wells are almost unconstrained by biostratigraphy and, therefore, their
284 interpretation is difficult and varies from one study to the other. For these sequences, we

285 preferred to follow the interpretation of Kadima et al. (2011a; 2015), which is based on
286 unpublished exploration reports, instead of the one presented in Linol et al. (2015b).

287 The oldest sequences of the CB are illustrated by the Mesoproterozoic Mbuji-Maji
288 Supergroup, which is found in two NW-trending depressions between the Kasai Craton and
289 the Kibara belt of Katanga (Fig. 2). They comprise a lower BI Group of mostly clastic
290 sediments, dolomitized on top, and an upper BII Group of dolomitic limestones, surmounted
291 by dolerite lava (Raucq, 1957, 1970; François et al., 2017; Balukiday et al., 2018).

292 The Neoproterozoic sequences are typified by the Lindi Supergroup, which outcrops
293 in the northern part of the CB (Fig. 2) and was intensively studied by Verbeek (1970). Their
294 correlation with the well and seismic data in the CB was proposed by Daly et al. (1992).

295 The lower Paleozoic sequences are represented by thick cross-bedded red arkosic
296 sandstones outcropping along the margin of the CB (Fernandez-Alonso et al., 2017) as the
297 Inkisi Group (Alvarez et al., 1995; Affaton et al., 2015), Banalia Group (Verbeek, 1970) and
298 Bianco Group (Cailteux and de Putter, 2019) and which are found also in the Samba and
299 Dekese wells (Cahen et al., 1959, 1960).

300 The overlying Karoo series comprise from top to bottom, red-sandstones of the Lueki
301 (ex-Haute-Lueki) Group (Triassic), coal-bearing mudstones and psammitic sandstones of the
302 Upper Lukuga Group (Late Carboniferous to Upper Permian), and glacial to periglacial tillite
303 and varval black shales of the Lower Lukuga Group (Upper Permian). Their age is relatively
304 well constrained by spores and pollens (Boulouard and Calendra, 1963; Boze and Kar, 1976,
305 1978; Cahen and Lepersonne, 1978). The Lower Lukuga Group is well known in the Dekese
306 well cores (Cahen et al., 1960), with a thickness of up to 1000 m of glacial-lacustrine tillites
307 and periglacial varval black shales (not present in the Samba Well). The entire Karoo series is
308 exposed along the Lukuga River valley and in the Lukuga Coal field (Fourmarier, 1914;
309 Jamotte, 1931), in the Luama graben along the Tanganyika rift valley. The Upper Lukuga

310 Group and its transition to the Lueki Group is well evidenced in a coal exploration drill well
311 (Cahen and Lepersonne, 1971). The Lueki Group is present in small thickness in the Dekese
312 Well, but not in the Samba Well (Lombard, 1961) and known as part of the Casanje Group in
313 Angola (Cahen, 1981). The Lukuga and Lueki sediments are also present in the Gilson and
314 Mbandaka wells, but the dominant clastic facies of these wells does not allow to precise their
315 biostratigraphic correlations.

316 The Jurassic to Cretaceous series are the best studied ones in terms of biostratigraphy,
317 sequence stratigraphy and lithostratigraphy. They were dated by ostracods (Grekoff, 1957;
318 1960), phyllopo ds (Defretin Lefranc, 1967), pelecypods (Cox, 1960); spores/pollen
319 (Boulouard and Calendra, 1963; Masheshwari et al., 1977) and fishes (de Saint-Seine, 1955;
320 de Saint-Seine and Casier, 1962; Casier, 1965; Taverne, 1975a, 1975b). Their biostratigraphy
321 has been revised by Colin (1994) and presented in detail in Linol et al. (2015b, c). Their
322 sequence stratigraphy and depositional environment were studied by Linol (2015c) and
323 Roberts (2015). These series start by the late Jurassic (Kimmeridgian) Kisangani (ex-
324 Stanleyville) Group, well developed along the Lualaba River (i.e. the Congo River upstream
325 Kisangani) where it forms a large basin (Passau, 1923). In this region the series starts by
326 organic-rich lacustrine calcareous siltstones and shales (Type I kerogen; Sachse et al., 2012)
327 and grades upward to more oxidized sandstones and siltstones in a dryer environment
328 (Caillaud et al., 2017). They overly limestones with stromatolites of probable Neoproterozoic
329 age, themselves resting over basement quartzites and gneisses.

330 Jurassic sediments are present in the Samba well (Cahen et al., 1959) consisting of a
331 lacustrine sequence at the base, locally organic-rich, surmounted by red siltstones and
332 sandstones with geochemical evidence for hot and arid conditions (Myers et al., 2011). They
333 have also been recognized in small thicknesses the Gilson and Samba Wells (Esso-Zaire
334 SARL, 1981a, 1981b; Linol et al., 2015b), in boreholes in Kinshasa and Brazzaville, lying

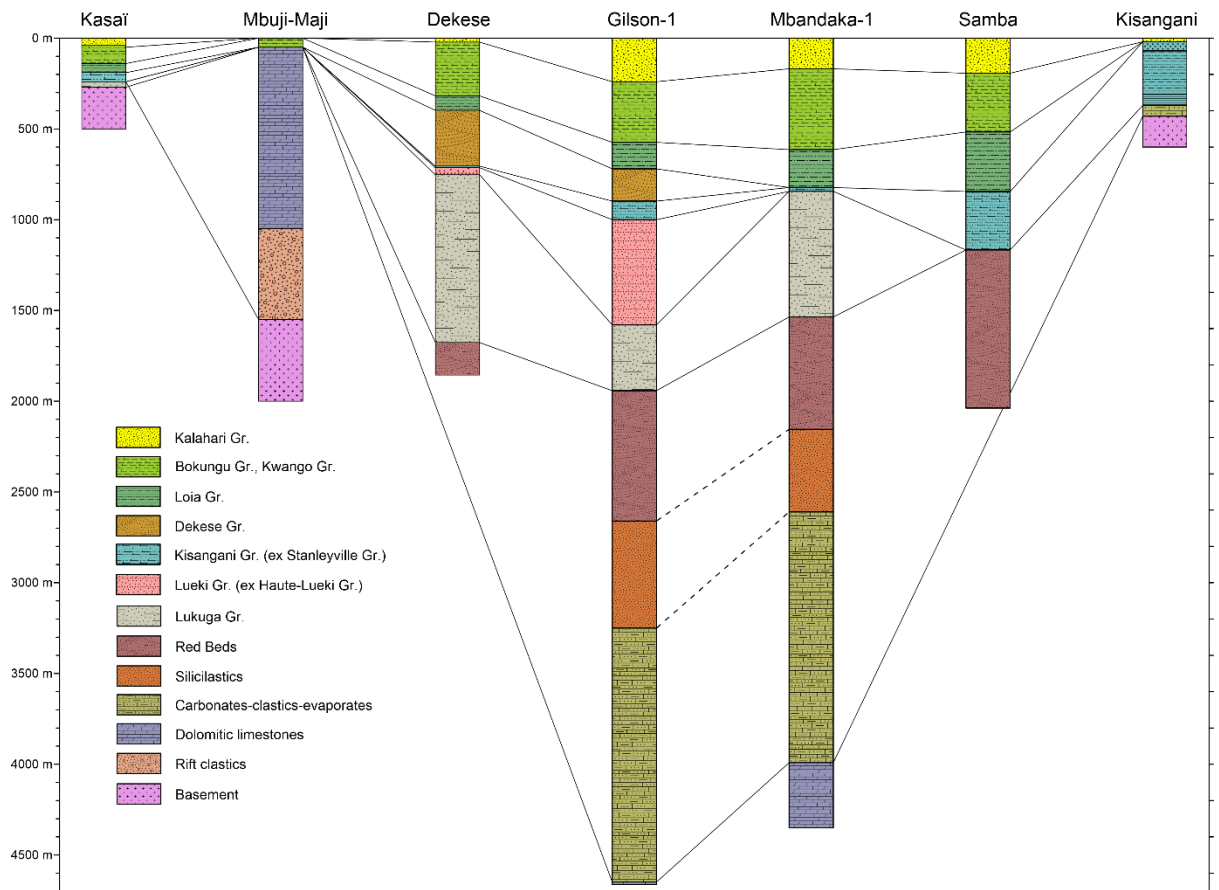
335 directly over the Inkisi red sandstones (Egoroff and Lombard, 1962; Defrétin-Lefranc, S.,
336 1967), and in the cover series of the Kasai Craton in the Tshikapa area (Roberts et al., 2015).

337 Arid conditions then developed, with deposition of eolian cross-bedded sandstones,
338 recently identified in Dekese and Gilson wells, which define the new Dekese Group (Linol et
339 al., 2015c). Its age is indirectly constrained as early Cretaceous from the surrounding
340 sediments. More humid conditions followed in Albian – Cenomanian as evidenced by the
341 deposition of sandstones and mudstones of the Loia and Bokungu Groups (Colin, 1994).
342 Deposition started in a lacustrine environment, locally anoxic with black shales (mixture of
343 kerogens of Type I and II; Sachse et al., 2012), then evolved into a shallower, fluvial
344 environment with carbonated mudstones.

345 The Kwango Group is known mainly in the southern and western parts of the basin
346 (Cahen and Lepersonne, 1954; Linol et al., 2015c) and as cover of the Kasai Craton (Roberts
347 et al., 2015). It may have had a marine influence and its lower part is dated mainly by fishes,
348 suggesting a Cenomanian-Turonian age (Casier, 1965; Taverne, 1976a, b) or Campanian-
349 Maastrichtian (Gobbo-Rodrigues et al, 2003).

350 The cover sequences are regrouped in the Kalahari Group (Linol et al., 2015e;
351 Fernandez-Alonso et al., 2015), with silcretes, calcretes and ferricretes covered by aeolian
352 sandstones. They represent the weathering and denudation ‘African Surface’ of King (1963)
353 and were formed under a regionally humid and hot climate of Central Africa. They are
354 described as ‘Polymorph sandstones’ (grès polymorphes) by Lepersonne (1945). Thermal
355 evolution modeling constrained by vitrinite data shows that during the late Cretaceous-
356 Paleogene evolution of the landscape (Guillocheau et al., 2015), an estimate of 1000m
357 (Sachse et al., 2012) or more (Lucazeau et al., 2015) of sediments were removed.

358



359

360 **Figure 3** : Regional lithostratigraphic correlations of the wells across the CB. Data in tables
 361 in the Supplementary Materials.

362

363 *4.2 New seismo-stratigraphic model*

364

365 Starting from the existing seismo-stratigraphic models of Kadima et al., (2011a;
 366 2015), we reinterpreted the entire seismic stratigraphy of the CB, using a new comprehensive
 367 analysis of the seismic profiles, integrated with the most recent works on the CB. This new
 368 stratigraphy of the CB with the description of the seismic sequences is displayed in Figure 4.

Stratigraphy	Seismic reflectors	Seismic sequences	Super - groups	Groups / Series	Context	Age max	Age min
Paleogene				Kalahari Gr.		66	
Cretaceous	R9 Base Bukungu	Seq. 7: Cret. - Paleogene	Congo	Sankuru Sup. Gr.	Drift to equator	Hot, dry	66
	R8: Base Cretaceous					Kwango Gr. Bokungu Gr. Loia. Gr. Dekese Gr.	Fluvial, ephemeral lakes
late Jurassic	R7: Base Jurassic	Seq. 6: Jura.		Kisangani Gr. (ex. Stanleyville Gr.)	Shallow lacustrine	157	132
Hiatus		Base Jurassic unconformity		Gondwana breakup		200	157
Triassic	R6: Base Triassic	Seq. 5: Karoo	Karoo	Lueki Gr. (ex-Haute-Lueki Gr.)	N-ward drift	Continental (dry, warm)	200
Permian				Lukuga Gr.		Deglacial (glacio-lacustrine)	250
Pennsylvanian	R5: Base Karoo						
Late Devonian-Early Carb. Ice House		Gondwana glaciation		Gondwana glaciation Congo Basin at South pole (3)		380	320
Paleozoic	Devonian	Seq. 4 : Red Beds	Aruwimi	Samba - Dekese Gr.	Gondwana	Post-orogenic Central Gondwana Super-fan	500
	Silurian						
	Ordovician			Inkisi - Banalia - Bianco Gr., Nama Gr.			
	Cambrian						
Pan-African deformation		Pan-African unconformity		Final Gondwana assembly (2)		580	500
Neoproterozoic	Cryogenian	R3 Base Siliciclastics	Lindi	Lokoma Gr.	Rodinia breakup	Rodinia breakup	1000
	Tonian	R2: Base Carb.-Clast.-Evap.		Seq. 3: Siliciclastics		Ituri Gr.	
Mesoproterozoic (Stenian)		R1: Base Dol. limestones	Mbuji-Mayi	BII Gr. (1)	Rodinia assembly	Carbonate ramp	1000
		R0: Top Basement		Seq. 1: Dol. limestones		BI Gr. (1)	Rifting
Top crystalline basement unconformity				Paleoproterozoic & Mesoproterozoic orogenies			
Mesoproterozoic - Archean		Acoustic Basement		Crystalline basement	Mobile belts & Archean cores		

369

370 **Figure 4.** Composite seismo-stratigraphic model integrating well and outcrop data and
371 seismic reflection profiles (Cahen et al., 1959; Esso-Zaire SARL, 1981a, 1981b; Sachse et al.,
372 2012; Linol 2013; Delvaux and Fernandez-Alonso, 2015; Fernandez-Alonso et al., 2012;
373 2015 ; Kadima et al., 2015; Roberts et al., 2015; François et al., 2017; Caillaud et al., 2017).
374 Age estimations from: François et al., 2017⁽¹⁾; Fritz et al., 2011⁽²⁾ and Torsvik and Cocks,
375 2011, 2013⁽³⁾. The thick coloured lines refer to the interpreted seismic reflectors in the
376 profiles (Figs. 7-12).

377

378 The Mesozoic and late Paleozoic strata are directly constrained by the Samba and
379 Dekese cored wells (Cahen et al., 1959, 1960), but the early Paleozoic and Proterozoic rocks
380 remain poorly dated, as they do not contain datable material, except for the basal series. Their
381 stratigraphic age is indirectly constrained by analogy with the Supergroups outcropping along
382 the margins of the basin, and with the help of the two Gilson-1 and Mbandaka-1 wells (Esso-
383 Zaire SARL, 1981a, b) and the first interpretation of the Esso-Texaco reflection seismic
384 profiles. The “infracambrian” stratigraphy was first correlated with the West Congo and the
385 Katanga Supergroups, respectively to the west and south-east of the CB (Lawrence and
386 Makazu, 1988). Daly et al. (1992) correlated it with the Lindi Supergroup (Verbeek, 1970) on
387 the northern side of the CB.

388 The seismo-stratigraphy of the CB was later revised by Delpomdor et al. (2013b) and
389 Kadima et al. (2015) with additional references to the Mbuji-Mayi Supergroup defined by
390 (Raucq, 1957, 1970). This Supergroup outcrops against the Kasai craton along the SE edge of
391 the CB in the Sankuru-Mbuji-Mayi-Lomami-Lovoy (SMLL) sedimentary basin, which is
392 considered to be a lateral equivalent of the basal units of the CB. The Mbuji-Mayi
393 Supergroup has been deposited in a intracratonic failed-rift basin with a lower clastic
394 sequence (BI) and an upper carbonate sequence (BII) indicative of a restricted marine
395 carbonate ramp environment (Delpomdor et al., 2013a). It is covered and intruded by dolerite
396 lavas, which mark the end of the deposition for the Supergroup, thus constraining its
397 minimum age. Cahen et al. (1984) obtained a K-Ar age of 940 ± 20 Ma for these dolerites. In
398 contrast, Delpomdor et al. (2013b) dated the depositional interval of the Mbuji-Mayi
399 Supergroup between 1174 ± 22 Ma and ca. 800 Ma using $\delta^{13}\text{C}$ of carbonates and obtained an
400 Ar/Ar age of 882.2 ± 8.8 Ma for the dolerites. However, recent U-Th-Pb (François et al.,
401 2017) dating shows that the diagenesis of the BI subgroup is between 1065 Ma and 1030 Ma.
402 Similarly, conventional $^{207}\text{Pb}/^{206}\text{Pb}$ ages of 1040 Ma and 1065 Ma for galena samples in

403 the upper part of the BI group were obtained by Cahen (1954), attributed to syngenetic
404 growth of galena during diagenesis. Therefore, we consider that the Mbuji-Mayi Supergroup
405 has a terminal Mesoproterozoic age and correlates with / represents the basal series of the
406 CB. Despite its age, this sedimentary sequence remained in a low-grade thermal maturity,
407 mostly restricted to the diagenesis domain (Balukiday et al., 2018).

408 We subdivided the seismic stratigraphy of the CB in a similar approach as Kadima et
409 al. (2015), but consider 8 sequences (instead of 6), overlying the crystalline/metamorphic
410 basement. Separated by the prominent Pan-African and Basal Jurassic regional
411 unconformities identified by Lawrence and Makazu (1988), a first-order subdivision in three
412 age groups can be made: (1) Meso-Neoproterozoic (sequences 0-3), (2) Paleozoic-Triassic
413 (sequences 4-5) and (3) Jurassic-Paleogene (sequences 6-7) (Fig. 4).

414

415 4.2.1 Proterozoic (sequences 0-3)

416

417 The Proterozoic sedimentary sequences formed in a succession of rift and post-rift
418 events, during the final stages of the Rodinia supercontinent amalgamation in (De Waele et
419 al. 2008).

420 The Mesoproterozoic corresponds to the syn-rift sequences:

- 421 • Sequence 0 (rift clastics): low-amplitude, discontinuous, and transparent seismic
422 patterns, which represent coarse siliciclastics, by analogy with the lower BI Group of
423 the Mbuji-Mayi Supergroup;
- 424 • Sequence 1 (dolomitic limestones): highly continuous and parallel reflectors,
425 considered an equivalent to the BII Group of the Mbuji-Mayi Supergroup. The top of
426 this sequence was reached in the Gilson well at 4503 m deep and in the Mbandaka
427 well at 3960 m. The latter stopped in interstratified massive salt, at 4350 m deep.

428

429 The Neoproterozoic is marked by continuous subsidence with carbonates and
430 siliciclastics. It has been correlated (Lawrence and Makazu, 1988; Daly et al., 1992) with the
431 Ituri (mostly carbonates) and Lokoma (siliciclastics and carbonates) groups of the Lindi
432 Supergroup, separated by the Akwokwo tillite (Verbeek,1970):

- 433 • Sequence 2 (carbonates-evaporates-clastics): transparent seismic pattern with some
434 medium to strong continuous reflectors, which could represent dominant carbonates
435 and clastics (eq. Ituri Gr.), locally with some evaporates.
- 436 • Sequence 3 (siliciclastics): banded seismic pattern of moderately continuous reflectors
437 representing dominantly siliciclastic sediments (eq. Lokoma Gr.).

438 As reported in Kadima et al. (2011b), Sr-isotope stratigraphy of the Akwokwo tillite
439 allowed researchers to postulate that it corresponds to a Sturtian event (720 ± 30 Ma), and
440 therefore, the Ituri group would be of Tonian age (1000-720 Ma), and the Lokoma group of
441 Cryogenian age (720-635 Ma).

442 Sequences 1 to 3 are locally folded, faulted, and truncated by the Pan-African
443 unconformity. The related tectonic deformation and subsequent denudation are explained as
444 the result of intraplate deformation in response to the amalgamation of the continental blocks
445 against the Congo Craton (Collins and Pisarevsky, 2005; Kadima et al., 2011a), as described
446 above.

447

448 *4.2.2 Paleozoic-Triassic (sequences 4-5)*

449

450 Below the Basal Jurassic unconformity, the whole Paleozoic and Triassic was
451 considered as a single sequence by Kadima et al. (2015). Here, it is further subdivided in two
452 sequences, corresponding respectively to a newly defined Aruwimi Supergroup (see below)

453 and the Karoo Supergroup, separated by the late Devonian – early Carboniferous Ice House
454 event, during which the CB was close to the South Pole,:

455 • Sequence 4 (Red Beds): moderate to continuous parallel reflectors, wavier on top. The
456 basal part of this sequence has been considered as equivalent to post-Pan-African
457 early Paleozoic red arkoses (“red beds”) outcropping at the periphery of the CB: the
458 Inkisi Group in the Bas-Congo (now Kongo Central) region in the DRC, but also in
459 the Republic of Congo and northern Angola (Alvarez et al., 1995; Straathof, 2011;
460 Affaton et al., 2015), the Banalia Group in the Lindi region (Tait et al., 2011), the
461 Bianco Group in Katanga (Cailteux and De Putter, 2019), and the Upper Nama Group
462 in Namibia (Blanco et al., 2011). The upper part of this sequence was reached in the
463 Samba well from 1167 m to 2038 m and in the Dekese well from 1677 m to 1856 m,
464 down to the bottom of the wells. The drill cores did not provided biostratigraphic
465 material for dating. Detrital zircons in the Inkisi Group gave a maximum age of $581 \pm$
466 18 Ma (Straathof, 2011). The age of this sequence could be up to the late Devonian,
467 just before the late Paleozoic Icehouse and late Devonian - early Permian “Karoo”
468 glaciation over Gondwana.

469 • Sequence 5 (Karoo): discontinuous to moderately continuous parallel reflectors, more
470 transparent than sequence 4. It was drilled in the Dekese well between 714 and 1677
471 m. The cores reveal alternating sequences of glacial diamictites (initially described as
472 tillites) and varval clays of late Carboniferous to early Triassic (Karoo) age (Cahen et
473 al., 1960), deposited in a large glacial lake (Linol et al., 2015). They correspond to
474 glacial - deglacial sequences under glacial to cool climate (Lukuga Group), and end in
475 a postglacial environment (Lueki Group), while the South Pole was migrating towards
476 central Antarctica (Wopfner, 1999).

477

478 Between sequences 4 and 5, the Dekese well shows a stratigraphic break at 1677 m
479 depth. The cored transition from sequence 4 to 5 shows a typical dark-brown diamictite with
480 poorly sorted irregular rock fragments up to 14 cm large overlying, in an irregular contact,
481 massive red-brown micaceous feldspathic sandstone with soft clay pebbles, locally weakly
482 calcareous and cross-bedded downwards. This evidences an episode of erosion (and therefore
483 a hiatus) before the beginning of the deglacial Karoo sequence.

484 The Karoo and Red Beds sequences are locally folded and truncated by the Basal
485 Jurassic unconformity, which is marked by a stratigraphic hiatus, localized tectonic
486 deformation and erosion related to far-field stresses caused by the Gondwanide Orogen
487 (Trouw and de Wit, 1999). This intracratonic deformation caused tectonic activations in the
488 CB (Daly et al., 1991) and in the Cape Fold Belt of South Africa (de Wit and Ransome,
489 1992).

490

491 *4.2.3 Jurassic-Paleogene (sequences 6-7)*

492

493 The Jurassic-Paleogene sequences appear as a continuous blanket over the entire
494 basin. They overlie the Basal Jurassic unconformity (Lawrence and Makazu, 1988; Kadima,
495 2011a) that truncates all the Paleozoic to Triassic sequences and correspond to the sequence 5
496 of Kadima et al (2015):

- 497 • Sequences 6 (Jurassic) and 7 (Cretaceous): parallel highly continuous reflectors
498 grading upward to wavier reflectors. They correspond to the late Jurassic Kisangani
499 and Cretaceous Dekese (sensu Linol et al., 2016), Loia, Bokungu and Kwango
500 Groups, assembled into the Congo Supergroup, and a thin Paleogene cover (Kalahari
501 Group) (Linol et al., 2016). They were deposited in tropical to equatorial conditions,
502 in shallow ephemeral-lakes, fluvial-deltaic and aeolian environments (Cahen 1954;

503 Lepersonne 1974; Cahen 1983a, 1983b, Colin, 1994; Linol et al., 2015c; Roberts et
504 al., 2015; Caillaud et al. 2017). This sequence is the best known of the CB, as it has
505 been reported in the four deep wells drilled in the CB and in outcrops and contains
506 fossils that allow biostratigraphic determinations (for the late Jurassic-Cretaceous).

507

508 In the explanatory notice of the new geological map of the DRC at 1/2.500.000
509 (Fernandez-Alonso et al., 2015), the Jurassic Stanleyville formation has been redefined as
510 Kisangani Group, and the continental Cretaceous series of the CB (Loia, Bokungu, Kwango
511 of Lepersonne, 1974) grouped into the Sankuru Supergroup. Linol et al. (2016) proposed to
512 regroup them altogether in a Congo Supergroup, which is consistent with the seismic
513 stratigraphy, since they all appear as a single macro sequence, without seismic
514 discontinuities.

515

516 **5. Refraction seismics**

517

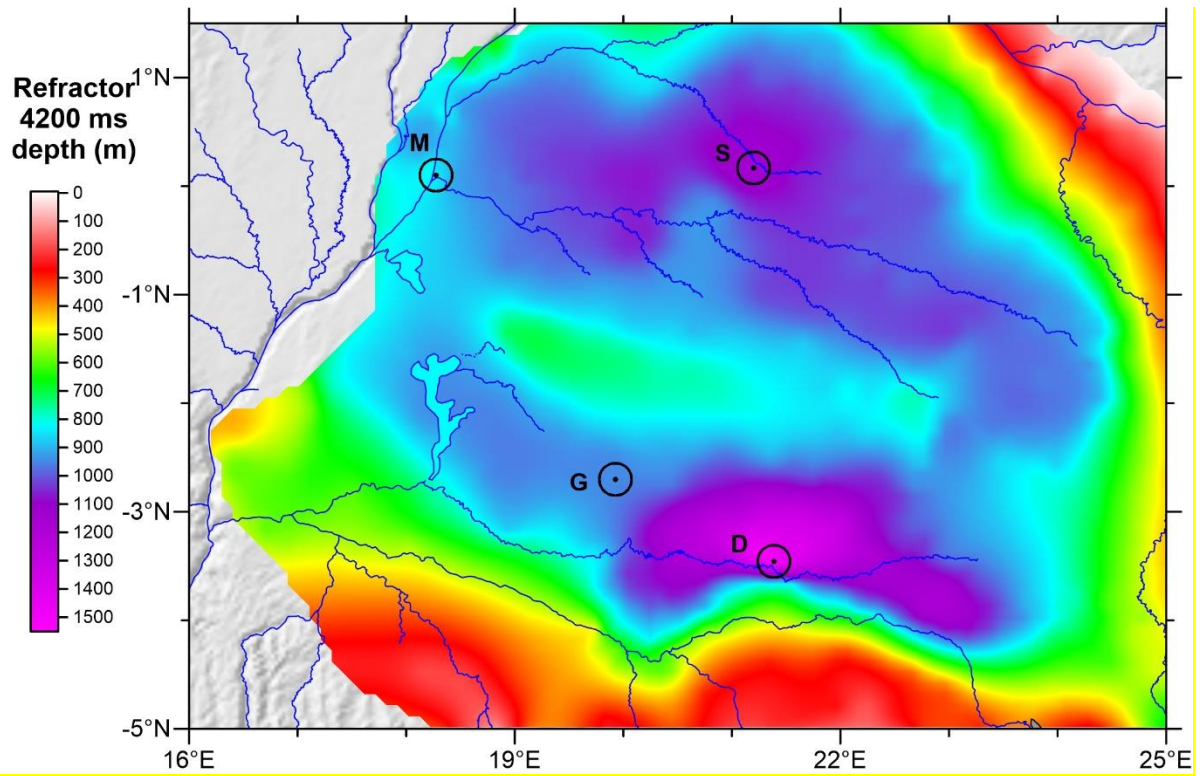
518 Three field geophysical campaigns were conducted by the REMINA in the CB
519 between 1952 and 1956 (Evrard, 1957). Among others, a refraction seismic survey was
520 carried out with 117 points regularly positioned over the entire CB. The depth of refractors
521 was obtained for these points, and isobaths were traced on a map (Evrard, 1960).

522 The sedimentary sequences characterized by velocities less than 3600 m/s were
523 considered by Evrard (1957; 1960) as “cover series” (Jurassic to Paleogene, our sequences 5
524 and 6) on the base of the correlations with outcropping series and the Samba and Dekese
525 cored wells. The 4200 m/s reflector was correlated with the top of the red arkoses (Red Beds)
526 in the northern part of the basin and the top of the Triassic Lueki and Permian Lukuga groups
527 (Karoo) in the southern part (our sequence 5). The Red Beds define our seismic sequence 4,

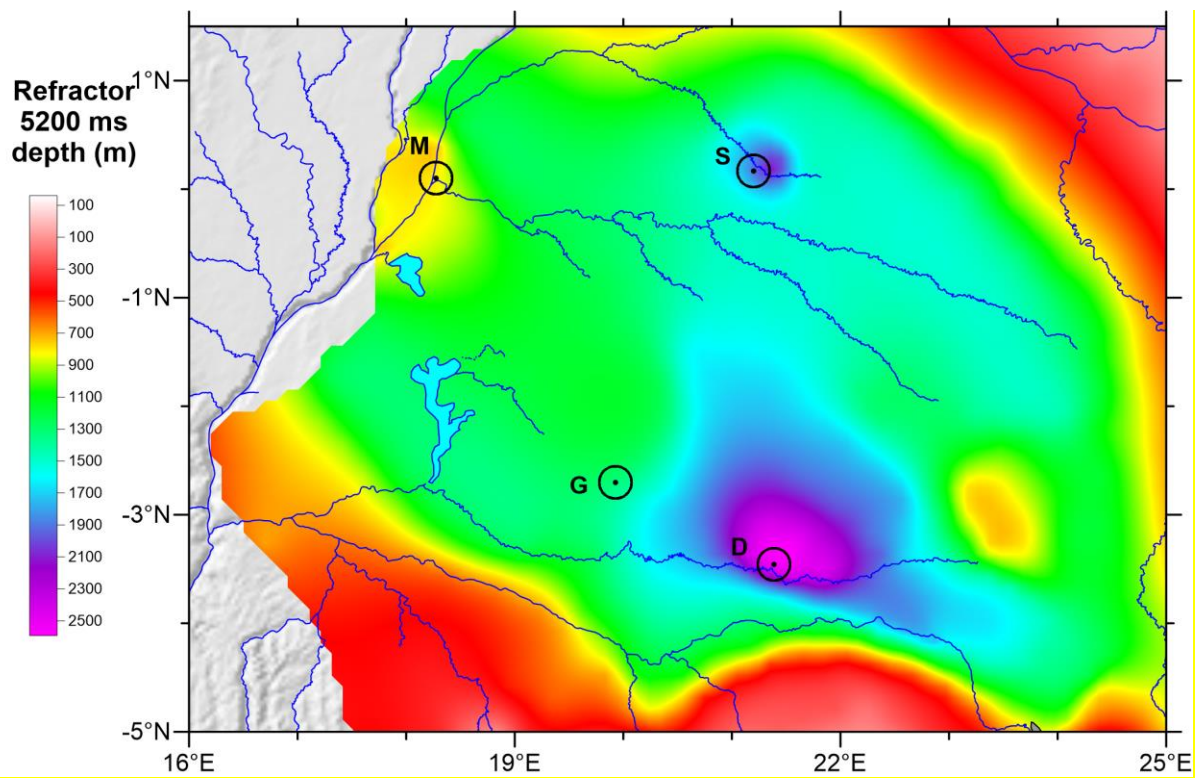
528 which was considered at that time as the top of the Neoproterozoic “substratum” (Veach,
529 1935; Cahen, 1954; Lepersonne, 1977). Evrard (1957) also recognized the ambiguity of the
530 nature of the substratum deduced from the sole measured velocities. An important outcome of
531 that survey was to recognize that the basin is likely much deeper than originally thought.

532 Here, we digitized the isobaths of the 4200 m/s and 5200 m/s refractors and
533 interpolated them using a standard kriging method (SURFER, Golden Software package)
534 with a grid spacing of 0.1 degree. The interpolated maps (Fig. 5a, b), show the internal
535 structure of the basin, with a WNW-ESE structural high separating the CB into two parts (the
536 Kiri High), coinciding with the axial magnetic zone (Kadima et al., 2011a; Maddaloni et al.,
537 2020). Two main depocenters were identified, that motivated the drilling of the Samba and
538 Dekese wells (Fig. 5a, b). The southern limit of the deep part of the basin remarkably
539 corresponds to the limit of the Kasai craton under the sediment cover, as defined using the
540 aeromagnetic data (Maddaloni et al., 2020).

541



542



543

544 **Figure 5.** Refraction seismics (kriging interpolation of the data from Evrard 1960). Depth of
 545 the (a) 4200 ms and (b) 5200 ms refractor. Black circles show the location of the four wells
 546 drilled in the study area: D=Dekese; G=Gilson-1; M=Mbandaka-1; S=Samba.

547

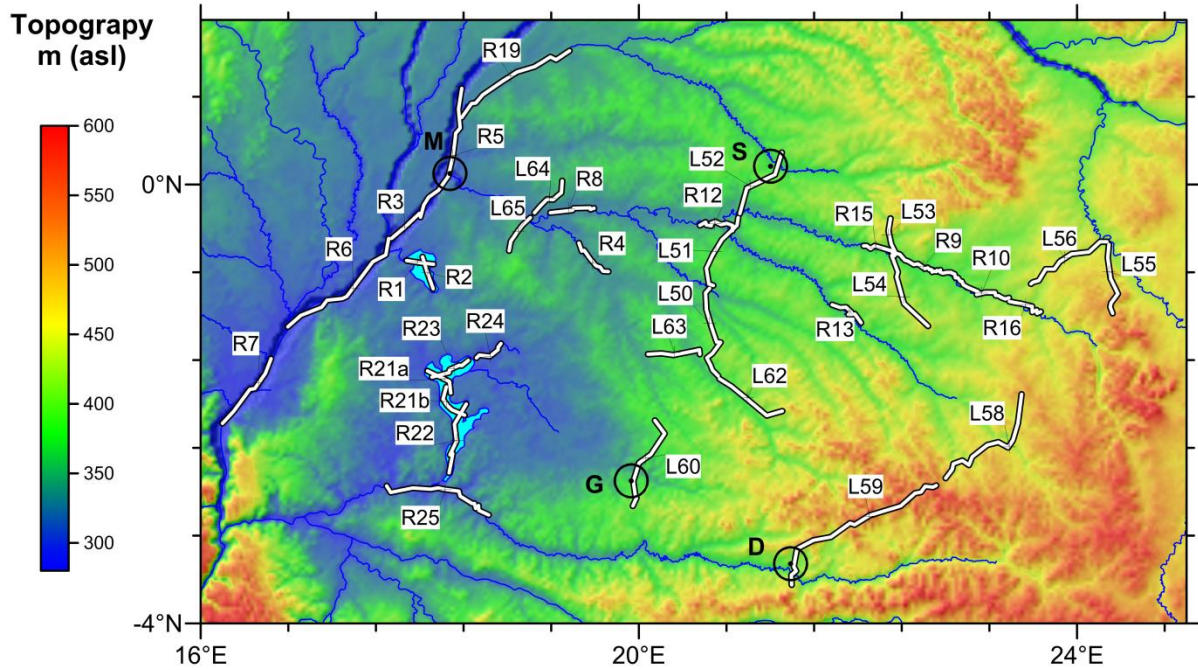
548 **6. Reflection seismics**

549

550 As part of a second field exploration campaign, an extensive coverage of the central
551 part of the CB by reflection seismic profiles has been performed by the Compagnie General
552 de Géophysique in 1974. They were recorded with sources at 100 m interval consisting of
553 groups of 3 vibrators 12.5 m apart, and geophones in series spaced by 5 m. The records were
554 processed by the Geophysical Development Corporation (Houston, Texas) in 1986.
555 Unfortunately, the original (digital) records are lost. The reflection profiles from scanned
556 paper copies and their location map come from Kadima (2011).

557 There are 35 profiles for 2623 km in total (Fig. 6), 21 deployed along rivers and
558 lakes (R profiles) and 14 along roads (L profiles). They were shot mainly at a high angle to
559 the Kiri High, in order to better image the structure of the basin, with also some transversal
560 lines. They cover in a rather homogeneous way the central part of the basin, from 1°N to
561 3.5°S and from 16.5°E to 24°E. In this work, the profiles were registered and analyzed using
562 the Golden Software SURFER program. The geographic coordinates (WGS84 projection) of
563 the seismic lines were digitized and the line lengths calibrated accordingly. In a reverse
564 operation, the digitized points of the profile interpretations were re-located as geographic
565 coordinates. The Common Depth Point boxes (CDP) giving the relation between TWT,
566 seismic velocity and depth were used to compute depth-time curves for each profile by a third
567 degree polynomial interpolation, needed for converting TWT to depth. For each profile, we
568 used the most central CDP boxes as average for the entire profile.

569



570

571 **Figure 6.** Topography map of the CB using (ETOPO 1, Amante et al., 2009). Black labels
 572 show the names of the seismic reflection profiles (white broken line). The hydrological
 573 system is displayed in blue. Black circles show the location of the four wells drilled in the
 574 study area: D=Dekese; G=Gilson-1; M=Mbandaka-1; S=Samba.

575

576 A preliminary interpretation of the seismic reflection profiles, calibrated with the
 577 Mbandaka-1 well, identified three major seismic units separated by major unconformities
 578 (Kadima et al., 2011a). Based on the interpretation of all available seismic reflection profiles
 579 inside the CB, we can identify now ten seismic reflectors (R0 – R9), of which seven can be
 580 recognized over the entire basin and two correspond to major tectonic unconformities. They
 581 define the eight (S0 - S7) seismic sequences overlying the acoustic basement (Fig. 4).

582 Some profiles were shot in series and thus have been assembled into combined
 583 profiles, generally calibrated by one or two wells. Some profiles intersect each other. From
 584 NW to SE, we distinguish:

- 585 • the SSW-NNE combined profile (R7-6-3-5-19), along the Congo River and calibrated
586 by the Mbandaka 4350 m deep well;
- 587 • a group of profiles recorded along roads and rivers, near Ingende (L64-65, R4, R8);
- 588 • the series of profiles along Lake Tumba (R1, R2) and Lake Mai-Ndombe (R22, R24),
589 together with profile R25 along the Lukenie river;
- 590 • the N-S Gilson-Samba combined land profile (L60-50-51-52), calibrated by the
591 Gilson (4563 m deep) and Samba (2039 m deep) wells and intersected by three E-W
592 oriented profiles (R12, L63, L62);
- 593 • a series of river and land profiles in the NE part of the basin, along the Tshuapa River
594 between Bokungu and Ikela (R15-9-10-16) and across it (L53-54), along the Lomela
595 River (R13) and near Opala on the Lomami River (L55, L56);
- 596 • two long WSW-ENE profiles (L59-L58), calibrated by the Dekese well (1856 m
597 deep).

598

599 All the seismic profiles with the raw seismic line, the interpreted seismic lines and the
600 depth-converted lines are displayed in the supplementary information S1. In the following
601 sections, we present only detailed portions of some seismic profiles which illustrate the key
602 features of the structure and stratigraphy of the CB.

603

604 *6.1 Congo River seismic profile R7-6-3-5-19*

605

606 This combined seismic profile shot along the Congo River shows an alternation of
607 highs and deep depressions (up to nearly 10 km deep), corresponding from SW to NW to the
608 Bololo Basin, Inongo High, Lokoro Basin, Kiri High and Busira Basin (Fig. 7). Line R5, as
609 shown in Kadima et al. (2011a), has been used to calibrate the stratigraphy of the CB using

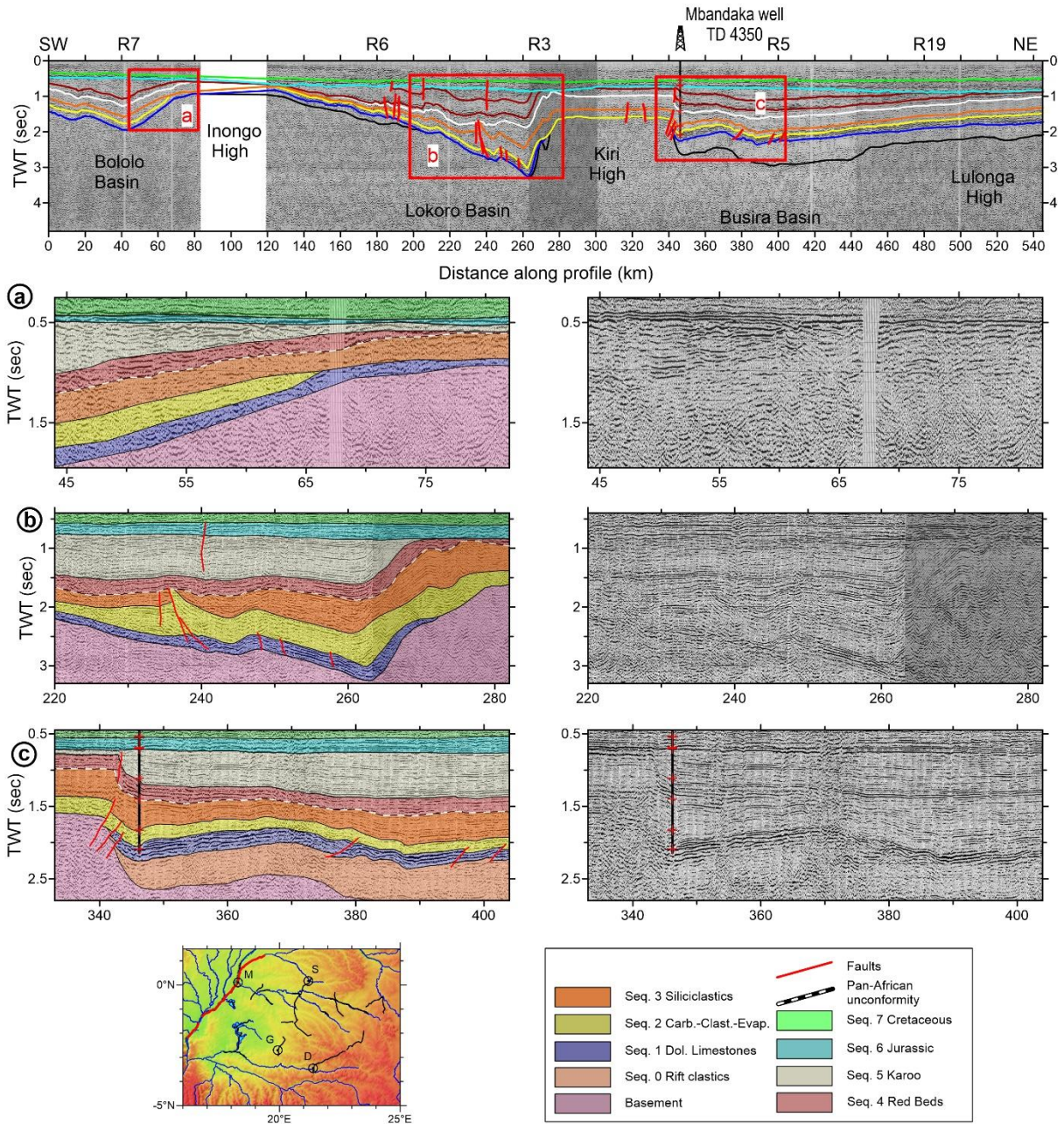
610 the Mbandaka well in the Busira Basin (Fig. 7c). This profile shows on the left (northern)
611 side the full succession of the 8 seismic sequences overlying the acoustic basement in a sub-
612 horizontal and undisturbed way. There are a series of small reverse faults affecting the
613 Proterozoic layers below the Pan-African unconformity, while the Paleozoic to Triassic
614 sequences are only locally dislocated by younger faults.

615 The highs are overlain by a regular cover of mostly undisturbed post-rift sediments,
616 about 3 km thick over the Kiri High (Figs 7b, c), thinning over the Inongo High (Fig. 7a).
617 Over these structural highs, the syn-rift sequences (0, 1), as well as the entire Paleozoic to
618 Triassic sequences (4, 5) are almost absent. The rift clastics (sequence 0) are absent in the
619 Lokoro basin, south of the Kiri High (Fig. 7b), while they reach up to 23 km thick in the
620 Busira Basin, north to the Kiri High (Fig. 7c). In contrast, the dolomitic limestones (sequence
621 1) are present in the basins on both side of the Kiri High. Detailed seismic interpretation (Fig.
622 7b, c) suggest that the synrift sequences do not onlap against the high and/or are not
623 condensed over its top. The sudden transitions with the adjacent Lokoro (Fig. 6b) and Busira
624 Basins (Fig. 7c) were interpreted by Daly et al. (1992) as controlled by normal faulting
625 during the initial failed rift stage, but the seismic profiles do not show clearly the existence of
626 such normal faults.

627 Above the Kiri High (Figs. 7b, c), there are about 2 km of Neoproterozoic sediments
628 (sequences 2 & 3), directly overlying the crystalline basement. The Red Beds (sequence 4)
629 overly the Pan-African unconformity with a similar thickness in the Kiri High as in adjacent
630 basins, except for the southern side, where they were probably partly eroded. The Karoo
631 sediments (sequence 5) , which form a thick layer in all the basins, are instead only present
632 over the Kiri High as a thin sheet on its northern side and are absent on its southern side. The
633 Pan-African unconformity appears weakly marked and passively deformed (Figs. 7b, c). In
634 contrast, the Basal Jurassic unconformity truncates the Paleozoic sediments over the Kiri

635 High and marks the expansion of the basin by regular sedimentation over the deformed pre-
636 Jurassic part of the basin. This pattern led Daly et al. (1991, 1992) to suggest an ‘inversion’
637 of the Kiri High in the late Paleozoic, controlled by the pre-existing “rift” structures inherited
638 from the initial opening of the CB. The latter would have caused uplift of the Kiri High and
639 overlying sediments, which were partly eroded before the deposition of the Jurassic
640 sediments. As we have no clear evidence for rift structure in the seismic profiles, we prefer to
641 consider these structures as a product of compressional reactivation instead of inversion.

642 All the tectonic structures identified along the combined line remained inactive since
643 the Jurassic, as indicated by the Jurassic to Paleogene layers lying undisturbed over the Basal
644 Jurassic unconformity over the entire line.



645

646 **Fig. 7.** Interpreted seismic profile of combined river lines R7-6-3-5-19 along the Congo River
 647 with details of three zones (a-c). Upper part: interpreted profile, a-c: details with
 648 superimposed interpretation (left) and raw profile (right). Bottom: profile location and
 649 legend. Colour of seismic horizons as in Figure 3.

650

651 *6.2 Gilson-Samba seismic profile L60-50-51-52*

652

653 This seismic profile with combined land lines, calibrated by the Gilson-1 and Samba
654 wells, provides a general SSW-NNE section across the central part of the CB (Fig. 8). It
655 shows a significant lateral variability of the depth of the basement and thickness of the
656 sedimentary sequences up to the Basal Jurassic unconformity. There is unfortunately a gap in
657 seismic recording in the vicinity of the Gilson well but recording was good at the Samba
658 well.

659 On the southern extremity of the profile, just south of the Gilson well, a zone of tectonic
660 deformation caused uplift of the northern compartment (with the Gilson well area) relative to
661 the southern extremity of the profile (Fig. 8a). It affected the entire Proterozoic and Paleozoic
662 series causing a general bending of the Pan-African unconformity, amplified by top-to-the-
663 south reverse and thrust faulting. In contrast, the Basal Jurassic unconformity is not affected.
664 The Karoo series appear to thicken markedly at the southern extremity of the profile. We
665 have indicated (Fig. 8a) the possible limit between the Permian Lukuga Group and the
666 Triassic Lueki Group, based on the interpretation of the Gilson well. However, this is poorly
667 constrained due to the lack of biostratigraphic control (Linol et al., 2015 b) in this well.

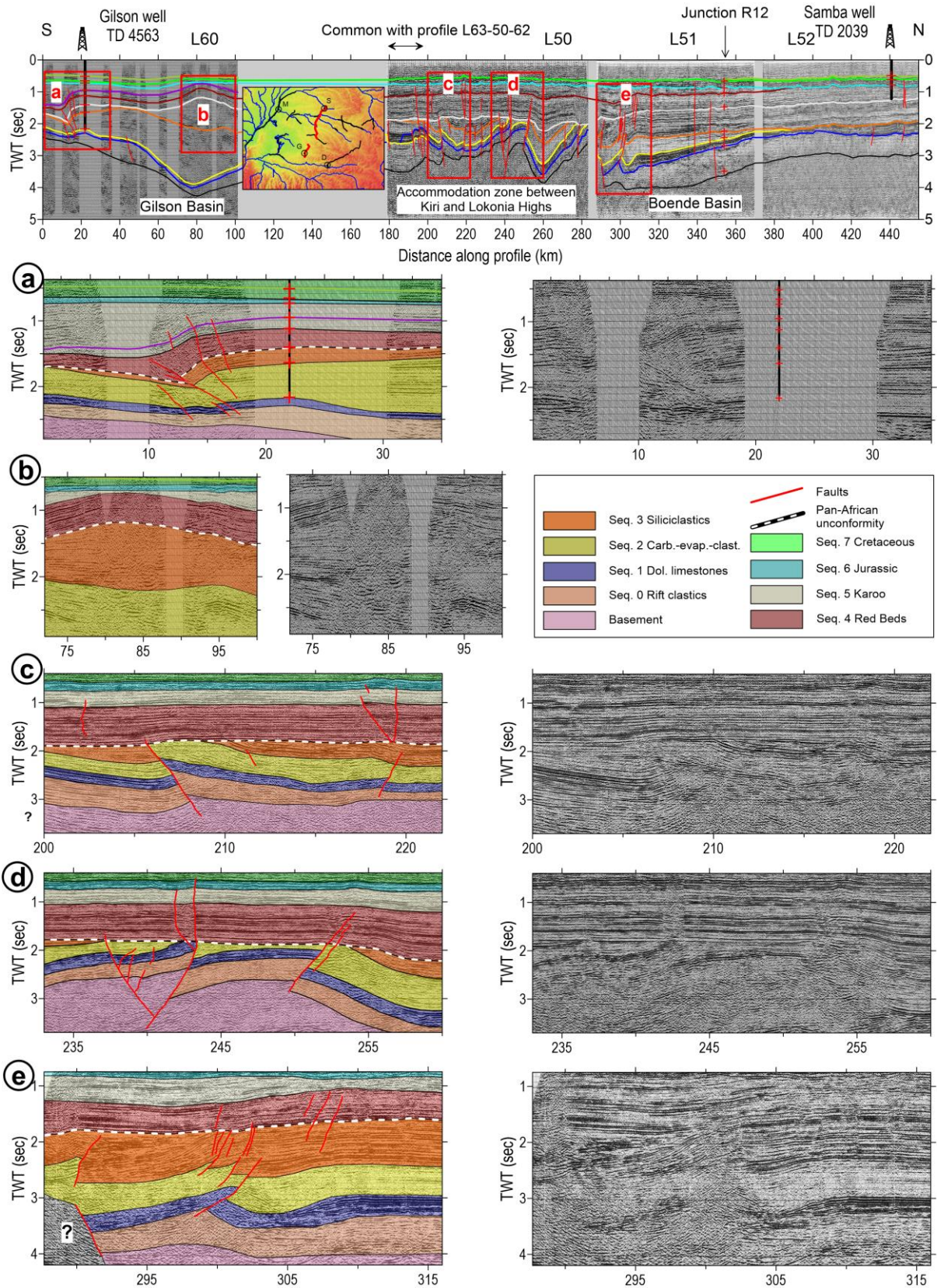
668 Between km 60 and 100 along profile L60, the basement and the overlying very thin rift
669 clastics and dolomitic limestones (sequences 0-1) are deflected downward and deepen up to a
670 maximum depth of about 11 km (Fig. 8b). This area corresponds to an important
671 overthickening of the Neoproterozoic series (sandstones and shales, rare limestones in the
672 well) over a distance of 50 and 100 km along the profile. The Karoo sediments appear
673 truncated by the Basal Jurassic unconformity.

674 After a hiatus in the profile, the N-trending line L50 shows an intensely folded and
675 faulted crystalline basement and overlying Proterozoic series (sequences 0-3), truncated by
676 the Pan-African unconformity (Figs. 8c, d). This one, in turn, has been (more locally)
677 deformed in continuity with the deformations underneath. This illustrates the presence of

678 well-developed Pan-African compressional structures (reverse faulting and folding) in the
679 center of the basin and suggests also a reactivation and influence of these structures on the
680 further evolution of the basin during Paleozoic-Triassic times (sequences 4-5). Above the
681 Basal Jurassic unconformity, the Jurassic to Paleogene sediments (sequences 6-7) are mainly
682 concordant with the underneath ones.

683 The Samba well in the northern extremity of the section (line L52) fixes the limit
684 between the Jurassic-Paleogene sequence (sequence 6) and the Red Beds (sequence 4) at
685 1167 m, since the Karoo (sequence 5) is entirely missing. The red sandstones present until the
686 well bottom (2038 m) represent the upper part of the Red Beds (the Samba-Dekese Group as
687 defined below). We identified a pronounced reflector just below the bottom of the Samba
688 well which we correlate with the Pan-African unconformity recognized on the left (southern)
689 side of line L51 (Fig. 8e). On this segment, the dolomitic limestones and overlying
690 Neoproterozoic series are affected by thrusting deformation, truncated by a prominent
691 reflector in continuity with the Pan-African unconformity seen in line L50 (Figs. 8c-d).

692



697 location map, Right of detail zone b: legend. Part of seismic line L50 is common with profile
698 L63-50-62 (Fig. 9, details in 9b). Colour of seismic horizons as in Figure 4.

699

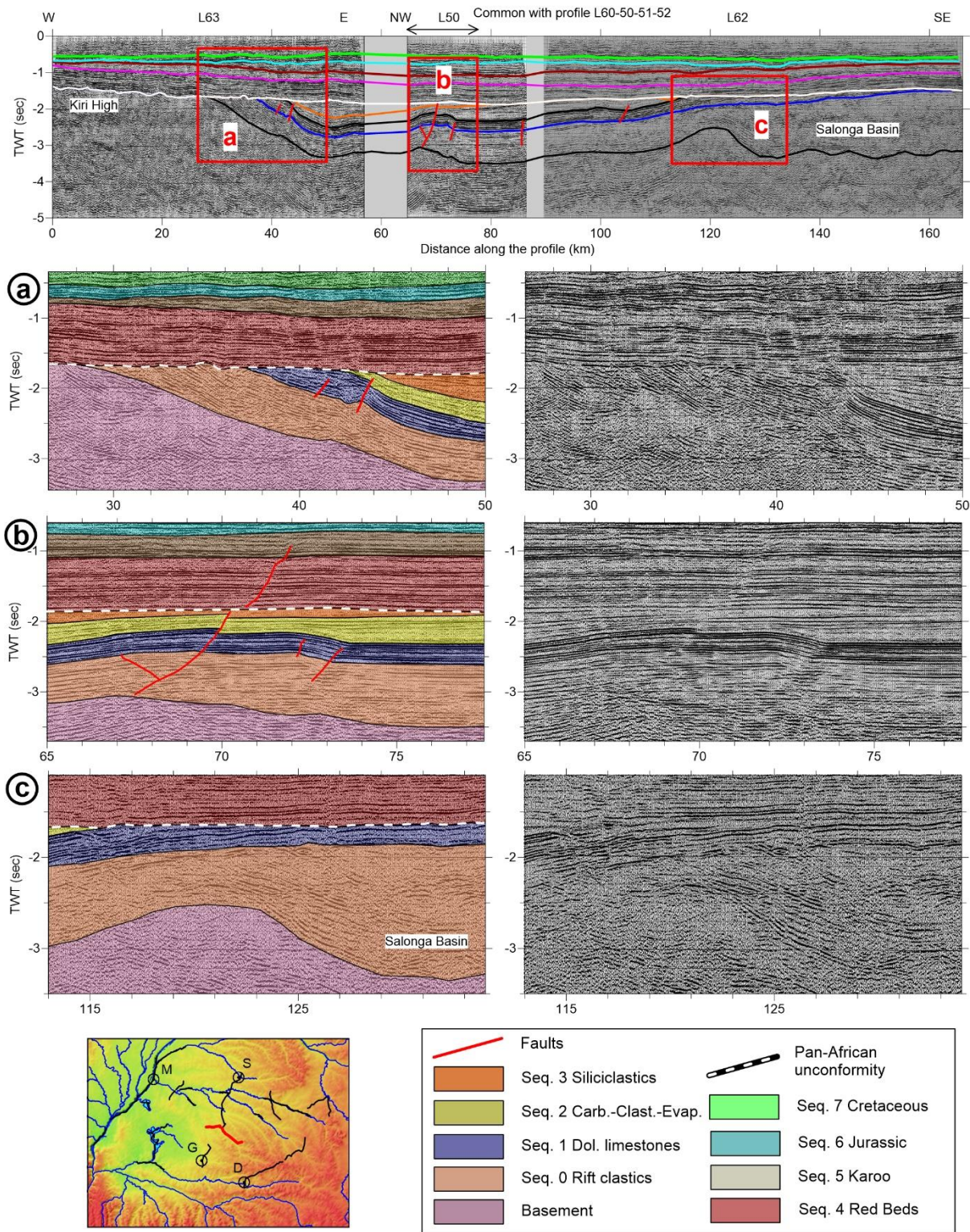
700 *6.3 E-W combined seismic profile L63-50-62*

701

702 This seismic profile with combined land lines cross-cuts the previous one in a general
703 E-W orientation (Fig. 9), with part of line 50 in common with profile L60-50-51-52. It shows
704 the Pan-African uniformity truncating the entire Proterozoic sequences (sequences 0-3). The
705 Neoproterozoic sequences (sequences 2-3) are present only in the central part, as a large and
706 flat depression. On the western side, the Red-Beds (sequence 4) rest directly over the
707 basement (Fig. 9a), and over the late Mesoproterozoic dolomitic limestones (sequence 1) on
708 the eastern side (Fig. 9c). The rift clastics (sequence 0) are particularly well developed in the
709 central part of the profile and seem to strongly thicken on the SE extremity of line 62. Here,
710 the deep reflectors are not so clear, but we see around 120 km along the profile, an upwarp
711 deflection of the seismic reflector which then deepens strongly until 130 km (Fig. 9c). This
712 implies that there should be a deep depocenter (Salonga Basin) that developed during the
713 initiation of the basin and accomodated a great thikness (4-5 km) of rift clastics.

714 In line L50, the dolomitic limestones layer appears slightly deformed by fault-assisted
715 kinking (Fig. 9b). This deformation does not affect the Pan-African unconformity, but some
716 possible faulting could also exist above it, in the Red Beds and the Karoo.

717



718

719 **Fig. 9.** Interpreted seismic profile of combined land lines L63-50-62 with details of three
 720 zones (a-c). Upper part: interpreted profile, a-c: details with superimposed interpretation (left)
 721 and raw profile (right). Bottom: location map and legend. Part of seismic line L50 is common
 722 with profile L60-50-51-52 (Fig. 8). Colour of seismic horizons as in Figure 4.

723

724 *6.4 Dekese seismic profile L59*

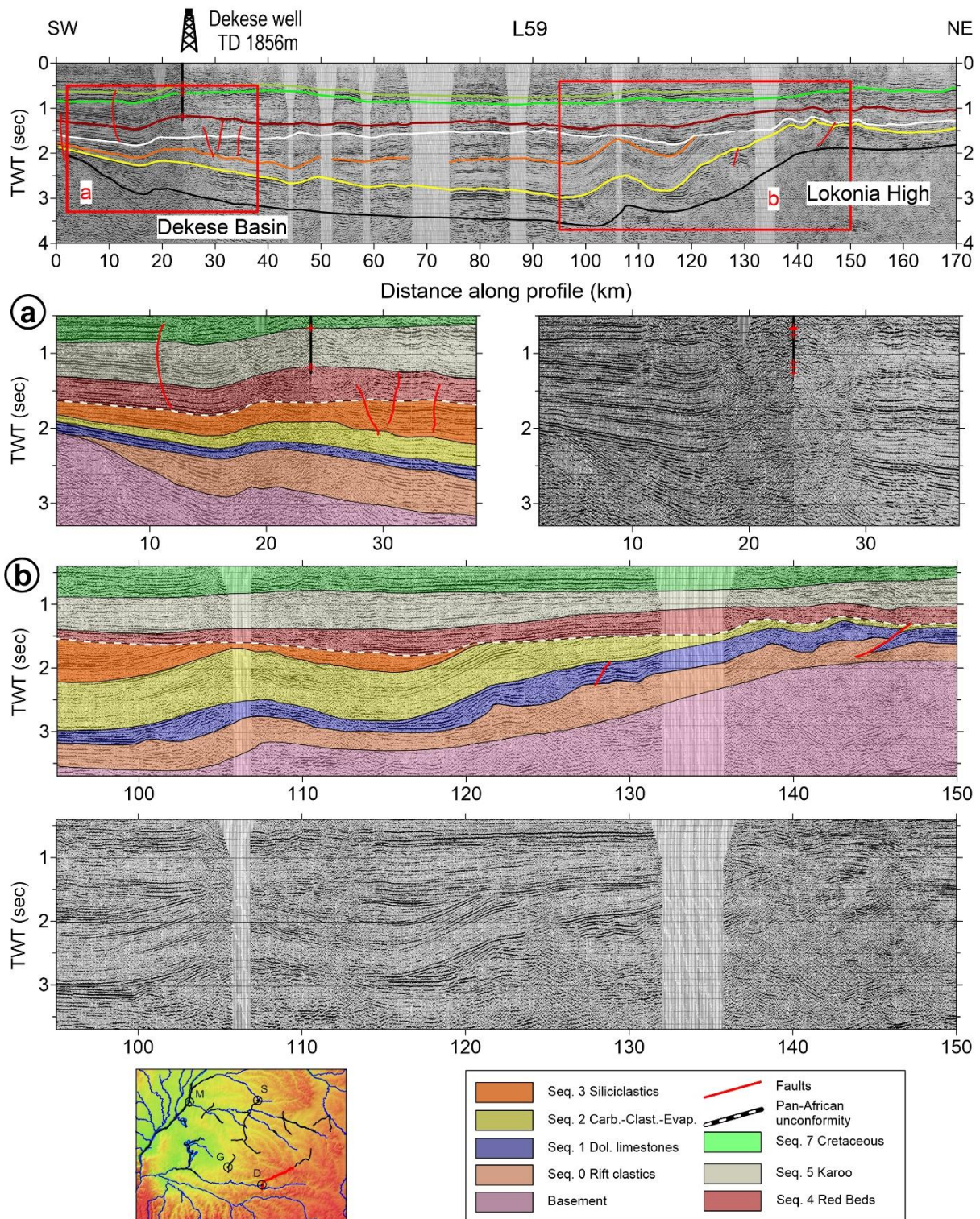
725

726 This WSW-ENE oriented profile, located in the southeastern part of the CB (Fig. 10),
727 passes through the Dekese well. The rift clastics reach a thickness of more than 2.5 km in
728 proximity of the Dekese well (Fig. 10a). This depocenter, named Dekese basin, reaches a
729 maximum depth of about 8 km. Between 100 and 130 km along the profile, the Pan-African
730 unconformity truncates the folded Neoproterozoic sequences (Fig. 10b). Some small-scale
731 compressional deformation (folds and reverse faults) affects the carbonate level (sequence 1),
732 suggesting it behaved during deformation as a mechanically strong layer between weaker
733 layers (km 140-150 long the profile, Fig. 10b).

734 The Dekese well, on the SW edge of the profile, is located in a highly perturbed zone
735 of the profile, most likely corresponding to a zone of intense tectonic deformation (Fig. 10a).
736 The drill cores of the well show locally intense deformation by folding and faulting, mainly
737 in the Karoo sequence, where some large parts reach verticality. These deformation signs
738 have sometimes been interpreted as due to glacio-tectonic movements (Giresse, 2005; Linol
739 et al., 2015b), but a detailed re-examination of the structures in the cores suggests rather a
740 tectonic origin (Delvaux et al., 2015). It caused also the uplift of the northern part relative to
741 the southern part, involving the basement as seen in the southern extremity of line L60 near
742 the Gilson well.

743 The syn-rift sediments (sequences 0-1) are reduced to a thickness of few hundred
744 meters in the SW side of the profile (toward the Kasai craton). They seem partly eroded
745 under the Pan-African unconformity on NE side (Lokonia High). The sedimentary sequences
746 deposited above the Pan-African unconformity appear almost undisturbed.

747



749

750 **Fig. 10.** Interpreted profile of land seismic lines L59 through the Dekese well, with details of
 751 two zones (a-b). Upper part: interpreted profile, a-b: details with superimposed interpretation
 752 (left/above) and raw profile (right/below). Bottom: location map and legend. Colour of
 753 seismic horizons as in Figure 4.

754

755 *6.5 Tshuapa River seismic profile R15-9-10-16*

756

757 This combined WNW-trending profile of rivers lines (Fig. 11) is located in the
758 northeastern part of the CB, along the Tshuapa River between Boende and Ikela. It shows a
759 long-wavelength anticlinal folding of the entire Precambrian-Paleozoic series (sequences 0-
760 5), which appears regularly stratified. The anticline forms an elevation (Maringa Ridge),
761 which has been truncated by the Basal Jurassic unconformity. It extends laterally in the
762 direction of the L53 and L54) seismic lines and thus has a NNW-SSE axis. The southeastern
763 flank of the anticline shows minor faults and reverse faults in the dolomitic limestones level
764 (sequence 1). In the central and southeastern part of the profile, the sedimentary sequences lie
765 horizontally undisturbed, forming the Lomami basin.

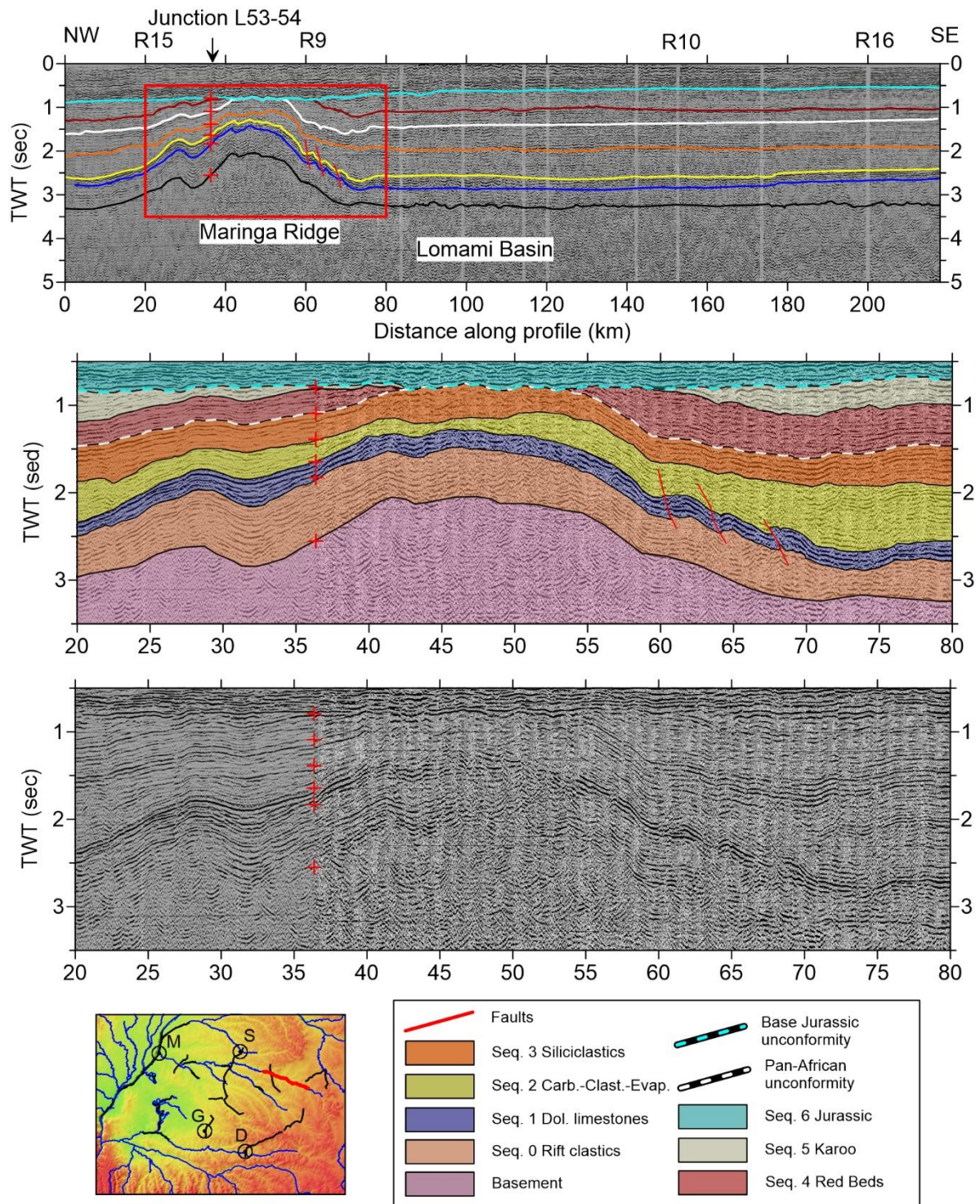
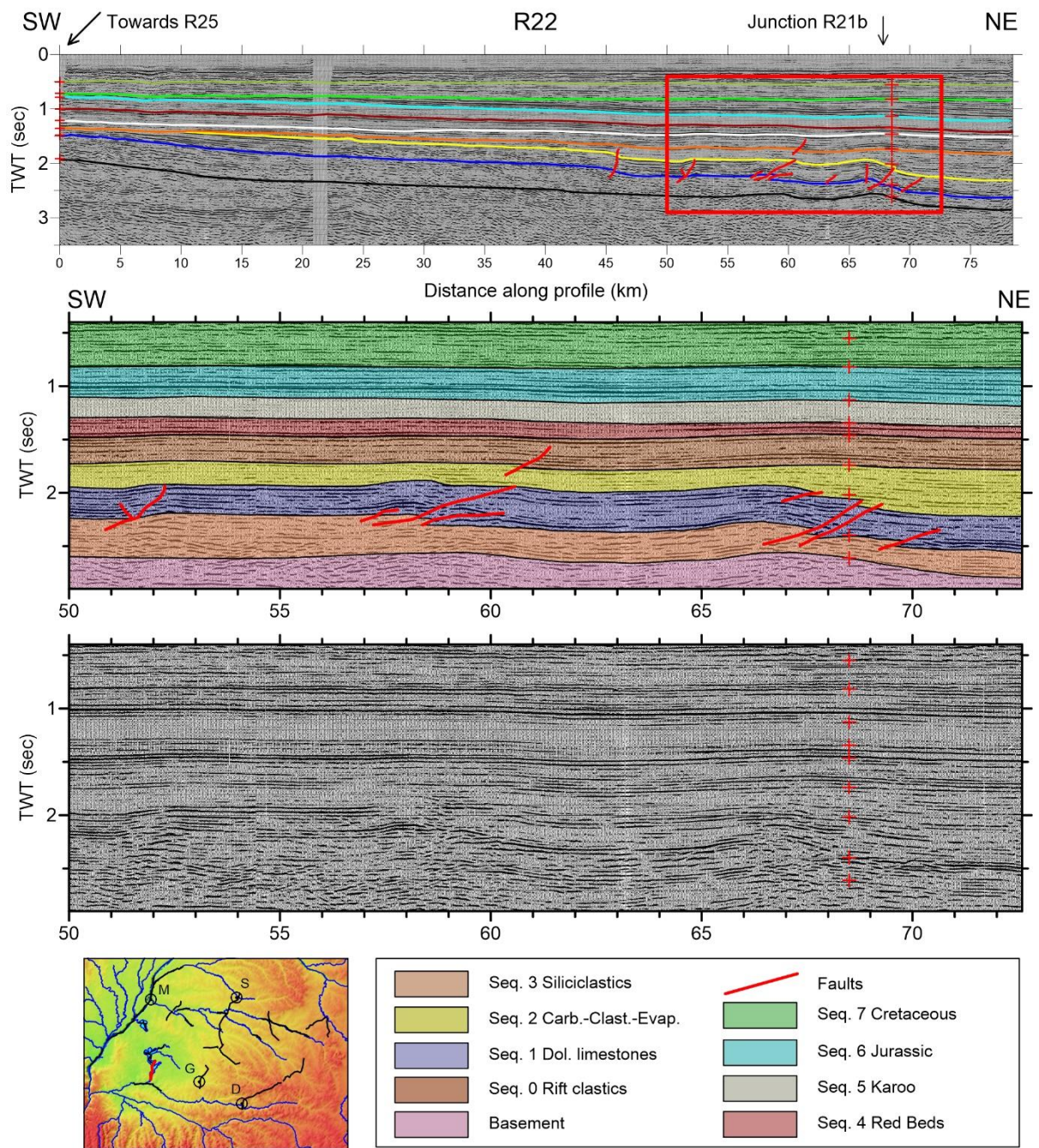


Fig. 11. Interpreted seismic profile of composite river lines R15-R9-R10, with detail of the zone around the Maringa Ridge anticline. Upper part: interpreted profile, middle part: details with superimposed interpretation, lower part: raw profile. Bottom: location map and legend. Colour of seismic horizons as in Figure 4.

772 *6.6 Lake Mai-Ndombe seismic profile R22*

773

774 Along Lake Mai-Ndombe in the southern part of the CB, the NNE-trending line R22
775 (Fig. 12), shows a northeastward deepening of the basement from about 3.5 to 6.5 km and of
776 the overlying sedimentary sequence. In the northeastern part of the profile, until the junction
777 with line R21b, we observe a pattern of small faults dislocating the late Mesoproterozoic
778 dolomitic limestones (sequence 1) and overlying Neoproterozoic sediments, while the
779 sedimentary sequences above the Pan-African unconformity lie undeformed. This suggests
780 that the carbonates layer formed a more competent layer relative to the surrounding ones
781 during the Pan-African deformation.



782

783 **Fig. 12.** Interpreted profile of land seismic line R22 with detail of the deformed dolomitic
 784 limestones sequence. Upper part: interpreted profile, middle part: details with superimposed
 785 interpretation, lower part: raw profile. Bottom: location map and legend.

786

787 **7. Model of the sedimentary sequences of the Congo Basin**

788

789 All the interpreted seismic horizons converted to depth were interpolated using a
790 standard kriging method (SURFER, Golden Software package) with a grid spacing of 0.05
791 degree (about 5.5 km) to generate depth maps of the main seismic horizons, R0-R5 & R7
792 (Figs. 13, 14). The R6, R8 and R9 seismic horizons, dividing the Karoo and the Mesozoic,
793 have not been recognized in all seismic lines and thus have not been computed. The thickness
794 of the seismic sequences (isopach maps) has been further derived by making the difference
795 between the depth maps of the top and bottom layers. They were computed for each
796 sequences (S0 to S7, Fig. 15) and for groups of sequences obtained considering the 4 main
797 stages of evolution of the basin (S0-1, S2-3, S4-5 and S6-S7, supplementary information).
798 They reveal a different behavior of the basin during the successive stages of evolution, with a
799 progressively decrease in the influence of the initial rift structure.

800 Both depth and isopach maps are limited to the data available, between 1.4°N-3.8° S,
801 16°E-24.5°E.

802

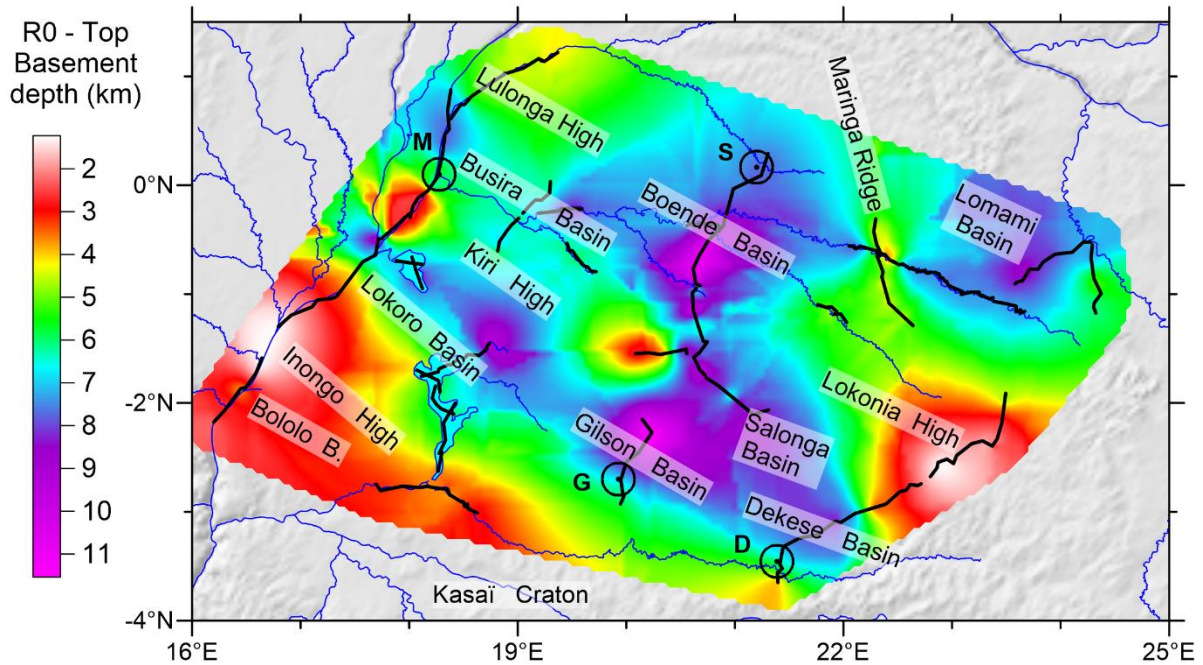
803 *7.1 Top of basement architecture and main sedimentary depocenters*

804

805 The top of the basement depth (reflector R0) shows significant variations, with major
806 and minor elevated zones, alternated by several sedimentary depocenters (Fig. 13). The
807 WNW-ESE Kiri High, well expressed between the Congo River and Line 63 in the center of
808 the basin, separates the CB into two parts. It appears formed by two domes, in the places
809 constrained by data, separated by a saddle, where there are no data. We interpret this last
810 feature as an artefact of the interpolation and assume that the Kiri High is probably a
811 continuous high between the Congo River and Line 63. In the eastern side of the basin, the
812 Lokonia High appears in a similar orientation as the Kiri High, but with a shift to the north.

813 The relay zone between the two is illustrated by the intensely deformed seismic line L50 Line
 814 (Fig. 8).

815



816

817 **Fig. 13.** Main tectonic structures identified at the depth of the top of the basement. Broken
 818 white lines show location of the seismic reflection profiles. Black circles show the location of
 819 the four wells drilled in the study area: D= Dekese; G=Gilson-1; M=Mbandaka-1; S=Samba.

820

821 The NW-SE oriented central elevated zone, formed by the Kiri and Lokonia Highs,
 822 separates the CB into two major depocenters. On the SW side, the depocenter is defined by a
 823 continuous alignment of three basins (Lokoro, Gilson, and Dekese Basins), with a maximum
 824 depth of 11.5 km observed in the Gilson Basin. It is limited to the SW by the Inongo High
 825 and, further to the south, by the Kasai craton, which rises below the Karoo to the Cretaceous
 826 cover. The Lokoro Basin is composed of two main depocenters, one very large in the south (~
 827 10 km deep) and another smaller and shallower (~ 8 km deep) in the north. The deep Salonga
 828 Basin lies in the alignment of the Kiri High, after the relay zone between the Kiri and
 829 Lokonia Highs.

830 On the northern side of the axial zone, the Busira Basin (7.6 km deep) is flanking the
831 Kiri High. The large Boende basin (10.6 km deep), well evidenced in the seismic line L51, is
832 separated from the Gilson Basin by the Kiri High - Lokonia High relay zone. The Lomami
833 Basin (8.6 km deep) on the NE extremity is separated from the Boende Basin by the Maringa
834 Ridge. The latter appears to result from an anticlinal folding, followed by erosion of the
835 whole pre-Jurassic series before the deposition of the Jurassic-recent series (lines R15-9-10-
836 16, Fig. 11). The Boende and Lomami Basins could therefore have been formed initially as a
837 single large basin.

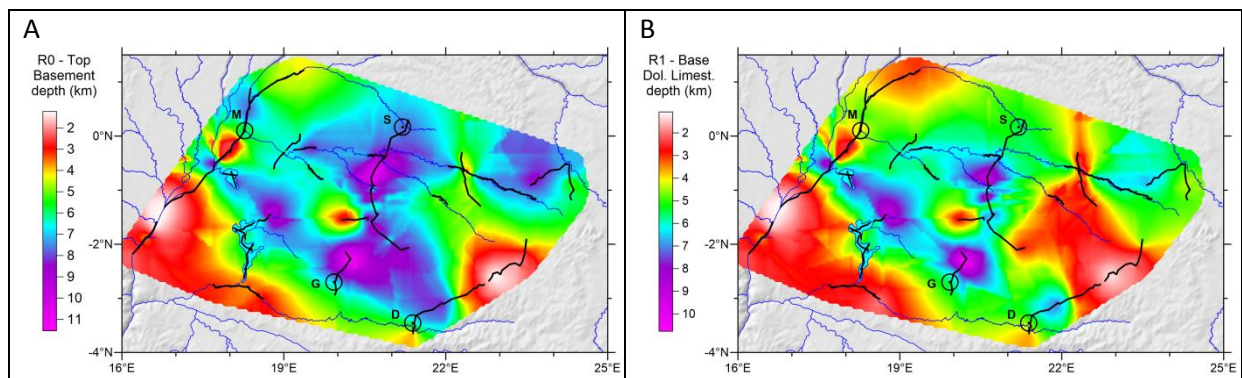
840

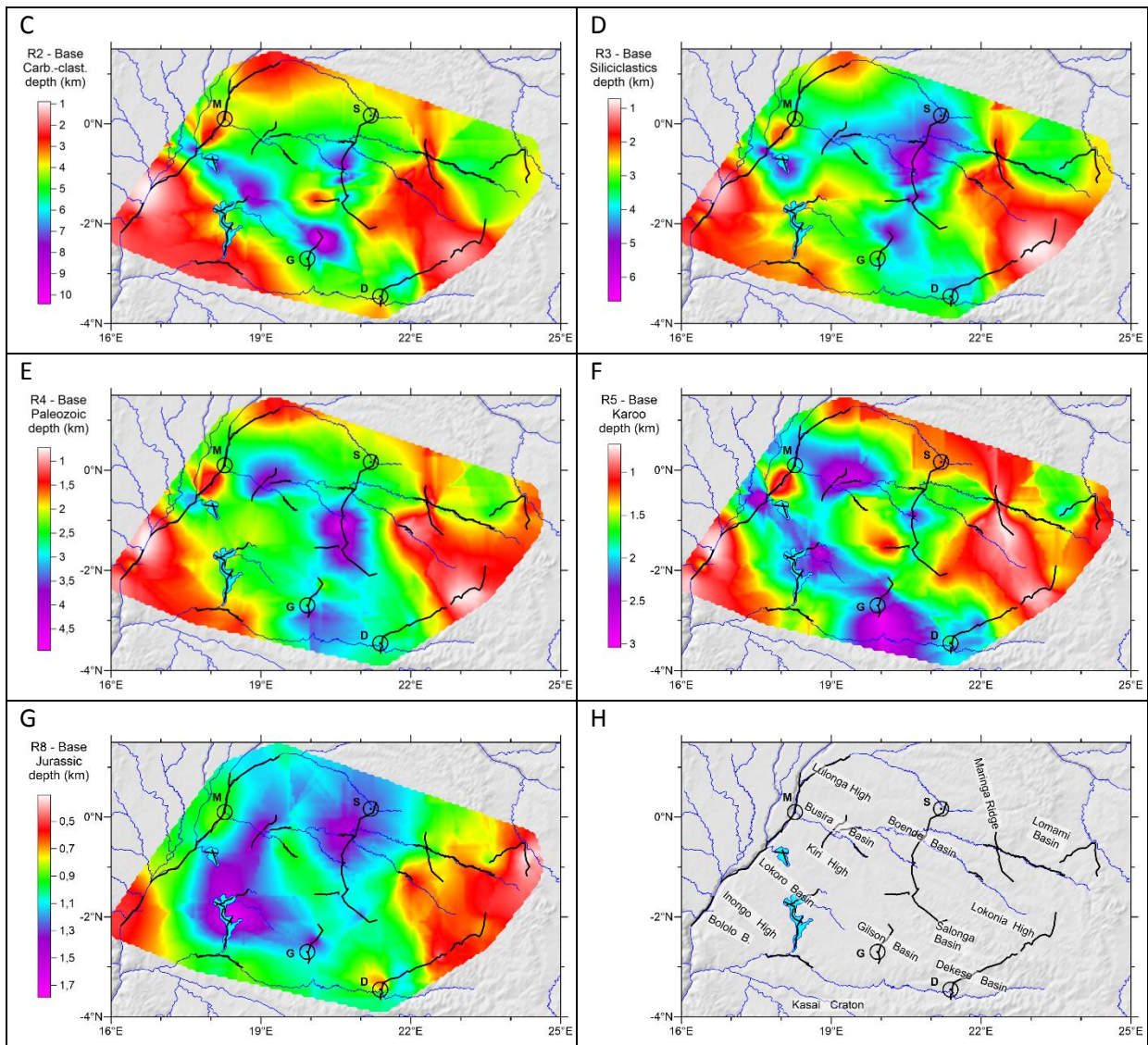
841 7.2. Evolution of the depocenters with time

842

843 The results of the interpolation of the seismic reflection profiles for the different
844 seismic horizons show the migration of the depocenters from the Proterozoic to Jurassic
845 times (Fig. 14) and the lateral thickness variations of the different sedimentary layers (Fig.
846 15). They reveal a different behavior of the basin during the successive stages of evolution,
847 with a progressive decrease in influence of the initial rift structure.

848

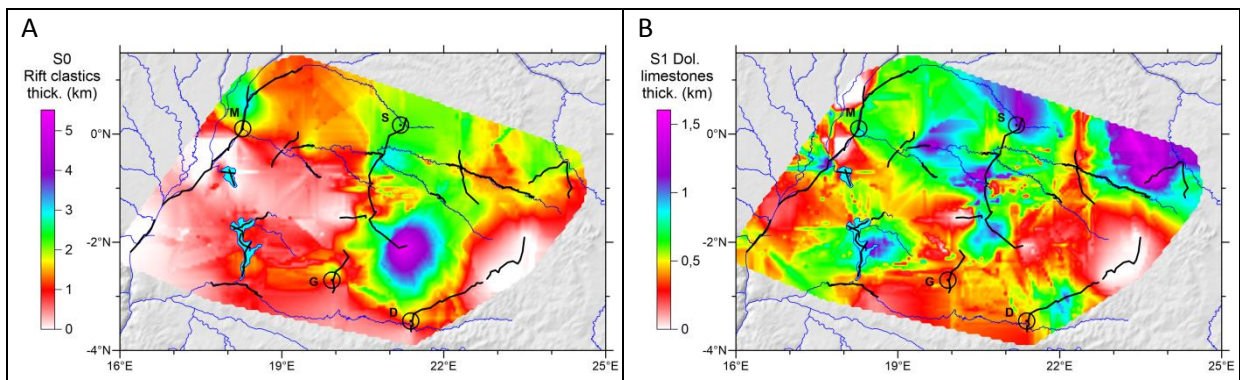


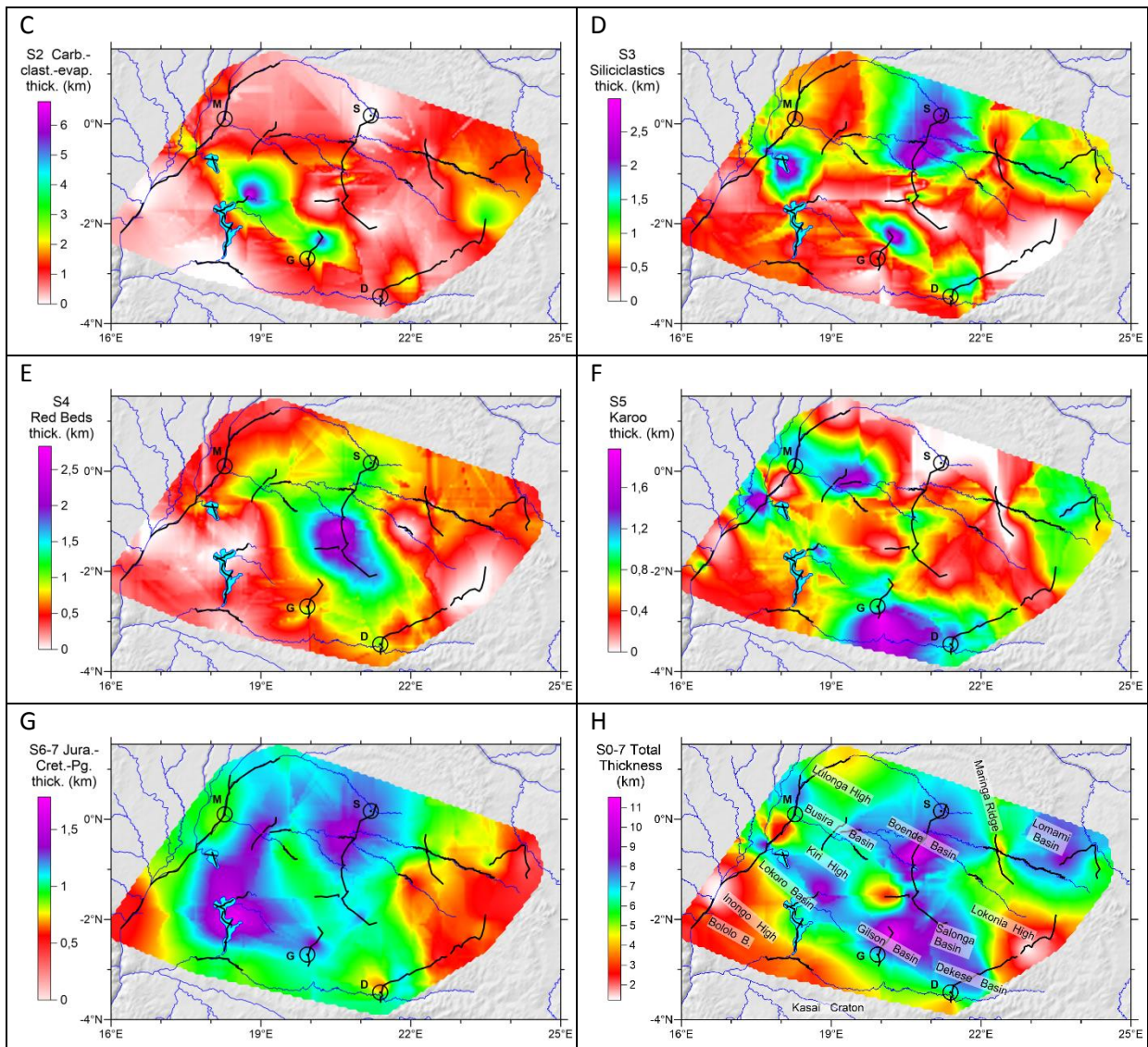


851

852 **Fig. 14.** Depths maps of the main seismic horizons (A-G). Names of the CB structures (H).
 853 Broken black lines show location of the seismic reflection profiles.

854





856

857 **Fig. 15.** Thickness maps (isopach) of the main stratigraphic sequences (A-G) and of the total
 858 sedimentary fill, with the names of the CB structures (H). Broken black lines show location
 859 of the seismic reflection profiles.

860

861 *7.2.1 Late Mesoproterozoic rifting (sequences 0 and 1)*

862

863 Sequences 0 and 1 (Fig. 15A, B) have been proposed to correspond to the initial failed
 864 rift stage, of possible late Mesoproterozoic age. The Kiri High is devoid of late
 865 Mesoproterozoic sediments, as shown by the seismic line R3 (Fig. 7b) and the western half of

866 line L63 (Fig. 9a). Between these two lines, we assume a similar situation, even if the
867 interpolation suggests some sediment. As explained above, this might be an artefact of the
868 interpolation. This indicates that the Kiri High appeared during the rifting stage of the CB. It
869 separates the basin into two large depressions from the beginning of its history. Globally, the
870 CB is asymmetric at this stage, with the northern depression deeper than the southern one.
871 The Kiri High extends laterally to line L63 in the center of the basin and forms a left-stepping
872 relay with the Lokonia High (Fig. 13).

873 The rift clastics (sequence 0) are thicker in the northern part of the CB, immediately
874 against the Kiri High, and become especially thick north of the Mbandaka well, in the Busira
875 basin. South of the Kiri High, the rift clastics are present as a blanket in the region of Lake
876 Inongo (group of profiles R21-25). The over-thickening in the Salonga Basin appears to be
877 caused by important subsidence at the time of deposition of the rift clastics, close to the relay
878 zone between the Kiri and Lokonia highs.

879 The Dolomitic limestones (sequence 1) are absent over the Kiri and Lokonia High and
880 have a relatively constant thickness over the rest of the basin, fluctuating between 0.5 and 1
881 km. They have their greatest thickness in the northern part of the basin where they reach up to
882 1.6 km.

883

884 *7.2.2 Neoproterozoic post-rift evolution (sequences 2 and 3)*

885

886 During the Neoproterozoic, the geography of the basin changed and new basins
887 developed. Sequences 2 and 3 (Fig. 15C, D) are the thickest in the southern depressions
888 (Lokoro and Gilson basins), close to the Kiri High and also in the Boende Basin. The Lokoro
889 Basin accumulated up to 6 km of carbonates-clastics (sequence 2) and the Gilson Basin, up to
890 5 km (Fig. 15C). The Boende Basin started to develop during the deposition of the

891 siliciclastics (sequence 3), and the two others (Lokoro and Gilson) continued to accumulate
892 sediments with about 2.5 km in all the tree basins, Fig. 15D). The rest of the CB
893 accommodated a much less thickness (about 2 km), with a maximum of 3.2 km in the
894 Lomami basin and a similar thickness over the Kiri High and the Busira Basin north of it
895 (line R5, Fig. 7c). Over the Kiri High, they cover directly the basement (Line R3, Fig. 7b).
896 The depocenter of the Lokoro basin fluctuated in time, with the deepest part on the eastern
897 side (line R24) during deposition of sequence 2 and then in the western side (Lake Tumba),
898 during deposition of sequence 3 (Fig. 14C-D).

899 The post-rift sequences are locally not present over the eastern extremity of the Kiri
900 high (Line 63; Fig. 9a) and some parts of the Lokonia High (Line 59, Fig. 10b) and the
901 Salonga Basin (line L63, Fig. 9). They might have been deposited and removed after the Pan-
902 African deformation, as the Pan-African unconformity truncates the entire Proterozoic
903 sequences.

904

905 *7.2.3 Paleozoic post-orogenic and deglacial sedimentation (sequences S4 and S5)*

906

907 After the Pan-African orogenic period, the configuration of the CB changed
908 drastically. During the deposition of the Red Beds (sequence 4; Fig. 15E), the depocenter
909 migrated towards a central NW-SE oriented depression, open towards the north. This
910 depression, centered on lines L50, L60, L62 & L63 (Fig. 8, 9) lies between the Boende and
911 the Gilson basins, with a maximum of 2.8 km of sediments. During the Karoo period
912 (sequence 5; Fig. 15F), depocenters developed between the Gilson and Dekese wells in the
913 south (1.97 km deep), against the Kasai Craton and in the Busira and Lokoro basins on both
914 sides of the Kiri High. Little sediments were deposited in the area of the former depocenter of
915 the Red Beds. No angular unconformity can be observed on the seismic profiles between the

916 Red Beds and the Karoo sequences. Instead, as mentioned above, we observe a sedimentary
917 hiatus with evidence for erosion in the transition between these series in the Dekese well at
918 1677 m deep.

919

920 *7.2.4 Jurassic-Cretaceous transgressive cover (sequences S6-S7)*

921

922 The late Jurassic-Cretaceous-Paleogene sequences (6-7) form a transgressive cover
923 over the Basal Jurassic unconformity (Fig. 15G, H). Sedimentation was no more influenced
924 by the initial rift structure. The depocenter of the CB now lies in the region of Lake May
925 Ndombe with a maximum of 1.8 km of sediments (group of lines L21-24). It extends across
926 the Kiri High towards the in the Busira basin (lines L64-65). Another depocenter developed
927 over the Boende Basin (lines L51-52 and R12), with a maximum of 1.4 km of sediments.

928

929 **8. Tectono-stratigraphic evolution of the CB**

930

931 The CB had a long-lived evolution in an intracontinental setting at the center of the
932 Congo Craton that stabilized during the Mesoproterozoic. Since then, it recorded a long
933 geological history driven by global processes (plate tectonics and climate change) with
934 several episodes of basin subsidence and sedimentation in intracontinental settings,
935 interrupted by tectonic and erosional events (Pan-African near field, Gondwana far field).
936 Sedimentation was also controlled by global climatic fluctuations and affected by several Ice
937 House events.

938 Our study confirms the subdivision of the stratigraphy of the CB into three major
939 units, representing the Proterozoic, Palaeozoic-Triassic, and the Jurassic-Cretaceous
940 sediments (Kadima et al., 2015). They are separated by two major tectonic unconformities at

941 the Neoproterozoic-Palaeozoic transition (related to the Pan-African deformation) and at the
942 Triassic-Jurassic transition (related to far-field intraplate compression).

943 The initial rift and post-rift phases in the Meso- and Neoproterozoic produced
944 significant subsidence of the basement in the northern part of the basin, where it currently
945 reaches an average depth of 7-8 km (Fig. 13). In most of this area, the sedimentary sequences
946 appear unaffected by successive tectonic events and the basement depth is sub-horizontal or
947 shows small undulations, likely reflecting inherited heterogeneity. In the same area, the syn-
948 rift clastics and carbonate ramp layers are well developed and reach in total an average
949 thickness of 3 km. The overlying Proterozoic sediments reach a thickness of 4-5 km (Fig.
950 14C-D).

951 The thickness maps of the main stratigraphic units show that the migration of the
952 depocenters with time was clearly influenced by the WNW-trending Kiri basement High, and
953 to a lesser extent, the Lokonia High which are considered to be the axial zone of the paleorift
954 (Kadima et al., 2011b) that separates the CB into two parts (Fig. 15). The Kiri High had a
955 strong control on the sedimentation and basin architecture during the late Mesoproterozoic
956 and Neoproterozoic. This control weakened during the Palaeozoic and Mesozoic.

957 The basin sedimentation and structure have been further influenced by global climate
958 fluctuations (ice/greenhouse ages), the paleo-geographic position of the CB (South Pole to
959 the Equator), as well as by tectonic phases (folding and thrusting) and local/regional
960 denudation stages.

961

962 *8.1 Late Mesoproterozoic basin initiation*

963

964 The age of initiation of the CB remained controversial for a long time, but tends to get
965 older with the increasing geological knowledge and data analyses. It was initially considered

966 to be Carboniferous to recent (Veach, 1935; Cahen, 1954; Lepersonne, 1977), as these
967 authors considered that the pre-Carboniferous sediments were part of the “Congo platform
968 cover”. After integration and synthesis of the results collected during the second exploration
969 campaign, and by correlation with the Lindian studied by Verbeek (1970), the CB was
970 considered to be Neoproterozoic in age (Chorowicz et al., 1990; Daly et al., 1991, 1992)
971 More recently, Delpomdor et al. (2013b) correlated the basal series of the CB, within the
972 failed rift basin of Kadima et al. (2011a), with the Mbuji-Mayi Supergroup, which could
973 represent its outcropping southeastern prolongation. We also support this correlation, but
974 Delpomdor et al. (2013b) puts the age of the of BII group of the Mbuji-Mayi Supergroup
975 between 750 and 880 Ma, contemporaneous with the break-up of Rodinia and the initiation of
976 the Katanga basin (Cailteux and de Putter, 2019). However, François et al. (2017) dated the
977 Mbuji-Mayi Supergroup between 1065 and 1000 Ma, (Stenian, Upper Mesoproterozoic), thus
978 before the main collisional events at about 1000 Ma that led to the Rodinia supercontinent
979 assembly (Li et al., 2008). The initiation of the CB could therefore be contemporaneous with
980 the Taoudeni Basin (Martin-Monge et al., 2016; Beghin et al., 2017a, 2017b). It cannot be
981 related to the initial Neoproterozoic divergence that occurred along the southern
982 margin of the CB, recorded in the Zambezi and Lufilian basins belts between 880 and 820
983 Ma (first rift cycle of de Waele et al., 2008).

984 Four main depocenters where the basement reaches very large depths between 9 and
985 11 km have been identified. The Lokoro Basin and the combined Gilson, Dekese and Salonga
986 Basins flank on the southern side the Kiri and the Lokonia Highs while the Boende and
987 Lomami Basins flank these highs on their northern side. The latter two could have formed
988 initially as a single large basin, now disrupted by the Maringa Ridge. This alternation of
989 highs and deep basins, NW-SE oriented, is already known since the time of the first
990 explorations in the CB (e.g., Cahen, 1956; Kadima et al., 2011a), but we identified now new

991 basins such as the Dekese and Salonga Basins with a total sedimentary infill of about 7 km.
992 The difference in the shape of the basins and thickness of the syn-rift sequences can be
993 attributed to a non-uniform syn-rift extension, which affected more the northern than the
994 southern part of the CB. Another hypothesis is that inherited heterogeneity of the basement,
995 derived from different cratonic nuclei, influenced the shapes and sizes of the basins formed in
996 response to uniform (or non-uniform) extension, as well as the thickness of syn-rift
997 sediments. This would explain the great thickness of syn-rift sediments in the Salonga basin,
998 relative to the Lokoro and Gilson basins, which are almost devoid of them.

999 The paleorift structure is represented by the Kiri and the Lokonia Highs, which act as
1000 basement uplifts between opposed diverging monoclines. They were not covered by the rift
1001 clastics (sequence 0), nor by the dolomitic limestones (sequence 1), but by the post-rift
1002 sediments (sequences 2-3). They represent two offset highs, instead of a continuous rift
1003 structure, as proposed by Kadima et al. (2011a, b).

1004

1005 *8.2 Neoproterozoic evolution (Rodinia to Gondwana)*

1006

1007 New depocenters formed during the Neoproterozoic in the CB (Lokoro, Gilson and
1008 Boende basins), filled by sequences 2 and 3 in a relatively continuous sedimentation. No
1009 regional unconformity can be seen between these two units, which are sometimes difficult to
1010 distinguish in the seismic profiles. The apparent continuity in sedimentation also suggests
1011 that no tectonic events disturbed the basin. The general geodynamic conditions of the CB
1012 were that of a relatively stable intracontinental setting, probably in a general extensional
1013 context. It is difficult to invoke post-rift subsidence for the entire period (nearly 500 Ma) as
1014 during that time, complete Wilson-cycles occurred along the margins of the Congo Craton, in
1015 the West-Congo belt (Pedrosa-Soares et al., 2008), Damara (Gray et al., 2008) and Katanga

1016 (Lufilian) belts (Cailteux and De Putter, 2019), and possibly also along its south-eastern
1017 margin, in the Ubende belt (Boniface and Appel, 2017; Fig. 2).

1018

1019 *8.3 Pan-African deformation and unconformity*

1020

1021 Daly et al. (1991, 1992) already evidenced a distal effect of the late Paleozoic peri-
1022 Gondwana orogenies as major contractional deformation observed in the seismic profiles.
1023 Our analysis of the profiles reveals that the Pan-African orogenies that developed around the
1024 Congo Craton at the end of the Neoproterozoic, also caused locally intense far-field
1025 deformations in the CB. They are even better expressed than the late Paleozoic deformations
1026 in the center for the CB, as shown by profile L50 (Fig. 7) and L63-L62 (Fig. 8). The western
1027 extremity of profile L63 (Fig. 8a) shows that the entire Proterozoic succession has been
1028 eroded away before the deposition of the Paleozoic series over the Pan-African unconformity.

1029 In several profiles, such as R5 (Fig. 7c), R9 (Fig. 11) and R22 (Fig. 12), the dolomitic
1030 limestones (sequence 1), which is marked by strong parallel reflectors, is affected by reverse
1031 faults that disappear in the adjacent sequences below and above.

1032 At the periphery of the basin, the Mbuji-Maji series are folded and faulted at the
1033 contact with the Kibara belt in the Katanga region, in the area of the Lomami River (Cahen
1034 and Mortelmans, 1947). This deformation has been interpreted as a far-field effect of the
1035 Lufilian orogeny which could have reactivated the Kibaran structures.

1036

1037 *8.4 Paleozoic Gondwana Super-fan*

1038

1039 The compressional tectonics that led to the formation of the Gondwana continent was
1040 followed by post-orogenic extension and denudation (removal of several km of sediments) in

1041 the early Paleozoic, with consequent development of the of the Pan-African tectonic and
1042 erosional unconformity during the Cambrian (Lucazeau et al. 2015).

1043 The seismic sequence 4, interpreted to represent the Red Beds, shows a well-defined
1044 depocenter in the middle of the basin, opened towards the north and terminating towards the
1045 South in the region of the Dekese well, against the Kasai Craton (Fig.15E). This sequence
1046 was not observed over the Kasai craton (Roberts et al., 2015). These Red Beds be the
1047 extension into the CB of the Cambrian-Ordovician North Gondwana Super-fan System of
1048 quartz-rich sandstone (Squire et al., 2006; Meinhold et al., 2013; Lewin, 2020). Quartz-rich
1049 arkosic sandstones are known to have been deposited during the Cambrian-Ordovician times
1050 in Northern Africa and the Arabian Peninsula (Burke et al., 2003; Avigad et al., 2005; Squire
1051 et al., 2006). They originate from Pan-African terranes exposed by post-orogenic uplift and
1052 chemical weathering of the Transgondwanan Supermountain (Squire et al., 2006) of the East
1053 African – Antarctic Orogen (Fritz et al., 2013) that developed between East and West
1054 Gondwana.

1055 This enormous depositional system of continent derived sediments throughout
1056 Gondwana lasted at least 260 Ma, from late Cambrian to early Devonian (Squire et al., 2006).
1057 These sediments are characterized by typical detrital zircon age spectra with a prominent
1058 double peak at 550-650 Ma (dominant) and 900-1200 Ma (secondary), with a minor
1059 Paleoproterozoic contribution. Using this pattern, Squire et al. (2006) proposed that the post-
1060 530 Ma sediments deposited over the Kuunga Suture, between the Congo and Kalahari
1061 cratons (Damara and Katanga belts), could also be originating from the East African orogen.

1062 The Red Beds in the Samba well in the CB have also detrital zircons with two major
1063 peaks, at 560-830 Ma and 930-1160 Ma, and minor peaks at 1.2-1.5 Ga and 1.9-2.1 Ga (Linol
1064 et al., 2015b). This unit is considered the equivalent to the similar red arkoses of the Dekese
1065 well (Cahen et al., 1960), which are below the Permo-Triassic series, but Linol et al. (2015b),

1066 without further data, considered them as Triassic. The small contribution of Ectasian-aged
1067 zircons (1.3-1.4 Ga) indicates that the Karagwe-Ankole and Kibara belts on the eastern
1068 margin of the CB (Tack et al., 2010; Fernandez-Alonso et al., 2012) cannot be an important
1069 source for these sediments. Similarly, as the Paleoproterozoic-aged zircons are also rare, a
1070 contribution from the Ubende and Rusizi belts (Lenoir et al., 1995) is also minor if any. A
1071 sample of red arkoses from the Red Beds sequence at the bottom of the Dekese well (1853 m
1072 deep) was also studied (Linol et al., 2016), providing a similar detrital zircon pattern, with
1073 major peaks, at 610-830 Ma and 880-1100 Ma, respectively, and minor peaks, at 2.0-2.1 Ga
1074 and 2.4-2.6 Ga, respectively. This is a further argument to support a lateral correlation
1075 between the red arkoses encountered in the lower part of these two wells.

1076 We propose here that the Red Beds (sequence 4) of the CB could at least partly have
1077 been fed by the erosion products of the Transgondwanan Supermountain coming from the
1078 East African – Antarctic Orogen. They could represent the extension of the Gondwana Super-
1079 fan System in Central Africa, as giant distal sedimentary fans in major intracontinental
1080 basins, as already proposed by Squire et al. (2006). The morphology of the sequence 4 unit,
1081 stopping against the Kasai Craton in the south, suggests an origin of the fan in the CB from
1082 the north.

1083 Along the margins of the CB, Red Beds are known as the red arkoses of the Banalia
1084 Group which crop out on the northern margin of the CB (Verbeek, 1970) as those of the
1085 Bianco group in the Katanga fold belt (Cailteux and Deputter, 2019), but no detrital zircon
1086 data are available for these units. The red arkoses of the Inkisi Group in the West-Congo belt
1087 contain a high abundance of 500-800 Ma zircons with two major peaks, at 500-800 Ma and
1088 900-1200 Ma and minor peaks at 1.8-2.2 Ga and 2.5-2.8 Ga (Straathof, 2011; Affaton et al.,
1089 2015), pointing to a possible origin in the Brasiliano Araçuaí orogeny.

1090 Verbeek (1970) proposed already to correlate the Banalia arkoses with the red arkoses
1091 of the Samba and Dekese wells. He noticed the common abundant presence of relatively
1092 fresh feldspar, from 40% in the Samba and Dekese wells (Cahen et al., 1959, 1960) up to
1093 70% in the Banalia Group (Verbeek, 1970). They contain a relative importance of detrital
1094 micas, similar to the composition of granitic rocks. The arkoses are well-sorted and fine-
1095 grained, with the presence of clay pebbles. They occur in an alternation of layers with cross-
1096 bedding and parallel bedding, with intercalations of red clay layers. They contain ripple-
1097 marks and intraformational folds. These are also the characteristics of the Inkisi red arkoses,
1098 with the difference that they contain in addition well-rounded pebbles of quartz, quartzite,
1099 magmatic, and metamorphic rocks of different origin (Alvarez et al., 1995).

1100 From the arguments given above, we consider the Banalia, Banalia and Inkisi arkoses
1101 as stratigraphically equivalent and forming lower unit within the Red Beds, overlying the
1102 Precambrian basement. The Samba and Dekese arkoses would be a stratigraphically upper
1103 unit of the same Red Beds, under the Karoo or directly the Jurassic in places (core of the
1104 Maringa Ridge). It is not clear how these series connect laterally in the CB as the
1105 biostratigraphic control is inexistant.

1106 Building on Tack et al. (2008) and Fernandez-Alonso et al. (2015) who introduced the
1107 correlation of the Bianco, Banalia and Inkisi units as a single distinct lithostratigraphic Group
1108 between the Neoproterozoic and Karoo Supergroups, we can now propose that this be
1109 expanded to incorporate all the Red Beds in the CB, defining a new lithostratigraphic
1110 supergroup that we propose to name Aruwimi Supergroup, from the name of the river where
1111 Verbeek (1975) described for the first time to the Aruwimi sequence, which forms the upper
1112 part of the his 'Lindian' and includes a.o. the Banalia arkoses. Indirect stratigraphic
1113 constraints show that it is broadly of Cambrian to Devonian age. It is composed the lower
1114 Inkisi-Banalia-Biano Group and the upper Samba-Dekese Group. The Inkisi-Banalia-Biano

1115 Group is observable along the margins of the CB, as molassic deposits in the foreland of the
1116 Pan-African fold belts. The Upper Nama Group can be considered as the equivalent over the
1117 Damara belt on the SW margin of the CB in Namibia (Blanco et al., 2011). The Samba-
1118 Dekese Group is seen only in the wells drilled in the Cuvette Centrale, and particularly in the
1119 fully cored Samba and Dekese wells.

1120 The depositional environment and provenance of the Red Beds has been already
1121 discussed by Verbeek (1970). Good sorting and fine-grain imply a long-distance transport,
1122 while the freshness of the feldspars indicates non-aggressive chemical conditions. The
1123 mineralogical composition indicates a granitic source under denudation. The deposition
1124 conditions are typically continental, compatible with a large braided-river system without
1125 vegetation. The great thickness (up to 2.5 km in the CB) and homogeneity of the entire
1126 sequence of arkoses point to a long-duration and major size of the source area, compatible
1127 with the suggestion that this seismo-stratigraphic unit could represent a new branch of the
1128 Gondwana Super-fan in Central Africa. During the entire late Cambrian to Devonian, Central
1129 Africa remained in southern latitude above 40° and in relatively cool climatic conditions
1130 (Torsvik and Cocks, 2013). We found no evidence that the deposition of the Red Beds
1131 sedimentation was interrupted or influenced by the late Ordovician glaciation and ice sheet,
1132 which affected most of Northern Africa (e.g. Ghienne et al., 2007).

1133

1134 *8.5 Karoo deglacial sequence*

1135

1136 The CB was close to the South Pole in the earliest Carboniferous at the time of the
1137 Gondwana glaciation. Not much is left of this period in the CB, except for the depositional
1138 hiatus, which marks the transition between the Red Beds (sequence 4) and Karoo (sequence

1139 5) in the Samba and Dekese wells. The effect of this climatic event has been recorded in the
1140 Karoo deglacial sequence, from the periglacial Lukuga unit to the post-glacial Lueki unit.

1141 The paleogeography of the CB during the Permo-Triassic is clearly different from that
1142 of earlier stages. The marked N-S central depocenter of the Red Beds sequence is no more
1143 the dominant feature. There are no Karoo sediments in the Samba well and along the L50-52
1144 N-S seismic lines (Fig. 8), while new depocenters appear on each side of the Kiri High, in the
1145 Busira and Dekese basins. The latter was probably part of a large intracontinental lake during
1146 the Permian deglacial period (Wopfner, 1999; Linol et al., 2015b), evolving into a warmer
1147 post-glacial basin in the Triassic. Recycled vitrinite in the sediments of the Lukuga Group
1148 (Permian) suggests their provenance from a sedimentary source, not older than late Devonian
1149 (Sachse et al., 2012). A detrital zircons profile (Linol et al., 2015b) shows the same age
1150 ranges as for the Red Beds, but with markedly different proportions. The age range 950-1150
1151 Ma is the dominant peak, followed by the Paleoproterozoic contribution between 1.8 Ga and
1152 2.1 Ga. These terranes are common to the east of the CB, with the ~ 980 Ma leucogranites of
1153 the Kibara and Karagwe-Ankole belts (Tack et al., 2010), the 1860-2100 Ma Ubende - Rusizi
1154 belt (Lenoir et al., 1995) and in the East African orogen (Fritz et al., 2013). A late
1155 Neoproterozoic contribution (600-850 Ma) is the third in importance, indicating a significant
1156 contribution from the Pan-African aged terrains. Minor contributions are noticed at 1350-
1157 1450 Ma, indicating a possible contribution of the Ectasian (1370-1380 Ma) magmatism in
1158 the Kibara and the Karagwa-Ankole belts (Tack et al., 2010) and at 2.5-2.7 Ga from the
1159 Paleoproterozoic to Neoproterozoic basement. Overall, this detrital zircon pattern is interpreted
1160 as a dominant contribution from the glacial erosion products of the basement East of the CB,
1161 from melting ice sheets, originating from the paleo-pole position at that time (over present-
1162 day Antarctica). The reworked vitrinite observed by Sachse et al (2012) also suggests a
1163 contribution from Southeastern Africa.

1164 In conclusion, we observe a major change in the depocenters and sediment source
1165 from the early Paleozoic (sequence 4) to the late Paleozoic-Triassic (sequence 5), even if no
1166 major unconformity is noticed between the two sequences. There might have been a
1167 sedimentation hiatus with some reworking, likely driven by global climate change, but not by
1168 major tectonic events.

1169

1170 *8.6 Late Permian-early Triassic deformation*

1171

1172 Late Paleozoic deformations in the CB were first evidenced by Daly et al. (1991,
1173 1992) who described compressional reactivations of the Kiri High, controlled by the pre-
1174 existing rift structures inherited from the initial opening of the CB (lines R3-R5, Fig. 7). In
1175 the seismic line L50 (Fig. 8), the Paleozoic series and Pan-African unconformity are both
1176 deformed in continuity with the Pan-African structures that affect the Paleoproterozoic
1177 sequences underneath, suggesting their reactivation. In contrast the Basal Jurassic
1178 unconformity and overlying sediments are not affected, constraining the deformation between
1179 the end of the Permian and the late Jurassic. The timing of the deformation relative to the
1180 Triassic Lueki Group is less clear. Some deformation could have occurred before and/or after
1181 it. Line 60 calibrated by the Gilson well (Fig. 8a) would suggest that the Lueki was affected
1182 by the deformation in the Gilson Basin before deposition of the Kisangani Group (Fig. 8b).

1183 Another expression of this deformation is illustrated in lines R15-16 (Fig. 11), where
1184 the entire Paleozoic to Proterozoic sequences were deformed in an anticlinal folding
1185 (Maringa Ridge) with a 70 km-long wavelength. This falls within the range of upper crustal
1186 lithospheric folding that typically develops in a layered lithosphere with an old
1187 thermotectonic age (> 500 Ma) submitted to horizontal compressional stresses (Cloetingh et

1188 al., 1999; Delvaux et al., 2013). The crest of the anticline has been completely eroded before
1189 the deposition of the Jurassic Kisangani series, which provide a clear age relationship.

1190

1191 *8.7 Jurassic-Cretaceous*

1192

1193 While the Permo-Triassic compressional event caused weaker and more localized
1194 deformation than the Pan-African deformation, it was still followed by important denudation.
1195 During the early Jurassic, up to 4000 m of sediments might have been removed as
1196 constrained by vitrinite reflectance in the Mbandaka and Dekese wells (Lucazeau et al., 2015),
1197 forming the Basal Jurassic Unconformity. The latter can be observed in-situ along the
1198 Lualaba segment of the Congo River, upstream of Kisangani (Caillaud et al., 2017), where
1199 sedimentation started in an anoxic lake, producing high quality lacustrine type II organic
1200 matter (Sachse et al, 2012).

1201 The overlying late Jurassic and Cretaceous to Paleogene seismic sequences (6 and S)
1202 cover not only the CB, but also its margins as a transgressive blanket, thus enlarging the size
1203 of the basin. Towards the south, it covers a large part of the Kasai craton, locally over a thin
1204 layer of Karoo sediments (Roberts et al., 2015). It contains lacustrine, fluvio-lacustrine and
1205 aeolian sequences, deposited in the context of Gondwana breakup and the African plate, with
1206 a more diverse source of sediments than during the Paleozoic, as indicated by detrital zircon
1207 age provenance (Linol et al., 2015c).

1208

1209 *8.8 Late Cretaceous-Cenozoic*

1210 As stated earlier, the CB underwent since the Late Cretaceous a new stage of erosion
1211 and denudation (Sachse et al., 2012; Lucazeau et al., 2015) with the formation of the 'African

1212 Surface', the Kalahari Group and the modern landscape (Giresse, 2005; Guillocheau et al.,
1213 2015; Linol et al., 2015e).

1214

1215 **9 Basin evolution in a broad context.**

1216

1217 The long geological history of the CB recorded a series of tectonic and climatic events
1218 that, given the size of the basin, located centrally in the Gondwana Supercontinent, are likely
1219 of global scale. It is thus useful to correlate the evolution of the CB in the broader context of
1220 Rodinia and Gondwana. The latter is illustrated in a schematic way in Figure 16.

1221

1222

1223 *9.1. Congo Basin in the context of Rodinia assembly and breakup*

1224

1225 The nucleation of the Congo Craton was completed with the “Kibaran” LIP magmatic
1226 event at around 1375 Ma in the eastern Congo Craton (de Waele et al., 2008; De Bruyne et
1227 al., 2015; Fernandez-Alonso et al. 2015). As the CB initiated during the final stages of the
1228 Rodinia Supercontinent amalgamation around 1 Ma, its geodynamic evolution can be put in
1229 parallelism with that of the Western Domain of the Karagwe-Ankole Belt (WD-KAB). The
1230 latter, which is relatively well known in Rwanda (Tack et al., 2010; Fernandez et al., 2012),
1231 extends westwards into the Kivu-Maniema region in the DRC (Lagmouch et al., 2018) and
1232 further west disappears below the CB sediments where it may form the crystalline and/or
1233 metamorphic basement in its northern part (Master, 2010). The metamorphic and tectonic
1234 evolution of the WD-KAB was recently revised and put into relation with the geodynamics
1235 evolution of Central Africa (Van Daele and Scherer, 2020; Van Daele et al., 2020). The
1236 Mesoproterozoic WD-KAB evolved in the context of Rodinia assembly in a prolonged but

1237 poorly defined extensional setting, with dominant quartzo-pelitic sedimentation and episodal
1238 magmatism and metamorphism.

1239 The oldest Mesoproterozoic sediments (Bugarama Gr.; 1420-1380 Ma) are intruded
1240 by widespread LIP bimodal magmatism, followed by dolerite dyke swarm intrusion at 1380-
1241 1360 Ma (Fernandez et al, 2012; Mäkitie et al., 2014). Sedimentation resumed after 1220 Ma
1242 (Rugezi and Cyohaha Gr.). At about 1000 Ma, a short-lived far-field fold-and thrust
1243 deformation occurred, followed by leucogranite intrusion and associated regional
1244 metasomatism and metamorphism up to 960 Ma (Fernandez et al, 2012; Van Daele et al.,
1245 2020). This marked the termination of sedimentation in the WD-KAB, which resumed in the
1246 Cryogenian (Itombwe Supergroup), just after carbonatitic magmatism, in the context of
1247 Rodinia breakup (820-750 Ma). A new phase of retrograde metamorphism and ductile-brittle
1248 deformation occurred (Van Daele & Scherer, 20200), in reaction to the East-African Orogeny
1249 (650-620 Ma and the final Gondwana assembly (580-500 Ma) (Fritz et al., 2010).

1250 In parallel, the CB started to develop at the end of the extensional stage of the Rodinia
1251 assembly, in late Mesoproterozoic. The ca. 1000 Ma ‘Rodinia assembly’ event is best
1252 expressed in the Irumides belt (Fig. 1; Fernandez-Alonso et al., 2012) and also expressed in
1253 the Kibara Belt (Fig. 2; Kokonyangi et al., 2002). It corresponds to the termination of the
1254 failed rift stage of the CB, transition from the dolomitic limestones (sequence 0) to the
1255 carbonates-evaporates-clastics (sequence 1). The siliciclastics (sequence 2) are coeval with
1256 the Itombwe Supergroup in eastern DRC and both were deposited in the context of Rodinia
1257 breakup. The Pan-African deformations and major unconformity in the CB are coeval with
1258 the last phase of metamorphism and deformation in the WD-KAB.

1259 Other Neoproterozoic basins developed over the West-African Craton: the huge
1260 Taoudeni and peripheral basins in the center and the Tindouf and Volta basins as peripheral
1261 forelands (Bertrand-Sarfati et al., 1991; Deynoux et al., 2006). Sedimentation started at about

1262 1100-1200 Ma in the Taoudeni basin (Rooney et al., 2010; Martin-Monge et al., 2016;
1263 Beghin et al., 2017a) and formed in a pericratonic to intracratonic unstable extensional
1264 tectonic context (Bronner et al., 1980; Beghin et al., 2017b). It recorded a discontinuous
1265 sedimentation history from late Mesoproterozoic to Paleozoic, including glacial deposits and
1266 was partly influenced by the Pan-African orogenic evolution (Villeneuve, 2005; Deynoux et
1267 al., 2006). The Taoudeni basin was deformed and uplifted by the Variscan deformation and
1268 covered by thin Mesozoic–Cenozoic units and Quaternary sand dunes (Trompette, 1973;
1269 Clauer, 1981; Deynoux et al., 2006; Balukiday et al., 2018).

1270 These basins are generally considered as intracontinental sag basins (Einsele, 1992;
1271 Allen and Allen, 2005). They form in continental interiors, affecting large areas with slow
1272 subsidence and a marked lateral continuity in the sedimentary layers. They can reach
1273 considerable thickness and remain active for long periods of time. They commonly form in
1274 the context of divergent plate motion and may have a central rift structure (Einsele, 1992).
1275 The CB with its suspected underlying failed rift is considered as one of them by Allen and
1276 Allen (2005). In the intracratonic basins, the initial failed rift likely formed by passive rifting
1277 rather than active rifting. In passive rifting, volcanism occurs during rifting and doming, as a
1278 consequence of lithospheric extension, while it occurs before in the active rifting model
1279 (Frizon de Lamotte et al., 2015).

1280 The Mbuji-Mayi Supergroup, which is considered as a proxy for the hidden rift below
1281 the CB, shows effectively a succession of rift clastics (BI Group) and dolomitic limestones
1282 (BII Group) terminating with basaltic lavas (François et al., 2017). Such a passive style of
1283 rifting tends to develop rather wide rifts at low strain rate in a thick and warm crust instead of
1284 narrow and well-focused rifts at high strain rate for an active style (Frizon de Lamotte et al.,
1285 2015).

1286

1287 *9.2. Congo Basin in the context of Gondwana assembly and breakup*

1288

1289 The Pan-African structures expressed by compressional deformation in the central
1290 part of the CB (this work) can be compared with the fold-and-thrust belt that developed in the
1291 Gourma basin on the eastern margin of the Taoudeni Basin (Villeneuve, 2005; Deynoux et
1292 al., 2006). In both cases, these structures are sealed by a major unconformity overlain by
1293 Paleozoic sediments. Elsewhere, in North Africa, Arabia and South America, numerous new
1294 Paleozoic basins formed over the Precambrian basement, all influenced by global climatic
1295 and tectonic events.

1296 The term ‘Inversion’ was used by the former authors (Daly et al., 1992; Kadima et al.,
1297 2011a). We recognize that this term is not fully appropriate, at least at the scale of the
1298 tectonic structures, as we cannot see precisely inverted structures in the profiles. For these,
1299 we preferred to use the term ‘compressional reactivation’. Within the general intraplate
1300 context, we can eventually use the term ‘inversion’ but at the basin-scale, considering that the
1301 major periods of sedimentation which occurred in an general (but poorly defined) extensional
1302 context have been interrupted by relatively short periods of far-field compressional tectonic
1303 deformation.

1304 The Paleozoic sag basins of NW Africa (Tindouf, Reggane, Ahnet, Mouydir
1305 Iolizi/Ghadames/Jefarah, Murzuk and Kufra basins in southern Algeria, Tunisia and Libya)
1306 formed over the Sahara Metacraton with a remarkably uniform early Paleozoic stratigraphy
1307 and a strong influence of the late Ordovician Hirnantian glacial event (Ghienne et al., 2007).
1308 Their development stopped in the Carboniferous as a consequence of the Variscan orogeny,
1309 before a new Mesozoic evolution (Selly, 1997; Jabir et al., 2020).

1310 The Great Arabian Basin recorded a history of sedimentation influenced by global
1311 climatic changes and tectonic movements from the Cambrian to the Triassic, with the major

1312 late Ordovician glaciation and Taconic (late Ordovician), Acadian (Devonian), and
1313 Hercynian (Carboniferous) tectonic movements (Laboun, 2010).

1314 In South America, several Paleozoic intracontinental sag basins also formed over the
1315 Precambrian basement. They initiated in Cambrian to late Ordovician and were filled
1316 essentially by siliciclastics with some evaporates and carbonates. Sedimentation was marked
1317 by a glacial influence between late Ordovician and Devonian, in function to their paleo-
1318 position relative to the South Pole. The Paraná Basin evolved in connection of the
1319 Gondwanide orogeny as a foreland basin (Milani and Zalan, 1999).

1320 The subsidence mechanism of these basins and in particular the CB during Paleozoic
1321 is not clear. If post-orogenic extension is likely in the peripheral Pan-African Belts for a
1322 relatively short time period (e.g. Kipata et al., 2013 for the Lufilian Arc), it cannot be invoked
1323 for the central part of the CB for its entire Paleozoic evolution. The seismic profiles show that
1324 the Pan-African deformation within the basin remained localized and most part of it remained
1325 tectonically undisturbed during the Pan-African time. Rather, a general extensional context
1326 probably established after the final Gondwana assembly.

1327

1328 *9.3. Congo Basin in the context of Pangea assembly and breakup*

1329

1330 The late Devonian – early Carboniferous saw the first stages of the Variscan collision
1331 between Gondwana and Laurussia that led to the formation of the Pangea Supercontinent. It
1332 affected the northern Gondwana margin by extensive vertical movements in the Sahara and
1333 Arabia domains, where Frizon de Lamotte et al. (2013) recognised a late Devonian
1334 unconformity associated with tectonic subsidence controlled by extensional deformation and
1335 subsequent erosion and peneplanation (“Eo-Variscan” event). The late Devonian - early
1336 Carboniferous was a period of major environmental crises with the onset of the Upper

1337 Paleozoic Ice House. It corresponds in Central Africa to the hiatus between the Red Beds (our
1338 new Aruwimi Supergroup) and the Karoo Supergroup and, in Southern Africa, between the
1339 Cape and the Karoo Supergroups (Catuneanu et al., 2005; Tankard et al., 2009). The tectonic
1340 versus climatic origin of the hiatus between the Red Beds and the Karoo in the CB is not
1341 clear. However, following Sachse et al. (2012), recycled detrital vitrinite are present in the
1342 Lukuga Group (Karoo) in the Dekese well. It must originate from eroded sediments not older
1343 than late Devonian (the oldest fossil evidence for angiosperms). This suggests that the
1344 Lukuga series were fed by an emerging and eroding area of late Devonian - early
1345 Carboniferous sediments.

1346 In the Carboniferous-Permian to early Triassic, the Gondwana domain of Pangea was
1347 affected on its southern and western sides by the Gondwanide accretionary orogeny as a
1348 consequence of the subduction of the Paleo-Pacific under the Gondwana margin (Cawood,
1349 2005). In South Africa, related tectonism is expressed by the Cape Fold Belt, recently dated
1350 at 525 Ma (Blewett & David, P., 2016). Hansma, 2013: 246-279 Ma

1351 At the same time, rifting developed along the Tethys side of Gondwana (Delvaux,
1352 2001), described as the Karoo I rifting period by Frizon de Lamotte et al. (2015), and the
1353 Tanzanian craton went through an important period of cooling and denudation (Kazanzu et
1354 al., 2016). In the center of Gondwana, the CB accumulated the Karoo Lukuga and Lueki
1355 groups. The late Triassic - lower Jurassic hiatus in the CB is coeval with a similar hiatus in
1356 Madagascar (Geiger et al., 2004), interpreted by Frizon de Lamotte et al. (2015) as a
1357 signature for doming. It was at least partly during this time interval that the late Permian -
1358 early Triassic tectonic deformation in the CB occurred, leading to the second widespread
1359 unconformity (Basal Jurassic unconformity). This period ends with the Karoo magmatism in
1360 Southern Africa and the giant Okavango dyke swarm, precisely dated at 179-180 Ma
1361 (Jourdan et al., 2004; Le Gall et al., 2005).

1362 Sedimentation in the CB resumed above the Basal Jurassic unconformity during the
1363 late Jurassic (Kimmeridgian), in a lacustrine continental setting (Caillaud et al., 2017). It
1364 continued until the Cenomanian (Colin, 1994; Delvaux and Fernandez-Alonso, 2015), after
1365 which the late Santonian inversion caused widespread basin inversion in North and Central
1366 Africa (Guiraud and Bosworth, 1977).

1367 The Cenozoic history of the CB is recorded in terms of denudation (Sachse et al.,
1368 2012), landform development (Guillocheau et al., 2015), neotectonics (Delvaux et al, 2016),
1369 and current seismotectonic activity (Delvaux and Barth., 2010), in the frame of the general
1370 uplift of Southern Africa Plateau (Braun et al., 2014) and development of the East African rift
1371 system (Macgregor, 2015), both resulting from a dynamic topography associated with the
1372 African superplume (Nyblade and Robinson, 1994).

1373

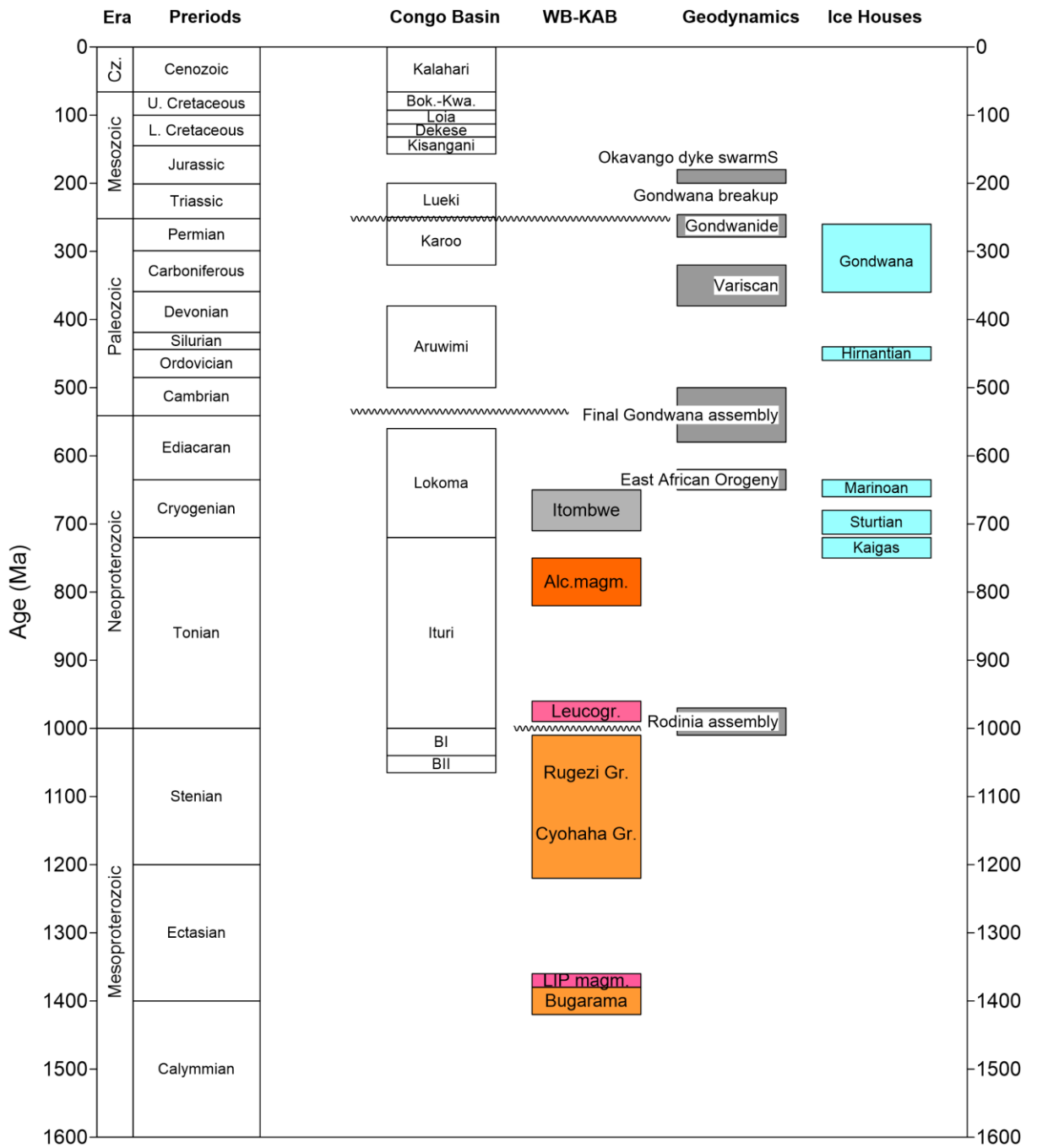
1374 *9.4 Congo Basin in the context of global climatic fluctuations*

1375

1376 The CB Basin recorded well the late Paleozoic Gondwana climatic event, marked by a
1377 hiatus after the Red Beds and the overlying Lukuga Group deglacial sequence, well-
1378 illustrated in the Dekese well. This was the consequence of its passage through the South
1379 Pole in late Devonian. In contrast, the other glacial periods that affected Africa are not well
1380 evidenced in the available geological data for the CB. The late Ordovician glacial period was
1381 relatively short-lived and affected mainly northern Africa (Ghienne et al., 2007). It might
1382 have influenced the source of the lower Red Beds by contributing well rounded and well
1383 sorted pebbles to the arkoses of the Inkisi Group (Alvarez et al., 2005).

1384 The Neoproterozoic glacial events (Hoffmann and Li, 2009) have been recognised in
1385 the Neoproterozoic belts surrounding the CB. The Kaigas (~750–720 Ma), Sturtian (~715-
1386 680) and Marinoan (~660-635 Ma) glacial events were described in the Damara belt on the

1387 southern edge of the Congo Craton (Hoffmann et al., 2015). The Sturtian and Marinoan are
1388 well known in the West-Congo Belt (Delpomdor et al., 2016) and in the Lufilian Arc in the
1389 Katanga Supergroup (Cailteux and de Putter, 2019). The Akwokwo diamictite in the Lindi
1390 Supergroup on the northern margin of the CB (Verbeek, 1970) is interpreted as a Sturtian
1391 event (Kadima et al., 2011b). The Gilson and Mbandaka deep wells drilled in the CB
1392 traversed almost the entire Neoproterozoic sequence, but the observation conditions (drill
1393 cuttings of mainly clastic sequences) did not allow recognising the Neoproterozoic glacial
1394 sediments.
1395



1396

1397 Figure 16: Synthesis of the stratigraphic evolution of the CB in relation with the evolution of
 1398 the Western Branch of the Karagwe-Ankole belt (WB-KAB), global geodynamic and glacial
 1399 events.

1400

1401 **10. Conclusion**

1402 We investigated the formation and evolution of the CB trough analysing all available
1403 geological and seismic data. This large data set makes it possible to reconstruct in greater
1404 detail than before the stratigraphic and tectonic history of this basin. We reconstructed the
1405 spatio-temporal evolution of the CB, integrating it in the evolution of the entire African
1406 continent during the last 1 billion years. After a review of the existing knowledge, we
1407 proposed a revised seismostratigraphic scheme for the CB, based on our interpretation of the
1408 seismic profile and the integration of well and outcrop data. We computed depth maps for the
1409 prominent reflectors and thickness maps for the seismostratigraphic units. This allowed us to
1410 highlight the three-dimensional evolution of the CB trough time.

1411 The CB is a remarkable intracontinental sag basin, which initiated in the late
1412 Mesoproterozoic, most probably as a failed rift basin. It recorded the deposition history of up
1413 to one billion years of sediments, one of the longest geological records on earth above a
1414 metamorphic basement. It registered several global glacial events in a geodynamic setting,
1415 evolving from the end of the Rodinia amalgamation to the Gondwana assembly and breakup
1416 while drifting over the South Pole and terminating at the Equator. Its early history parallels
1417 the evolution of the Mesoproterozoic-Neoproterozoic Kibaride belts of Central Africa.
1418 Surrounded by Pan-African orogenic belts in the late Neoproterozoic to Cambrian, it was
1419 affected by far-field deformations and associated vertical movements that left a prominent
1420 tectonic unconformity coeval with well-expressed Pan-African unconformities elsewhere in
1421 Gondwana. During its late Paleozoic to early Mesozoic evolution, sedimentation occurred in
1422 the context of the Gondwanide orogeny that occurred along the southern margin of
1423 Gondwana. It induced locally intense tectonic reactivation and general vertical movements,
1424 leading to the development of a second basin-scale unconformity (Basal Jurassic). The CB
1425 might also have been locally influenced by more distal tectonic events, but the current data
1426 available do not allow to precise that.

1427

1428 **12. Acknowledgements**

1429 A PhD grant to author Francesca Maddaloni was provided by Regione Friuli
1430 Venezia Giulia (Italy) through a European Social Fund (FSE) 50% cofounded fellowship.
1431 Magdala Tesauro acknowledges the grant “INTRACratonic basins TECTonic evolution: The
1432 Congo Basin (INTRA-TECTO)”. We are grateful to Dr. Alberto Pastorutti and Tommaso
1433 Pivetta for helpful discussions, assistance in program coding and informatics system
1434 management. Max Fernandez is thanked for his comments and careful proof-reading of the
1435 manuscript.

1436

1437 **13 Data sources:**

1438 The seismic profiles were obtained from the CNE, Kinshasa, D.R. Congo thanks to S.M.
1439 Kabeya.

1440

1441 **References**

1442 Abdelsalaam, M.G., Liégeois, J.-P., Stern, R.J., 2002. The Sahara Metacraton. *Journal of*
1443 *African Earth Sciences* 34, 119-136.

1444 Affaton, P., Kalsbeek, F., Boudzoumou, F., Trompette, R., Thrane, K., Frei, R., 2015. The
1445 Pan-African West Congo belt in the Republic of Congo (Congo Brazzaville):
1446 Stratigraphy of the Mayombe and West Congo Supergroups studied by detrital zircon
1447 geochronology. *Precambrian research* 272, 185-202.

1448 Allen, P.A., Allen, J.R., 2005. *Basin analysis: Principles and Applications*. Blackwell,
1449 Maldern, 549p.

- 1450 Alvarez P., Maurin J.-C., Vicat J.-P., 1995. La Formation de l'Inkisi (Supergroupe Ouest-
1451 Congolien) en Afrique Centrale (Congo et Bas-Zaïre): un delta d'âge Paléozoïque
1452 comblant un bassin en extension. *Journal of African Earth Sciences* 20(2), 119-131.
- 1453 Avigad, D., Sandler, A., Kolodner, K., Stern, R.J., McWilliams, M., Miller, N., Beyth, M.,
1454 2005. Mass-production of Cambro-Ordovician quartz-rich sandstones as a
1455 consequence of chemical weathering of Pan-African terranes: environmental
1456 implications. *Earth and Planetary Science Letters* 240, 818–826.
- 1457 Balukiday, B.K., François, C., Sforza, M.C., Beghin, J., Cornet, Y., Storme, J.-Y., Fagel, N.,
1458 Fontaine, F., Littke, R., Bauder, D., Delvaux, D., Javaux, E., 2018. Raman
1459 microspectroscopy, bitumen reflectance and illite crystallinity scale: comparison of
1460 different geothermometry methods on fossiliferous Proterozoic sedimentary basins
1461 (DR Congo, Mauritania and Australia). *International Journal of Coal Geology* 191,
1462 80-94, doi:org/10.1016/j.coal.2018.03.007.
- 1463 Barritt, S. D., 1983. The African Magnetic Mapping Project *ITC journal* 2, 122-131.
- 1464 Braitenberg, C., 2014. Exploration of tectonic structures with GOCE in Africa and across-
1465 continents. *International Journal of Applied Earth Observation and Geoinformation*
1466 35(A), 88-95. doi:10.1016/j.jag.2014.01.013
- 1467 Beghin, J., Storme, J.-Y., Blanpied, C., Gueneli, N., Brocks, J.J., Poulton, S.W., Javaux, E.J.,
1468 2017a. Microfossils from the late Mesoproterozoic – early Neoproterozoic Atar/El
1469 Mreïti Group, Taoudeni Basin, Mauritania, northwestern Africa. *Precambrian*
1470 *Research* 291, 63–82.
- 1471 Beghin, J., Guilbaud, R., Poulton, S.W., Gueneli, N., Brocks, J.J., Storme, J.-Y., Blanpied, C.,
1472 Javaux, E.J., 2017b. A palaeoecological model for the late Mesoproterozoic – early

- 1473 Neoproterozoic Atar/El Mreïti Group, Taoudeni Basin, Mauritania, northwestern
1474 Africa. *Precambrian Research* 299, 1-14.
- 1475 Blewett, S., David, P., 2016. An Overview of Cape Fold Belt Geochronology: Implications
1476 for Sediment Provenance and the Timing of Orogenesis. In: Linol., B. and de Wit,
1477 M.J. (Eds.) *Origin and evolution of the Cape Mountains and Karoo Basin*. Springer,
1478 Berlin, pp. 45-56. DOI: 10.1007/978-3-319-40859-0_5
- 1479 Bertrand-Sarfati, J., Moussine-Pouchikne, Z.A., Affaton, P., Trompette, R., Bellion, Y., 1991.
1480 Cover sequences of the West-African Craton. In: Dallmeyer, R.D. & Lecorché, J.P.
1481 (Eds.). *The West African Orogens and Circum-Atlantic Correlatives*. Springer, Berlin,
1482 65-82.
- 1483 Blanco, G., Germs, G.J.B., Rajesh, H.M., Chemale Jr. F., Dussin, I.A., Justino, D., 2011.
1484 Provenance and paleogeography of the Nama Group (Ediacaran to early Palaeozoic,
1485 Namibia): Petrography, geochemistry and U–Pb detrital zircon geochronology.
1486 *Precambrian Research* 187, 15–32.
- 1487 Boniface, N., Appel, P., 2017. Stenian - Tonian and Ediacaran metamorphic imprints in the
1488 southern Paleoproterozoic Ubendian Belt, Tanzania: Constraints from in situ monazite
1489 ages. *Journal of African Earth Sciences* 133, 25-35.
- 1490 Boulouard, C., Calendra, F., 1963. Etude palynologique de quelques sondages de la
1491 République du Congo (Congo ex-belge). Unpublished report R/ST-no7376, SNPA
1492 Direction Exploration et Production Pau, France.
- 1493 Bose, M.N., Kar, R.K., 1976. Paleozoic sporaefrom Zaïre (Congo). XI: Assises
1494 glaciaires et periglaciaires from the Lukuga Valley. *Ann. Mus. Roy. Congo belge*,
1495 Tervuren (Belgique), série in-8, *Sci. géol.*, 77, 1-19.

- 1496 Bose, M.N., Kar, R.K., 1978. Biostratigraphy of the Lukuga Group in Zaïre. *Ann. Mus. Roy.*
1497 *Congo belge, Tervuren (Belgique), série in-8, Sci. géol.*, 82, 97-114.
- 1498 Braun, J., Guillocheau, F., Robin, C., Baby, G., Jelsma, H., 2014. Rapid erosion of the
1499 Southern African Plateau as it climbs over a mantle superswell. *J. Geophys. Res.*
1500 *Solid Earth* 119, 6093–6112, doi:10.1002/2014JB010998.
- 1501 Bronner, G., Roussel, J., Trompette, R., Clauer, N., 1980. Genesis and geodynamic evolution
1502 of the Taoudeni Cratonic Basin (Upper Precambrian and Paleozoic), western Africa.
1503 In: Bally, A.W. (Ed.), *Dynamics of Plate Interiors. Geodyn. Series 1*, 81–90. AGU-
1504 GSA.
- 1505 Buitter, S.J.H., Steinberger, B., Medvedev, S., Tetreault, J.L., 2012. Could the mantle have
1506 caused subsidence of the Congo Basin? *Tectonophysics* 514-517, 62-80.
- 1507 Burke, K., MacGregor, D.S., Cameron, N.R., 2003. Africa's petroleum systems: four tectonic
1508 'Aces' in the past 600 million years. In: Arthur, T.J., MacGregor, D.S., Cameron,
1509 N.R. (Eds.), and *Petroleum geology of Africa: new themes and developing*
1510 *technologies: Geological Society of London, Special Publication 207*, 21–60.
- 1511 Burke, K., Gunnell, Y., 2008. The African erosion surface: a continental-scale synthesis
1512 geomorphology, tectonics, and environmental change over the past 180 million years.
1513 *Geological Society of America Memoir* 201, 66pp.
- 1514 Cahen, L., 1954. *Géologie du Congo Belge*. Vaillant-Caramane, Liège, 577pp.
- 1515 Cahen, L., 1981. Précisions sur la stratigraphie et les corrélations du Groupe de la Haute-
1516 Lueki et des formations comparables (Triassique à Liasique? d'Afrique Centrale).
1517 *Dépt. Géol. Min., Mus. Roy. Afr. Centr., Rapp. Ann.* 1980, 81-96.
- 1518 Cahen, L., 1983a. Brèves précisions sur l'âge des groupes crétaciques post-Wealdien (Loia,
1519 Bokungu, Kwango) du Bassin intérieur du Congo (Republique du Zaïre). *Rapport*

- 1520 annuel du Musée Royal de l’Afrique centrale, Tervuren (Belgique), Département de
1521 Géologie et de Minéralogie, pp 61–72.
- 1522 Cahen, L., 1983b. Le Groupe de Stanleyville (Jurassic supérieur et Wealdien de l’intérieur
1523 de la République du Zaïre): Révision des connaissances. Rapport annuel du Musée
1524 Royal de l’Afrique centrale, Tervuren (Belgique), Département de Géologie et de
1525 Minéralogie, pp 73–91.
- 1526 Cahen, L., Ferrand, J.J., Haarsma, M.J.F., Lepersonne, J., Verbeek, Th., 1959. Description du
1527 sondage de Samba. Ann. Mus. Royal Congo Belge, Tervuren (Belgique), Série in-8°,
1528 Sc. géol., 29, 210pp.
- 1529 Cahen, L., Ferrand, J.J., Haarsma, M.J.F., Lepersonne, J., Verbeek, Th., 1960. Description du
1530 sondage de Dekese. Ann. Mus. Royal Congo Belge, Tervuren (Belgique), Série in-8°,
1531 Sc. géol., 34, 115pp.
- 1532 Cahen, L., Lepersonne, J., 1971. La stratigraphie de la série des roches rouges et ses relations
1533 avec la série de la Haute-Lueki. (Annexe : Coupe du sondage n°11 dans le bassin
1534 charbonnier de la Lukuga). Dépt. Géol. Min., Mus. Roy. Afr. Centr., Rapp. Ann.,
1535 1970, 94-121.
- 1536 Cahen, L., Lepersonne, J., 1978 Synthèse des connaissances relatives au Groupe
1537 (anciennement Série) de la Lukuga (Permien du Zaïre). Ann. Mus. Roy. Congo belge,
1538 Tervuren (Belgique), série in-8, Sci. géol., 82, 115-152.
- 1539 Cahen, L., Mortelmans, G., 1947. Le système de la Bushimae au Katanga. Bull. Société belge
1540 de Géologie 56, 217-252.
- 1541 Cahen, L., Snelling, N.J., Delhal, J., Vail, J.R., Bonhomme, M. and Ledent, D., 1984.
1542 Geochronology and Evolution of Africa. Clarendon, Oxford, 512 p.

- 1543 Caillaud, A., Blanpied, C., Guillocheau, F., Delvaux, D., 2017. The Jurassic Stanleyville
1544 formation in the eastern margin of the Congo basin: an example of a shallow
1545 balanced-fill lake basin. *Journal of African Earth Sciences* 132, 80-98.
- 1546 Cailteux, J.L.H., De Putter, T., 2019. The Neoproterozoic Katanga Supergroup (D. R.
1547 Congo): State-of-the-art and revisions of the lithostratigraphy, sedimentary basin and
1548 geodynamic evolution. *Journal of African Earth Sciences* 150, 522–531.
- 1549 Casier, E., 1965. Poissons fossils de la série du Kwango (Congo). *Ann. Mus. royal Afrique*
1550 *centrale, Tervuren (Belgique), série in-8, Sci. géol., 50, 69p.*
- 1551 Catueanu, O., Wopfner, H., Eriksson, P.G., Cairncross, B.S., Rubridge, B.S., Smith, R.M.H.,
1552 Hancox, P.J., 2005. The Karoo basins of south-central Africa. *Journal of African*
1553 *Earth Sciences* 43, 211-253.
- 1554 Cawood, P.A., 2005. Terra Australis Orogen: Rodinia breakup and development of the
1555 Pacific and Iapetus margins of Gondwana during the Neoproterozoic and Paleozoic.
1556 *Earth-Science Reviews* 69, 249-279.
- 1557 Celli, N.L., Lebedev, S., Schaeffer, A.J., Gaina, C., 2020. African cratonic lithosphere carved
1558 by mantle plumes. *Nature Communications* 11, 92, doi:10.1038/s41467-019-13871-2.
- 1559 Chorowicz, J., Le Fournier, J., Mvumbi, M.M., 1990. La Cuvette Centrale du Zaïre: un bassin
1560 initié au Proterozoïque supérieur. *Contribution de l'analyse du réseau hydrographique.*
1561 *C. R. Acad. Sci. Paris, t. 311, Serie II, p. 349-356.*
- 1562 Clauer, N., 1981. Rb–Sr and K–Ar dating of Precambrian clays and glauconies. *Precambrian*
1563 *Res.* 15, 331–352.
- 1564 Cloetingh, S., Burov, E.B., Poliakov, A., 1999. Lithospheric folding: primary response to
1565 compression? (From central Asia to Paris basin). *Tectonics* 18, 1064–1083.

- 1566 Colin, J.P., 1994. Mesozoic-Cenozoic lacustrine sediments of the Zaïre Interior Basin. In:
1567 Gierlowski-Kordesch, E., Kelts, K. (eds.) Global Geological record of lake basins,
1568 Vol.1. Cambridge University Press, UK, pp. 31-36.
- 1569 Collins, A.S., Pisarevsky, S.A., 2005. Amalgamating eastern Gondwana: The evolution of the
1570 Circum-Indian Orogens. *Earth-Sciences Reviews* 71, 229-270.
- 1571 Cox, L.H., 1960. Further Mollusca from the Lualaba Beds of the Belgian Congo. *Ann. Mus.*
1572 *Roy. Afr. Cent., Tervuren (Belgique), série in-8, Sci. géol., 37, 15p.*
- 1573 Crosby, A.G., Fishwick, S., White, N., 2010. Structure and evolution of the intracratonic
1574 Congo Basin. *Geochemistry Geophysics Geosystems* 11(6), Q06010, doi:
1575 10.1029/2009GC003014.
- 1576 Daly, M.C., Lawrence, S.R., Kimun'a, D., Binga, M., 1991. Late Palaeozoic deformation in
1577 central Africa: a result of distant collision? *Nature* 350, 605-607.
- 1578 Daly, M.C., Lawrence, S.R., Diemu-Tshiband, K., Matouana, B., 1992. Tectonic evolution of
1579 the Cuvette Centrale, Zaire. *Journal of the Geological Society of London* 149, 539-
1580 546, doi:10.1144/gsjgs.149.4.0539.
- 1581 De Bruyne, D., Hulsbosch, Van Wilderode, J., Balcaen, L., Vanhaecke, F., Muchez, Ph.,
1582 2015. Regional geodynamic context for the Mesoproterozoic Kibara Belt (KIB) and
1583 the Karagwe-Ankole Belt: Evidence from geochemistry and isotopes in the KIB.
1584 *Precambrian Research* 264, 82–97.
- 1585 Defrétin-Lefranc, S., 1967. Etude sur les Phyllopoïdes du Bassin du Congo. *Ann. Mus. Roy.*
1586 *Afr. Cent., Tervuren (Belgique), série in-8, Sci. géol., 56, 122p.*
- 1587 Delpomdor, F., Blanpied, C., Virgone A., Prétat, A., 2013a. Paleoenvironments in Meso-
1588 Neoproterozoic carbonates of the Mbuji-Mayi Supergroup (Democratic Republic of

1589 Congo) - Microfacies analysis combined with C-O-Sr isotopes, major-trace elements
1590 and REE+Y distributions. *Journal of African Earth Sciences* 88, 72-100.

1591 Delpomdor, F., Linnemann, U., Boven, A., Gärtner, A., Travin, A., Blanpied, C., Virgone, A.,
1592 Jelsma, H., Pr at, A., 2013b. Depositional age, provenance, and tectonic and
1593 paleoclimatic settings of the late Mesoproterozoic–middle Neoproterozoic Mbuji-
1594 Mayi Supergroup, Democratic Republic of Congo. *Palaeogeography,*
1595 *Palaeoclimatology, Palaeoecology* 389, 35-47.

1596 Delpomdor, F., Eyeles, N., Tack, L., Pr at, A., 2016. Pr - and post-Marinoan carbonate facies
1597 of the Democratic Republic of the Congo: Glacially- or tectonically-influenced deep-
1598 water sediments? *Paleogeography, Paleoclimatology, Paleoecology* 457, 144-157.

1599 Delpomdor, F. and Pr at, A., 2015. Overview of the Neoproterozoic sedimentary series
1600 exposed along the margins of the Congo Basin. In: de Wit, M., Guillocheau, F., de
1601 Wit, M.C.J. (Eds.), *The Geology and Resource Potential of the Congo Basin.*
1602 Springer, Berlin, pp. 41-58, doi: 10.1007/978-3-642-29482-2_3.

1603 Delvaux, D., 2001. Karoo rifting in western Tanzania: precursor of Gondwana breakup ? In:
1604 *Contributions to Geology and Paleontology of Gondwana. In honour of Prof. Dr.*
1605 *Helmut Wopfner, Cologne, pp. 111-125. ISBN 3-934027-07-5.*

1606 Delvaux, D., Barth, A., 2010. African stress pattern from formal inversion of focal
1607 mechanism data. Implications for rifting dynamics. *Tectonophysics* 482, 105-128.

1608 Delvaux, D., Kervyn, F., Macheyeke, A.S., Temu, E.B., 2012. Geodynamic significance of
1609 the TRM segment in the East African Rift (W-Tanzania): active tectonics and
1610 paleostress in the Ufipa plateau and Rukwa basin. *Journal of Structural Geology* 37,
1611 161-180.

1612 Delvaux, D., Cloetingh, S., Beekman, F., Sokoutis, D., Burov, E., Buslov, M.M,
1613 Abdrakhmatov, E.E. (2013). Basin evolution in a folding lithosphere: Altai-Sayan and
1614 Tien Shan belts. *Tectonophysics* 602, 194-222.

1615 Delvaux, D., Fernandez-Alonso, M., 2015. Petroleum potential of the Congo Basin. In: de
1616 Wit, M., Guillocheau, F., de Wit, M.C.J. (Eds.), *The Geology and Resource Potential*
1617 *of the Congo Basin*. Springer, Berlin, pp. 371-391, doi: 10.1007/978-3-642-29482-
1618 2_18.

1619 Deynoux, M., Affaton, P., Trompette, R., Villeneuve, M., 2006. Pan-African tectonic
1620 evolution and glacial events registered in Neoproterozoic to Cambrian cratonic and
1621 foreland basins of West Africa. *Journal of African Earth Sciences* 46, 397–426.

1622 de Sainte Seine, P., 1955. Poissons fossiles de l'étage de Stanleyville (Congo belge). 1ère
1623 partie : la faune des argilites et schistes bitumineux. *Ann. Mus. royal Afrique centrale,*
1624 *Tervuren (Belgique), série in-8, Sci. géol., 14, 125p.*

1625 de Sainte Seine, P. and Casier, E., 1962. Poissons fossiles de l'étage de Stanleyville (Congo
1626 belge). 2ème partie : la faune marine des calcaires de Songa. *Ann. Mus. royal Afrique*
1627 *centrale, Tervuren (Belgique), série in-8, Sci. géol., 44, 52p.*

1628 De Waele, B., Johnson S.P. and Pisarevsky, S.A., 2008. Palaeoproterozoic to Neoproterozoic
1629 growth and evolution of the eastern Congo Craton: Its role in the Rodinia puzzle.
1630 *Precambrian Research* 160, 127-141.

1631 de Wit, M.J., Ransome, I.G.D., 1992. Regional inversion tectonics along the southern margin
1632 of Gondwana. In: de Wit, M.J., Ransome, I.G.D. (Eds.), *Inversion Tectonics of the*
1633 *Cape Fold Belt, Karoo and Cretaceous Basins of Southern Africa*. Balkema,
1634 Rotterdam, pp. 15-21.

1635 de Wit, M.J. and Linol, B., 2015. Precambrian basement of the Congo Basin and its flanking
1636 terrains. In: de Wit, M., Guillocheau, F., de Wit, M.C.J. (Eds.), *The Geology and*
1637 *Resource Potential of the Congo Basin*. Springer, Berlin, pp. 19-40, doi: 10.1007/978-
1638 3-642-29482-2_2.

1639 Downey, N.J., Gurnis, M., 2009. Instantaneous dynamics of the cratonic Congo basin.
1640 *Journal of Geophysical Research* 114, B06401, doi: 10.1029/2008JB006066.

1641 Downey, N., Gurnis, M., Avouac, J.-P., 2011. Subsidence history and geodynamic evolution
1642 of the cratonic Congo Basin. *Geophysical Research Abstracts* 13, EGU2011-388-1.

1643 ECL, 1988. *Hydrocarbon Potential of the Cuvette Centrale (Republic of Zaire)*. Exploration
1644 Consultants Limited, Cellule Technique Pétrolière, Pétrozaire, unpublished report,
1645 41pp.+figures, tables, appendices and enclosures.

1646 Einsele, G., 1992. *Sedimentary Basins. Evolution, Facies and Sediment Budget*. Springer-
1647 Verlag, Berlin, 628p.

1648 Egoroff, A., Lombard, A.L., 1962. Présence des couches de Stanleyville dans le sous-sol de
1649 Léopoldville, République du Congo (Note préliminaire). *Ann. Société géologique*
1650 *Belg.* 85, 103-109.

1651 Esso-Zaire SARL (1981a) Geological completion report: Gilson-1. Unpublished report

1652 Esso-Zaire SARL (1981b). Geological completion report: Mbandaka-1. Unpublished report

1653 Evrard, P., 1957. Les recherches géophysiques et géologiques et les travaux de sondage dans
1654 la Cuvette congolaise. Académie royale des Sciences coloniales, Classe des Sciences
1655 Techniques, *Mém. En 8°, Nouv. Sér.*, 7(1), 63p.

- 1656 Evrard, P., 1960. Sismique. Résultats scientifiques des missions du Syndicat pour l'étude
1657 géologique et minière de la Cuvette congolaise. Ann. Mus. Royal Congo Belge,
1658 Tervuren (Belgique), Série in-8°, Sc. géol. 33, 87p.
- 1659 Fernandez-Alonso, M., Cutten, H., De Waele, B., Tack, L., Tahon, A., Baudet, D., Barritt,
1660 S.D., 2012. The Mesoproterozoic Karagwe-Ankole Belt (formerly the NE Kibara
1661 Belt): The result of prolonged extensional intracratonic basin development punctuated
1662 by two short-lived far-field compressional events. *Precambrian Research* 216-219, 63-
1663 86.
- 1664 Fernandez-Alonso, M., Kampata, D., Mupande, J.-F., Dewaele, S., Laghmouch, M., Baudet,
1665 D., Lahogue, P., Badosa, T., Kalenga, H., Onya, F., Mawaya, P., Mwanza, B.,
1666 Mashagiro, H., Kanda-Nkula, V., Luamba, M., Mpoyi, J., Decrée, S. and Lambert, A.
1667 2015. Carte Géologique de la République Démocratique du Congo au 1 / 2.500.000 -
1668 Notice explicative. Ministère des Mines, République Démocratique du Congo,
1669 Kinshasa. ISBN: 978-9-4922-4481-9.
- 1670 Fernandez-Alonso, M., Kampata, D., Mupande, J.-F., Dewaele, S., Laghmouch, M., Baudet,
1671 D., Lahogue, P., Badosa, T., Kalenga, H., Onya, F., Mawaya, P., Mwanza, B.,
1672 Mashagiro, H., Kanda-Nkula, V., Luamba, M., Mpoyi, J., Decrée, S. and Lambert, A.
1673 2017. Carte Géologique de la République Démocratique du Congo au 1 / 2.500.000 -.
1674 Ministère des Mines, République Démocratique du Congo, Kinshasa. ISBN: 978-9-
1675 4922-4480-2.
- 1676 Foster, D. A., Goscombe, B. D., Newstead, B., Mapani, B. , Mueller, P. A., Gregory L. C.,
1677 Muvangua E., 2015. U–Pb age and Lu–Hf isotopic data of detrital zircons from the
1678 Neoproterozoic Damara Sequence: Implications for Congo and Kalahari before
1679 Gondwana, *Gondwana Research* 28(1), 179-190, doi:10.1016/j.gr.2014.04.011.

- 1680 Fourmarier, P., 1914. Le bassin charbonnier d'âge Permo-Triassique de la Lukuga. *Ann. Soc.*
1681 *Geol. Belg., Pub. rel. Congo belge*, 41, C77-C227.
- 1682 Frakes, L.A., Francis, J.E., Syktus, J.I., 1992. *Climate Modes of the Phanerozoic*. Cambridge
1683 University Press, Cambridge, 274p.
- 1684 François, C., Baludikay, B.K., Storme, J.Y., Baudet, D., Paquette, J.L., Fialin, M., Javaux,
1685 E.J., 2017. Contributions of U-Th-Pb dating on the diagenesis and sediment sources
1686 of the lower group (BI) of the Mbuji-Mayi Supergroup (Democratic Republic of
1687 Congo). *Precambrian Research* 298, 202-219.
- 1688 Frimmel, H. E., Tack, L., Basei, M. S., Nutman, A. P., Boven, A., 2006. Provenance and
1689 chemostratigraphy of the Neoproterozoic West Congolian Group in Democratic
1690 Republic of Congo: *Journal of African Earth Sciences* 46, 221-239.
- 1691 Frimmel, H. E., Basei, M. A. S., Gaucher, C., 2011. Neoproterozoic geodynamic evolution of
1692 SW-Gondwana: a southern African perspective, *International Journal of Earth*
1693 *Sciences*, 100, 323-354, doi: 10.1007/s00531-010-0571-9.
- 1694 Fritz, H., Abdelsalam, M., Ali, K.A., Bingen, B., Collins, A.S., Fowler, A.R., Ghebreab, W.
1695 Hauzenberger, C.A., Johnson, P.R., Kusky, T.M., Macey, P., Muhongo, S., Stern,
1696 R.J., Viola, G., 2013. Orogen styles in the East African Orogen: A review of the
1697 Neoproterozoic to Cambrian tectonic evolution. *Journal of African Earth Sciences* 86,
1698 65-106.
- 1699 Frizon de Lamotte, D., Tavakoli-Shirazi, S., Leturmy, P., Averbuch, O., Mouchot, N., Raulin,
1700 C., Leparmentier, F., Blanpied, C., Ringenbach, J.-C., 2013. Evidence for Late
1701 Devonian vertical movements and extensional deformation in northern Africa and
1702 Arabia: Integration in the geodynamics of the Devonian world. *Tectonics* 32, 1-16.

- 1703 Frizon de Lamotte, D., Fourdan, B., Leleu, S., Leparmentier, F., de Clarens, P., 2015. Style of
1704 rifting and the stages of Pangea breakup. *Tectonics* 34, 1009-1029.
- 1705 Geiger, M., Clark, D.M., Mette, W., 2004. Reappraisal of the timing of the breakup of
1706 Gondwana based on the sedimentological and seismic evidence for the Morondavia
1707 basin, Madagascar. *Journal of African earth Sciences* 38, 363-381.
- 1708 Giresse, P., 2005. Mesozoic-Cenozoic history of the Congo Basin. *Journal of African Earth*
1709 *Sciences* 43, 301-315.
- 1710 Ghienne, J.-F., Le Heron, D.P., Moreau, J., Denis, M., Deynoux, M., 2007. The Late
1711 Ordovician glacial sedimentary system of the North Gondwana platform. In: M.J.
1712 Hambrey, P. Christoffersen, N.F. Glasser, Bryn Hubbard (Eds.) *Glacial Sedimentary*
1713 *Processes and Products*, Wiley. Special Publication of the International Association of
1714 *Sedimentologists*, doi: 00.1002/9781444304435.ch17.
- 1715 Gobbo,-Rodrigues, S.R., Coimbra, S.R., Petri, S.R.J.B., 2003. Kwango Series (Congo),
1716 Bauru Group (Brazil) and Neuquen Basin (Argentina) ages, based on ostracods and
1717 vertebrates. XVIII Congresso Brasileiro de Paleontologia, Brasilia, Brazil, 152-153.
- 1718 Grecoff, N., 1957. Ostracodes du bassin du Congo. I. Jurassique supérieur et Crétacé inférieur
1719 du Nord du bassin. *Ann. Mus. Roy. Afr. Cent.*, Tervuren (Belgique), série in-8, *Sci.*
1720 *géol.*, 19, 97 p.
- 1721 Grecoff, N., 1960. Ostracodes du bassin du Congo. I. Crétacé. *Ann. Mus. Roy. Afr. Cent.*,
1722 Tervuren (Belgique), série in-8, *Sci. géol.*, 22, 36p.
- 1723 Guillocheau, F., Chelalou, R., Linol, B., Dauteuil, O., Robin, C., Mvondo, F., Callec, Y.,
1724 Colin, J.-P., 2015. Cenozoic landscape evolution in and around the Congo Basin:
1725 Constraints from sediments and planation surfaces. In: de Wit, M., Guillocheau, F., de

- 1726 Wit, M.C.J. (Eds.), *The Geology and Resource Potential of the Congo Basin*.
1727 Springer, Berlin, pp. 271-314, doi: 10.1007/978-3-642-29482-2_14.
- 1728 Guiraud, R., Bosworth, W., 1997. Senonian inversion and rejuvenation of rifting in Africa
1729 and Arabia: synthesis and implications to plate-tectonics. *Tectonophysics* 282, 39-
1730 82.
- 1731 Gray, D.R., Foster, D.A., Meert, J.G., Goscombe, B.D., Armstrong, R., Trouw, R.A.J.,
1732 Passchier, C.W., 2008. A Damara orogen perspective on the assembly of
1733 southwestern Gondwana. In: Pankhurst, R.J., Trouw, R.A.J., Brito Neves, B.B. & de
1734 Wit, M.J. (Eds.) *West Gondwana: Pre-Cenozoic Correlations Across the South*
1735 *Atlantic Region*. Geological Society, London, Special Publications, 294, 257–278.
- 1736 Hartley, R.W. and Allen, P.A., 1994. Interior cratonic basins of Africa: relation to continental
1737 break-up and the role of mantle convection. *Basin Research* 6, 65-113.
- 1738 Heine, C., Zoethout, J., Müller, R.D., 2013. Kinematics of the South Atlantic rift. *Solid Earth*
1739 4, 215-253.
- 1740 Hoffmann, P.F., Li, Z.-X., 2009. A palaeogeographic context for Neoproterozoic glaciation.
1741 *Palaeogeography, Palaeoclimatology, Palaeoecology* 277, 158-172.
- 1742 Hoffmann, M., Linnemann, U., Hoffmann, K.-H., Germs, G., Gerdes, A., Marko, L.,
1743 Eckelmann, K., Gärtner, A., Krause, R., 2015. The four Neoproterozoic glaciations of
1744 southern Namibia and their detrital zircon record: The fingerprints of four crustal
1745 growth events during two supercontinent cycles. *Precambrian Research* 259, 176-188.
- 1746 Hu, J. Faccenda, M., Zhou, Q., Fischer, K.M., Marshak, S., Lundstrom, C., 2018.
1747 Modification of the Western Gondwana craton by plume lithosphere interaction. *Nat.*
1748 *Geosci.* 11, 203–210.

- 1749 Jabir, A., Cerepi, A., Loisy, C., Rubino, J.-L., 2020. Stratigraphy, sedimentology and
1750 paleogeography of a Paleozoic succession, Ghadames and Jefarah basin, Libya and
1751 Tunisia. *Journal of African Earth Sciences* 163, 103642.
- 1752 Jamotte, A., 1931. Contribution à l'étude géologique du bassin charbonnier de la Lukuga.
1753 Comité Spécial du Katanga: *Annales du Service des Mines*, 2, 3-44.
- 1754 JNOC, 1984. Rapport des investigations géophysiques et géologiques dans la Cuvette
1755 centrale de la République du Zaïre. Japan National Oil Corporation, Report for
1756 Department of Mines and Energy, Government of Zaire, Unpublished, 205pp.
- 1757 Jones, L., Mathieu, P.L. and Strenger, H., 1960. Gravimétrie: Les résultats scientifiques des
1758 missions du syndicat pour l'étude géologique et minière de la Cuvette Congolaise et
1759 travaux connexes. *Ann. Mus. Roy. Congo belge, Tervuren (Belgique), série in-8, Sci.*
1760 *géol.* 36, 46pp.
- 1761 Jourdan, F., Féraud, G., Bertrand, H., Kampunzu, A.B., Tshoso, G., Le Gall, B., Tiercelin,
1762 J.J., Capiez, P., 2004. The Karoo triple junction questioned: Evidence from Jurassic
1763 and Proterozoic $^{40}\text{Ar}/^{39}\text{Ar}$ ages and geochemistry of the giant Okavango dyke swarm
1764 (Botswana). *Earth and Planetary Science Letters* 222, 989-1006.
- 1765 Kadima, E.K., 2011. Contribution géophysique à la connaissance du bassin de la Cuvette
1766 congolaise. Modélisation de la structure sédimentaire, Mécanisme de subsidence et
1767 structure de la lithosphère sous-jacente. PhD thesis, University of Lubumbashi,
1768 278pp.
- 1769 Kadima, E., Delvaux, D., Sebananzi, S.M.N., Tack, L. & Kabeya, S. M. 2011a. Structure and
1770 geological history of the Congo Basin: An integrated interpretation of gravity,
1771 magnetic, and reflection seismic data. *Basin Research* 23, 499-527.

- 1772 Kadima, E.K., Sebagenzi, S.M.N., Lucazeau, F., 2011b. A Proterozoic-rift origin for the
1773 structure and the evolution of the cratonic Congo Basin. *Earth and Planetary Science*
1774 *Letters* 304, 240-250.
- 1775 Kadima, K.E., Delvaux, D., Everaerts, M., Sebagenzi, S.M.N., Lucazeau, F., 2015.
1776 Neoproterozoic to Early Paleozoic sequences of Congo Shield: comparison of Congo
1777 Basin with the surrounding marginal basins. In: de Wit, M., Guillocheau, F., de Wit,
1778 M.C.J. (Eds.), *The Geology and Resource Potential of the Congo Basin*. Springer,
1779 Berlin, pp. 97-109, doi: 10.1007/978-3-642-29482-26.
- 1780 Kazanzu, C.H., Linol, B., de Wit, M., Rrown, R., Persano, C., Stuart, F.M., 2016. From
1781 source to sink in central Gondwana: Exhumation of the Precambrian basement rocks
1782 of Tanzania and sediment accumulation in the adjacent Congo basin. *Tectonics* 39,
1783 2034-2051.
- 1784 King, L.C., 1963. *South African scenery: a textbook of geomorphology*, 3rd. Edn. Oliver and
1785 Boyd, Edinburg, 308p.
- 1786 Kipata, M.L., Delvaux, D., Sebagenzi, M.N., Cailteux, J.-J., Sintubin M., 2013. Brittle
1787 tectonic and stress field evolution in the Pan-African Lufilian arc and its foreland
1788 (Katanga, DRC): from orogenic compression to extensional collapse, transpressional
1789 inversion and transition to rifting. *Geologica Belgica* 16/1-2, 001-017.
- 1790 Kokonyangi, J., Armstrong, R.A., Kampunzu, A.B., Yoshida, M., Okudaira, T., 2004. U-Pb
1791 zircon geochronology and petrology of granitoids from Mitwaba (Katanga, Congo):
1792 implications for the evolution of the Mesoproterozoic Kibaran belt. *Precambrian*
1793 *Research* 132, 79-106.
- 1794 Kröner, U., Römer, R.L., 2013. Two plates - Many subduction zones: The Variscan orogeny
1795 reconsidered. *Gondwana Research* 24, 298-329.

- 1796 Kuribara, Y., Tsunogae, T., Takamura, Y., Tsutsumi, Y., 2018. Petrology, geochemistry, and
1797 zircon U-Pb geochronology of the Zambezi Belt in Zimbabwe: Implications for
1798 terrane assembly in southern Africa. *Geoscience Frontiers* 10, 2021-2044, doi:
1799 10.1016/j.gsf.2018.05.019.
- 1800 Laboun, A.A., 2010. Paleozoic tectono-stratigraphic framework of the Arabian Peninsula.
1801 *Journal of King Saud University (Science)* 22, 41–50.
- 1802 Lagmouch, M., Mees, F., Delvaux, D. Kalikone, C., Ilombe, G., Ganza, G., Safari, E.,
1803 Bachinyaga, J., Mugisho, E., Wazi, N., Nzolang, C., Dewaele, S., Fernandez, M.,
1804 Nimpagaritse, G., Tack, L., Kervyn, F., 2018. Carte géologique du Kivu au
1805 1/1500.000. Musée royal de l’Afrique Centrale et Université Officielle de Bukavu.
1806 ISBN : 978-9-4926-6943-8.
- 1807 Lawrence, S., Makazu, M.M., 1988. Zaire’s Central basin: prospectivity outlook. *Oil Gas*
1808 *Journal* 86(38), 105-108.
- 1809 Le Gall, B., Tshoso, G., Dymont, J., Kampunzu, A.B., Jourdan, F., Féraud, G., Bertrand, H.,
1810 Aubourg, C., Vétel, W., 2005. The Okavango giant mafic dyke swarm (NE
1811 Botswana): its structural significance within the Karoo large igneous province.
1812 *Journal of Structural Geology* 27, 2234–2255.
- 1813 Lenoir, J.L., Liegeois, J.-P., Theunissen, K., Klerkx, J., 1995. The Palaeoproterozoic
1814 Ubendian shear belt in Tanzania: geochronology and structure. *Journal of African*
1815 *Earth Sciences* 19(3), 169-184.
- 1816 Lepersonne, J., 1945. La stratigraphie du Système du Kalahari et du Système du Karoo au
1817 Congo occidental. *Bulletin du Service géologique du Congo belge et du Rwanda-*
1818 *Urundi* 1, 27-50.

- 1819 Lepersonne, J. 1974. Carte géologique du Zaïre au 1: 2.000.000 + Notice explicative.
1820 Kinshasa, République du Zaïre: Direction de la Géologie/Musée Royal de l'Afrique
1821 centrale, Tervuren (Belgique)
- 1822 Lepersonne, J., 1977. Structure géologique du bassin intérieur du Zaïre. Bulletin de
1823 l'Académie royale de Belgique, Classe des Sciences, 5^e série, 63(12), 941-965.
- 1824 Lewin, A., Meinhold, G., Hinderer, M., Dawit, E.L., Bussert, R., Lünsdorf, N.K., 2020.
1825 Heavy minerals as provenance indicator in glaciogenic successions: An example from
1826 the Palaeozoic of Ethiopia. *Journal of African Earth Sciences* 165, 103813, doi:
1827 10.1016/j.jafrearsci.2020.103813.
- 1828 Lombard, A.L., 1961. La série de la Haute-Lueki (partie orientale de la cuvette congolaise).
1829 Bulletin de la Société belge de Géologie, de Paléontologie et d'Hydrologie 70, 65-72.
- 1830 Li, Z.X., Bogdanova, S.V., Collins, A.S., Davidson, A., De Waele, B., Ernst, R.E.,
1831 Fitzsimons, I.C.W., Fuck, R.A., Gladkochub, D.P., Jacoba, J., Karlstrom, K.E., Lu, S.,
1832 Napatov, L.M., Pease, V., Pisarevsky, S.A., Thrane, K., Vernikovsky, V., 2008.
1833 Assembly, configuration, and break-up history of Rodinia: A synthesis. *Precambrian*
1834 *Research* 160, 179-210.
- 1835 Liao, J., Wang, Q., Gerya, T., Ballmer, M.D., 2017. Modeling craton destruction by
1836 hydration-induced weakening of the upper mantle. *J. Geophys. Res.* 122, 7449–7466.
- 1837 Lindsay, J.F., 2002. Supersequences, superbasins, supercontinents-evidence from the
1838 Neoproterozoic-Early Paleozoic basins of Central Australia. *Basin Research* 14, 207-
1839 223.
- 1840 Linol, B. 2013. Sedimentology and sequence stratigraphy of the Congo and Kalahari Basins
1841 of south-central Africa and their evolution during the formation and break-up of
1842 West Gondwana. PhD thesis, Nelson Mandela Metropolitan University, 375p.

- 1843 Linol, B., de Wit, M.J., Guillocheau, F., Robin, C., Dauteuil, O., 2015a. Multiphase
1844 Phanerozoic subsidence and uplift history recorded in the Congo Basin: a Complex
1845 successor basin. In: de Wit, M., Guillocheau, F., de Wit, M.C.J. (Eds.), The Geology
1846 and Resource Potential of the Congo Basin. Springer, Berlin, pp. 213-227, doi:
1847 10.1007/978-3-642-29482-2_11.
- 1848 Linol, B., de Wit, M.J., Bartoon, E., Guillocheau, F., de Wit, M.C.J., Colin, J.P., 2015b.
1849 Paleogeography and tectono-stratigraphy of Carboniferous-Permian and Triassic
1850 ‘Karoo-like’ sequences of the Congo Basin In: de Wit, M., Guillocheau, F., de Wit,
1851 M.C.J. (Eds.), The Geology and Resource Potential of the Congo Basin. Springer,
1852 Berlin, pp. 111-134, 111-134, doi: 10.1007/978-3-642-29482-2_7.
- 1853 Linol, B., de Wit, M.J., Barton, E., Guillocheau, F., de Wit, M.C.J., Colin, J.P., 2015c. Facies
1854 analyses, chronostratigraphy and Paleo-environmental reconstructions of Jurassic to
1855 Cretaceous sequences of the Congo Basin. In: de Wit, M., Guillocheau, F., de Wit,
1856 M.C.J. (Eds.), The Geology and Resource Potential of the Congo Basin. Springer,
1857 Berlin, pp. 135-162, 135-161, doi: 10.1007/978-3-642-29482-2_8.
- 1858 Linol, B., de Wit, M.J., Milani, E.J., Guillocheau, F., Scherer, C., 2015d. New Regional
1859 Correlations Between the Congo, Parana´ and Cape-Karoo Basins of Southwest
1860 Gondwana. In: de Wit, M., Guillocheau, F., de Wit, M.C.J. (Eds.), The Geology and
1861 Resource Potential of the Congo Basin. Springer, Berlin, pp. 245-270, doi:
1862 10.1007/978-3-642-29482-2_13.
- 1863 Linol, B., de Wit, M.J., Guillocheau, F., de Wit, M.C.J., Anka, Z., Colin, J.-P., 2015e.
1864 Formation and collapse of the Kalahari Duricrust [‘African Surface’] across the
1865 Congo Basin, with implications for changes in rates of Cenozoic offshore
1866 sedimentation. In: de Wit, M., Guillocheau, F., de Wit, M.C.J. (Eds.), The Geology

- 1867 and Resource Potential of the Congo Basin. Springer, Berlin, pp. 193-212, doi:
1868 10.1007/978-3-642-29482-2_10.
- 1869 Linol, B., de Wit, M.J., Barton, E., de Wit, M.C.J., Guillocheau, F., 2016. U–Pb detrital
1870 zircon dates and source provenance analysis of Phanerozoic sequences of the Congo
1871 Basin, central Gondwana. *Gondwana Research* 29, 208-219.
- 1872 Lucazeau, F., Armitage, J., Kadima, E.K., 2015. Thermal regime and evolution of the Congo
1873 basin as an intracratonic basin. In: de Wit, M., Guillocheau, F., de Wit, M.C.J. (eds.),
1874 The Geology and Resource Potential of the Congo Basin. Springer, Berlin, pp. 229-
1875 224, doi: 10.1007/978-3-642-29482-2_12.
- 1876 Macgregor, D., 2015. History of the development of the East African Rift System: A series of
1877 interpreted maps through time. *Journal of African Earth Sciences* 101, 232–252.
- 1878 Maddaloni, F., Braiternberg, C., Kaban, M. K., Tesauro, M., Delvaux, D., 2020. The Congo
1879 Basin: Subsurface structure interpreted using potential field data and constrained by
1880 seismic data. (In preparation).
- 1881 Maheshwari, H., Bose, M.N., Kumaran, K.P., 1977. Mesozoic spora dispersae from Zaire:
1882 II. The Loia and Bokungu Groups in the Samba borehole. III. Some miospores from
1883 the Stanleyville Group. *Ann. Mus. royal Afrique centrale, Tervuren (Belgique), série*
1884 *in-8, Sci. géol.* 80, 60p.
- 1885 Mäkitie, H., Data, G., Isabirye, E., Mänttari, I., Huhma, H., Klausen, M.B., Pakkanen, L.,
1886 Virransalo, P., 2014. Petrology, geochronology and emplacement model of the giant
1887 1.37 Ga arcuate Lake Victoria Dyke Swarm on the margin of a large igneous province
1888 in eastern Africa. *Journal of African Earth Sciences* 97, 273-296.
- 1889 Martin-Monge, A., Baudino, R., Gairifo-Ferreira, L.M., Tocco, R., Badali, M., Ochoa, M.,
1890 Haryono, S., Soriano, S., El Hafiz, N., Hernan-Gomez, J., Chacon, B., Brisson, I.,

- 1891 Grammatico, G., Varade, R., Abdallah, H., 2016. An unusual Proterozoic petroleum
1892 play in Western Africa: the Atar Group carbonates (Taoudeni Basin, Mauritania). In:
1893 Sabato Ceraldi, T., Hodgkinson, R.A. & Backe, G. (Eds.) Petroleum Geoscience of
1894 the West Africa Margin. Geological Society, London, Special Publications 438.
- 1895 Master, S., 2010. Lac Télé structure, Republic of Congo: Geological setting of a
1896 cryptozoological and biodiversity hotspot, and evidence against an impact origin.
1897 *Journal of African Earth Sciences* 58, 667–679.
- 1898 Meinhold, G., Morton, A.C., Avigad, D., 2013. New insights into peri-Gondwana
1899 paleogeography and the Gondwana super-fan system from detrital zircon U–Pb ages.
1900 *Gondwana Research* 23, 661-665.
- 1901 Milani, E.J., de Wit, M.J., 2008. Correlations between the classic Paraná and Cape–Karoo
1902 sequences of South America and southern Africa and their basin infills flanking the
1903 Gondwanides: du Toit revisited. Geological Society, London, Special Publications
1904 294, 319-342. doi:10.1144/SP294.17.
- 1905 Milani, E.J., Zalan, P.V., 1999. An outline of the geology and petroleum systems of the
1906 Paleozoic interior basins of South America. *Episodes* 22(3), 199-205.
- 1907 Myers, T.S., Tabor, N.J., Jacobs, L.L., 2011. Late Jurassic paleoclimate of central Africa.
1908 *Palaeogeogr. Palaeoclimatol. Palaeoecol.* 311 (1-2), 111-125.
- 1909 Nyblade, A.A. Robinson, S.W., 1994. The African Superswell. *Geophysical Research*
1910 *Letters* 21, 765-768.
- 1911 Passau, G., 1923. La géologie du bassin des schistes bitumineux de Stanleyville (Congo
1912 belge). *Ann. Société géologique de Belgique. Publ. Rel. Congo belge* 45, 91-243.
- 1913 Pedrosa-Soares, A.C., Alkmim, F.F., Tack, L., Noce, C.M., Babinski, M., Silva, L.C.,
1914 Martins-Neto, M.A., 2008. Similarities and differences between the Brazilian and

- 1915 African counterparts of the Neoproterozoic Araçuaí-West Congo orogeny. Geological
1916 Society, London, Special Publications 294, 153-172.
- 1917 Poidevin, J.-L., 1985. Le Protérozoïque supérieur de la République Centrafricaine. Ann. Mus.
1918 Royal Afrique Centrale, Tervuren (Belgique), Série in-8°, Sc. géol. 91, 75p.
- 1919 Raucq, P., 1957. Contribution à la connaissance du Système de la Bushimay. Ann. Mus.
1920 Royal Congo Belge, Tervuren (Belgique), Série in-8°, Sc. géol. 18, 427p.
- 1921 Raucq, P., 1970. Nouvelles acquisitions sur le système de la Buchimay. Ann. Mus. Royal
1922 Congo Belge, Tervuren (Belgique), Série in-8°, Sc. géol. 69, 156p.
- 1923 Roberts, E.M., Jelsma, R. E., Hegna, T.A., 2015. Mesozoic sedimentary cover sequences of
1924 the Congo Basin in the Kasai Region, Democratic Republic of Congo. In: de Wit, M.,
1925 Guillocheau, F., de Wit, M.C.J. (Eds.), The Geology and Resource Potential of the
1926 Congo Basin. Springer, Berlin, pp. 163-191, doi: 10.1007/978-3-642-29482-2_9.
- 1927 Rooney, A.D., Selby, D., Houzay, J.-P., Renne, P.R., 2010. Re-Os geochronology of a
1928 Mesoproterozoic sedimentary succession, Taoudeni basin, Mauritania: Implications
1929 for basin-wide correlations and Re-Os organic-rich sediments systematics. Earth and
1930 Planetary Science Letters 289, 486-496.
- 1931 Sachse, V.F, Delvaux, D., Littke, R., 2012. Petrological and geochemical investigations of
1932 potential source rocks of the Central Congo Basin, DRC. AAPG bulletin 96 (2), 277-
1933 300.
- 1934 Santiago, R., de Andrade Caxito, F., Neves, M.A., Dantaz, E.L., de Medeiros Junior, E.B.,
1935 Queiroga, G.N., 2020. Two generations of mafic dyke swarms in the Southeastern
1936 Brazilian coast: reactivation of structural lineaments during the gravitational collapse
1937 of the Araçuaí-Ribeira Orogen (500 Ma) and West Gondwana breakup (140 Ma).
1938 Precambrian Research 340, 105344.

- 1939 Saha-Fouotsa, A.N., Vanderhaeghe, O., Barbey, P., Eglinger, A., Tchameni, R., Zeh, A.,
1940 Fosso Tchunte, P., Negue Nomo, E., 2019. The geologic record of the exhumed root
1941 of the Central African Orogenic Belt in the central Cameroon domain (Mbé – Sassa-
1942 Mbersi region). *Journal of African Earth Sciences* 151 286-314, doi:
1943 10.1016/j.jafrearsci.2018.12.008.
- 1944 Scotese, C.R., Boucot, A.J., Mckerrow, W.S., 1999. *Journal of African earth Sciences* 28(1),
1945 99-114.
- 1946 Selly, R.C., 1997: The Basins of Northwest Africa: Structural Evolution. In: R.C. Selly (ed.) *African*
1947 *Basins. Sedimentary Basins of the World*, 3, 17-26. Elsevier, Amsterdam.
- 1948 Sinha, S. T., Saha, S., Longacre, M., Basu, S., Jha, R., & Mondal, T., 2019. Crustal
1949 architecture and nature of continental breakup along a transform margin: New insights
1950 from Tanzania-Mozambique margin. *Tectonics* 38, 10.1029/2018TC005221.
- 1951 Squire, R.J., Campbell, I.H., Allen, C.M., Wilson, C.J.L., 2006. Did the Transgondwanan
1952 Supermountain trigger the explosive radiation of animals on Earth? *Earth and*
1953 *Planetary Science Letters* 250, 116-133.
- 1954 Straathof, G.B., 2011. Neoproterozoic low latitude glaciations: an African perspective. PhD
1955 thesis, University of Edinburg, 285p.
- 1956 Tack, L., Delvaux, D., Kadima, E., Delpomdor, F., Tahon, A., Dumont, P., Hanon, M.,
1957 Fernandez-Alonso, M., Baudet, D., Dewaele, S., Cibambula, E., Kanda Nkula, V.,
1958 Mpiana, Ch. (2008). The 1.000 m thick Redbeds sequence of the Congo River Basin
1959 (CRB): a generally overlooked testimony in Central Africa of post-Gondwana
1960 amalgamation (550 Ma) and pre-Karoo break-up (320 Ma). 22nd Colloquium of
1961 African Geology, Hammamet, Tunisia, November 4-6, 2008, Abstract book, 86-88.

- 1962 Tack, L., Wingate, M.T.D., De Waele, B., Meert, J., Belousova, E., Griffin, A., Tahon, A.,
 1963 Fernandez-Alonso, M, 2010. The 1375 Ma "Kibaran event" in Central Africa:
 1964 prominent emplacement of bimodal magmatism under extensional regime.
 1965 *Precambrian Research* 180, 63-84.
- 1966 Tait, J. Delpomdor, F. Pr at, A. Tack, L. Straathof, G., Nkula, V. K., 2011. Neoproterozoic
 1967 sequences of the West Congo and Lindi/Ubangi Supergroups in the Congo Craton,
 1968 Central Africa, in Arnaud, E. Halverson, G. P. and Shields-Zhou, G. Ed. The
 1969 geological record of Neoproterozoic glaciations, *Geological Society Memoir* 36, 185-
 1970 194.
- 1971 Tankard, A., Welsink, H., Aukes, P., Newton, R., Stettler, E., 2009. Tectonic evolution of the
 1972 Cape and Karoo basins of South Africa. *Marine and Petroleum Geology* 26, 1379-
 1973 1412.
- 1974 Taverne, L. (1975a). A propos de trois T el ost eens Salmoniformes du Cr etac e inf erieur
 1975 (Wealdien) du Za ire, pr ec edemment d ecrits dans les genres *Leptolepis* et *Culpavus*
 1976 (*Pisces Teleostei*). *Rev. Zool. Afr.* 89, 481-504.
- 1977 Taverne, L. (1975b). Etude ost eologique de *Leptolepis caheni*, T el ost een fossile du
 1978 Jurassique sup erieur (Kimm eridgien) de Kisangani (ex-Stanleyville, Za ire)
 1979 pr ec edemment d ecrit dans le genre *Paraclupavus*. *Rev. Zool. Afr.* 89, 821-853.
- 1980 Trouw, R.A.J., de Wit, M.J., 1999. Relation between the Gondwanide Orogen and
 1981 contemporaneous intracratonic deformation. *Journal of African Earth Sciences* 28,
 1982 203-213.
- 1983 Torsvik TH, Cocks LR, 2011. The Paleozoic paleogeography of central Gondwana. In: Van
 1984 Hinsbergen, D.J., Buiter, S.J.H., Torsvik, T.H., Gaina, C., Webb, S.J. (Eds). *The*

- 1985 formation and the evolution of the Africa: a synopsis of 3.8 Ga of earth history.
1986 Geological Society, London, Special publications 357, 137-166.
- 1987 Torsvik, T.H., Cocks, L.R., 2013. Gondwana from top to base in space and time. *Gondwana*
1988 *Research* 24, 999-1030.
- 1989 Toteu, S.F., Penaye, J., Poudjom Djomani, Y., 2004. Geodynamic evolution of the Pan-
1990 African belt in central Africa with special reference to Cameroon. *Can. J. Earth Sci.*
1991 41, 73–85.
- 1992 Trompette, R., 1973. Le Précambrien supérieur et le Paléozoïque inférieur de l'Adrar de
1993 Mauritanie (bordure occidentale de Bassin de Taoudeni, Afrique de l'Oust). Un
1994 exemple de sédimentation de craton. Etude stratigraphique et sédimentologique.
1995 Travaux des laboratoires des Sciences de la Terre St.-Jérôme, Marseille B-7, 702.
- 1996 Trouw, R.A.J., de Wit, M.J., 1999. Relation between the Gondwanide Orogen and
1997 contemporaneous intracratonic deformation. *Journal of African Earth Sciences* 28,
1998 203–213.
- 1999 Van Daele, J., Hulsbosch, N., Dewaele, S., Muchez, P., 2020. Metamorphic and metasomatic
2000 evolution in the Western Domain of the Karagwe-Ankole Belt (Central Africa).
2001 *Journal of African Earth Sciences* 165, 103783
- 2002 Van Daele, J. Scherer, E., 2020. Neoproterozoic pre- and post-deformational metamorphism
2003 in the Western Domain of the Karagwe-Ankole Belt reconstructed by Lu-Hf garnet
2004 geochronology in the Kibuye-Gatumba area, Rwanda. *Precambrian Research* 344,
2005 105744.
- 2006 Veach, A.C., 1935. Evolution of the Congo Basin. *Mem. Geol. Soc. Am.*, 3, 184p.

- 2007 Verbeek, T., 1970. Géologie et lithologie du Lindien (Précambrien Supérieur du nord de la
2008 République Démocratique du Congo). Ann. Mus. Roy. Afr. Cent., Tervuren
2009 (Belgique), série in-8, Sci. géol., 66, 311p.
- 2010 Villeneuve, M., 2005. Paleozoic basins in West Africa and the Mauritanide thrust belt.
2011 Journal of African Earth Sciences 43, 166–195.
- 2012 Wopfner, H., 1999 The Early Permian deglaciation event between East Africa and
2013 northwestern Australia. Journal of African earth Sciences 29(1), 77-90.
- 2014